Engineering Oxidase Activity in Flavocytochrome b_2

by Lars H. Østergaard

PhD
The University of Edinburgh
1997

Til min mor og far

Acknowledgements

I thank my supervisors, Graeme Reid and Stephen Chapman, for their excellent guidance during the last three years work. I am also grateful to the Darwin Trust of Edinburgh and its trustees for their generosity and financial support. The Danish Research Academy and Brian Clark are likewise acknowledged.

Several people at ICMB have been most helpful in providing technical assistance and biological material whenever needed. Hence, thank you to Sean McAteer, Noreen Murray, Annette Titheradge, Arnold van der Luit, Nicola Preston and many more... A special thanks to Medhat Khattar for many useful and enjoyable discussions (and several cups of coffee).

The contribution of cloned glycolate oxidase from Peter Macheroux of University of East Anglia, cloned *E. coli* L-lactate dehydrogenase from Ed Lin and Simon Lynch of Harvard Medical School, and tips on mutagenic PCR from Mark Osborne of Hoffman la Roche is also gratefully appreciated.

And last but not least, a BIG thanks to ALL people in the Reid-Chapman group for being such a friendly, helpful, and cheerful crowd. I would especially like to acknowledge Eryl Sharp, Simon Daff, Alexis Balme, and Forbes Manson for their help during the initial phase of my work. Finally, many thanks and best of luck to my ex-collaborator Martin Goble.

Abstract

Flavocytochrome b_2 from *Saccharomyces cerevisiae* is a L-lactate dehydrogenase. The enzyme structurally consists of two functional separate domains, a FMN-binding and a haem-binding domain. The active site residues, involved in L-lactate dehydrogenation, are all located in the FMN-binding domain. The bound flavin molecule becomes fully reduced upon substrate oxidation, and the electrons are subsequently passed individually onto cytochrome *c* via the cytochrome domain. The flavin-binding domain expressed separately in *E. coli* also functions as a L-lactate dehydrogenase. However, this enzyme only interacts efficiently with the artificial electron acceptor ferricyanide and not with cytochrome *c*.

The three-dimensional structure of the flavin-binding domain exhibits a very high degree of similarity to another member of the family of 2-hydroxy acid oxidases, glycolate oxidase from spinach. The structure of each enzyme consists of a TIM-barrel with FMN bound at the carboxyl end of the β-strands in the barrel. However, the similarity is not restricted to the barrel, but includes loops and non-barrel helices as well. The enzymes are thus likely to have evolved from a common ancestral gene.

Glycolate oxidase catalyses the oxidation of small 2-hydroxy acids, including L-lactate. However, the biochemistry of FMN reoxidation is completely different from that of flavocytochrome b_2. Glycolate oxidase reacts with molecular oxygen to produce hydrogen peroxide, whereas flavocytochrome b_2 only reacts very slowly with oxygen. The structural features controlling the reactivity of the bound FMN towards dioxygen are unknown, and the general understanding of the reaction itself is likewise very incomplete. These important questions have been addressed during this work by attempting to convert the L-lactate dehydrogenase, flavocytochrome b_2, into an oxidase.

One approach was based on protein engineering by introduction of site-specific mutations. The mutations were concerned with the problem of generating access to and space around the bound FMN. A number of modified enzymes with substitution of amino acid residues in close proximity to the co-factor were constructed, purified and characterised. Most mutations had negative effects on the dehydrogenase activity. However, their oxidase activity did not improve either, and suggests that a single mutation may not be sufficient to swing the activity. Another concern in the design of mutant enzymes is the extremely high degree of similarity between the two enzyme structures. There simply are no obvious differences to explain the different reactivity.

However, a loop region exhibits no amino acid sequence similarity between members of this family of enzymes. This loop is located close to the flavin, but is disordered in the electron density map of both flavocytochrome b_2 and glycolate oxidase. The function of this loop was studied by construction of various alterations in this region. The loop clearly interacted with the active site and its bound co-factor, as demonstrated by changes in absorption spectra and kinetic parameters. Unfortunately, none of these mutant enzymes exhibited the desired oxidase activity either.

The approach of forced evolution seems ideal, when considering the above described difficulties. The method includes random mutagenesis of the gene coupled with selection. A selection system based on expression of mutant enzymes in *E. coli* has been established. The mutagenesis has been performed by error-prone PCR, which offers control over the level of mutagenesis and may be targeted to specific areas. The techniques have been combined with DNA shuffling to mimic the process of natural evolution, and thus exploiting the benefits of homologous recombination. This technique may also be applied to mix the two genes of flavocytochrome b_2 and glycolate oxidase, which probably has the highest potential of success given the close relationship between the enzymes.

Table of Content

List of Figures

1. Introduction

1.1. Flavoproteins

The term flavoprotein is used to catalogue a group of proteins, that contain a flavin prosthetic group. Many flavoenzymes exist as nondissociable, but noncovalent, complexes of apoprotein and flavocoenzyme. However, the co-factor may also be covalently linked to the protein moiety (Mewies *et al.*, 1997) or merely be employed as a substrate (Fisher *et al.*, 1995). The name flavin originates from the Latin word for yellow, and refers to the chromophore riboflavin (vitamin B_2). Riboflavin is a tricyclic isoalloxazine molecule conjugated to ribose, that in biological systems is phosphorylated and then adenylated further to the two active redox coenzyme forms FMN (flavin mononucleotide) and FAD (flavin adenine dinucleotide) found in flavoproteins (Walsh, 1980).

Flavoproteins catalyse redox reactions, whereby one substrate is reduced and another oxidised. The flavin prosthetic groups are unique and highly versatile chemical molecules, which have the ability to serve as converters between two-electron and one-electron reactions. This leads to the wide range of reactions catalysed by the flavoproteins. Flavins are thus involved in the dehydrogenation of a variety of substrates, in one-electron transport processes and in the activation of molecular oxygen. The specificity and efficiency of the reaction catalysed is determined by interaction of the isoalloxazine nucleus of the flavin with the protein moiety, and presumably requires very fine tuning (Ghisla & Massey, 1986).

The flavoproteins may be divided into four subclasses dependent on their reactivity with molecular oxygen: oxidases, electron transferases, oxygenases, and dehydrogenases (Massey, 1994). Different groups display many properties that are characteristic of a particular group and not shared with other groups. These characteristics are summarised below:

The oxidases catalyse a two-electron reduction of molecular oxygen and yield hydrogen peroxide as the only observed product of oxygen reduction (Lindqvist & Brändén, 1985). Oxidases form a red anionic semiquinone on reduction by one electron.

Electron transferases react rapidly with molecular oxygen to produce superoxide (Leenders *et al.*, 1993).

The oxygenases catalyse insertion of molecular oxygen into the substrate. Mono-oxygenases catalyse insertion of one atom of dioxygen into an organic substrate and reduce the other atom to water (Willetts, 1997), whereas di-oxygenases catalyse the insertion of both atoms of dioxygen into an organic substrate (Keevil & Mason, 1978).

The dehydrogenases, as opposed to all other groups, have practically eliminated the reaction with molecular oxygen (Lederer, 1991). Instead, these enzymes utilise cytochromes, nonhaem iron proteins, quinones, oxidised pyridine nucleotides, or other flavoproteins as their physiological electron acceptors.

1.2. Chemistry of Molecular Oxygen

Oxidation based on molecular oxygen is the primary source of energy in many living organisms. It is one of the most extensively studied biochemical reactions, and the structures of several oxidising enzymes have been elucidated by crystallography. However, the nature of the attacking oxygen species involved is still a mystery.

Oxygen is the eight element in the Periodic Table. It is the most abundant element and makes up 46.6% (by weight) of rock on earths crust and 20.9% (by volume) of air. The chemistry of molecular oxygen or dioxygen is dominated by its relative reluctance with which the element reacts with most compounds. Molecular oxygen is thermodynamically a good oxidising agent, and most other elements and compounds are unstable to O_2. In practice however, few systems actually reacts with O_2 under normal conditions, as most processes are kinetically controlled by high activation energy. Hence, much of the interest in the chemistry of oxygen has been associated with different ways of activating O_2, using catalysts (Ebsworth *et al.*, 1975).

The electronic structure of the oxygen molecule is represented as O=O. This representation indicates that the O-O bond is short and strong, as it indeed is. The molecular orbital configuration for molecular oxygen is:

$$(1\sigma_g)^2(1\sigma_u)^2(2\sigma_g)^2(2\sigma_u)^2(3\sigma_g)^2(1\pi_u)^4(1\pi_g)^2$$

The inner electrons concentrate around the nuclei, $(1\sigma_g)^2(1\sigma_u)^2$, and probably contribute very little if anything to the formation of bonds. The rest of the electrons are considered valency electrons. The $2\sigma_g$ orbital builds up electron density between the two atoms, and is referred to as a bonding orbital. This bonding orbital is followed (in energy) by a $2\sigma_u$ antibonding orbital, which is an orbital with nodal planes between the

nuclei. These 2σ orbitals correspond to weak interactions arising from the 2s atomic orbitals. The next orbital on the energy scale is a $3\sigma_g$ bonding orbital, arising from the $2p_z$ orbitals on each atom, thus giving oxygen its fundamental σ bond. This is followed by the double-degenerate $1\pi_u$ bonding orbital. Finally, there are two electrons in the $1\pi_g$ antibonding orbital. Thus, the strong bonds holding the oxygen atoms together consist of one σ-bond and effectively one π-bond (the other is cancelled out by the π-antibond). The two electrons that give the molecule its paramagnetism are found in two degenerate antibonding π orbitals (Kasha & Brabham, 1979).

Most molecules are diamagnetic with ground states described as singlets. If a reaction is to take place with dioxygen in its ground state there must be a change of spin at some stage during the reaction. This is forbidden, which is the major reason for the kinetic inertness (Green & Hill, 1984). There are no unpaired electrons in H_2O_2 nor H_2O, so the reduction of O_2 actually involves a forbidden spin change. There are two ways to overcome this restriction. Reduction of dioxygen to superoxide removes the kinetic barrier associated with spin restriction. Alternatively, molecular oxygen could be activated by exitation to the singlet state which has paired electrons. However, the general reaction pattern of singlet oxygen is different from that of triplet oxygen, and it is more difficult to accomodate with the oxidation products formed in nature. Triplet oxygen is therefore the most plausible oxidative agent in biological reactions (Torssell, 1989).

1.3. Flavin mononucleotide (FMN)

Flavin mononucleotide is constituted of a tricyclic isoalloxazine ring molecule, which is connected to a phosphorylated ribityl side chain (Figure 1.1).

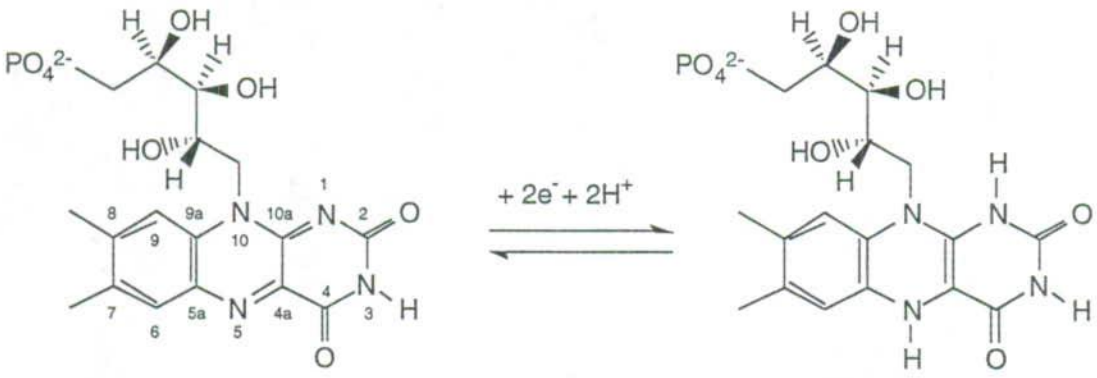

Figure 1.1. The structure of oxidised and reduced FMN, including the numbering system used to define the atoms in the isoalloxazine ring system.

The varied redox chemistry of FMN is restricted to the isoalloxazine skeleton, and is remarkably well-suited in having readily accessible one-electron and two-electron reduced states (Ghisla & Massey, 1986). This allows FMN a wide variety of redox choices and makes it a unique organic molecule as compared to the nicotinamide coenzymes (Walsh, 1980). The ribityl side chain is not involved in the redox process, but serves in anchoring the co-enzyme to the protein moiety.

The two-electron-reduced dihydro form is readily produced by reduction with dithionite (Figure 1.2). Changes affect the N5, C4a, C10a, and N1 positions of the isoalloxazine ring system, that comprise an enediamine (diaminoethylene) electron sink (Ghisla & Massey, 1989). The reduced (leuco) form is colourless, which makes the yellow chromophore of FMN invaluable as an absorbance and fluorescence probe. This feature of FMN is employed in analysis of the kinetics and the nature of chemical intermediates in both reductive and oxidative half-reactions. The colour of oxidised FMN is due to absorption of light in the blue region (430-480 nm) of the visible spectrum, but we perceive the compliementary colour yellow.

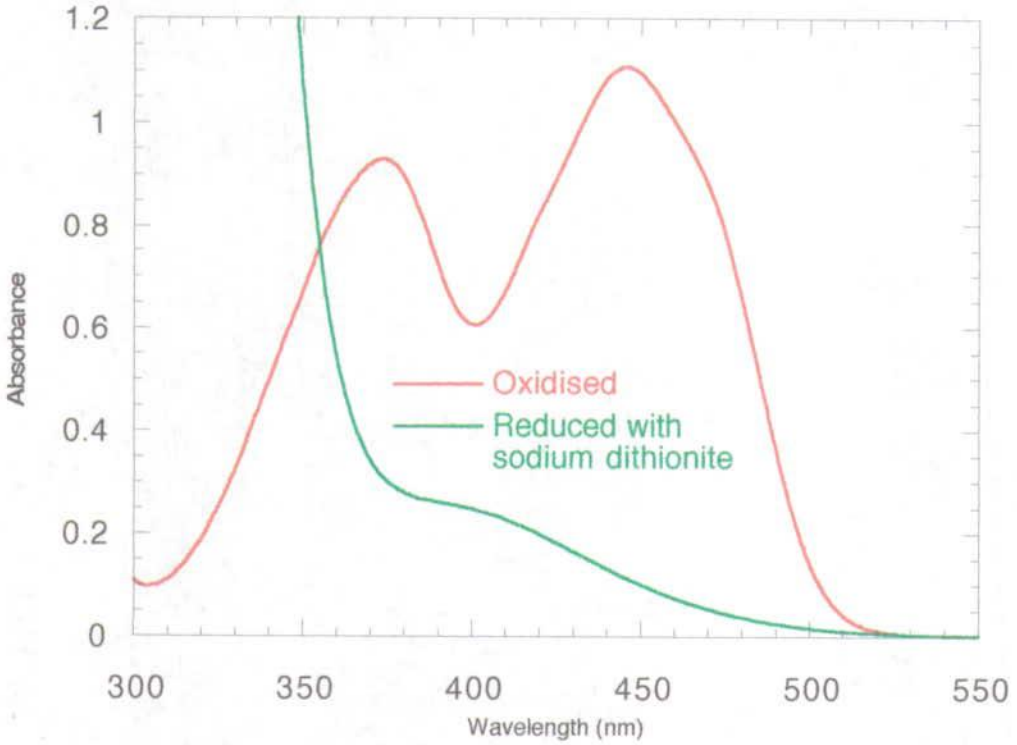

Figure 1.2. Absorption spectrum of 0.1 mM FMN dissolved in 10 mM Tris-HCl pH 7.5 (I = 0.1 M) recorded at 25°C using a 1 cm cuvette.

Reduced FMN can be oxidised with oxidants such as ferricyanide or molecular oxygen. Flavin is one of the few biocatalysts which can efficiently reduce dioxygen. The reoxidation of reduced flavin by molecular oxygen is a very complicated process (Figure 1.3). The dihydro form is autooxidised to the quinoid form by molecular

oxygen in a stepwise manner (Gibson & Hastings, 1962). The first encounter results in the transfer of an electron from reduced flavin to O_2 with the intermediate formation of the semiquinone radical and superoxide ion. The superoxide radical ion is generated at a low reduction potential (Kemal *et al.*, 1977). The reduction of oxygen weakens the strong O-O bond, as the electron goes into an unfilled antibonding orbital. It also removes the kinetic barrier associated with spin restriction, as one-electron reduction of fully reduced FMN produce a flavin radical. These two radicals may then rapidly recombine to form the covalent flavin-4a-hydroperoxide. The hydroperoxide itself can dissociate heterolytically to yield hydrogen peroxide and oxidised flavin (Malmström, 1982). However, as a base superoxide readily adds a proton to form the reactive hydrogen peroxide radical, $pK_s = 4.9$, thus at physiological pH only a few per cent are present in the acidic form (Torssell, 1989). By protonation, which proceeds extremely rapidly, the chemical character of the superoxide ion is drastically changed. From being a good nucleophile and mild reducing agent it is turned into a strong oxidant, and this change in oxidation potential may alter the route of reaction. Indeed, no radical species, superoxide or covalent hydroperoxides has ever been detected during catalysis in flavoprotein oxidases (Massey, 1994). Yet, the efficient reaction between reduced enzyme and molecular oxygen does lead to formation of oxidised enzyme and H_2O_2. The simplest explanation is that the reaction does not proceed via a C4a-hydroperoxide, but rather through a second one-electron transfer step. Alternatively, the covalent hydroperoxide is a transition state.

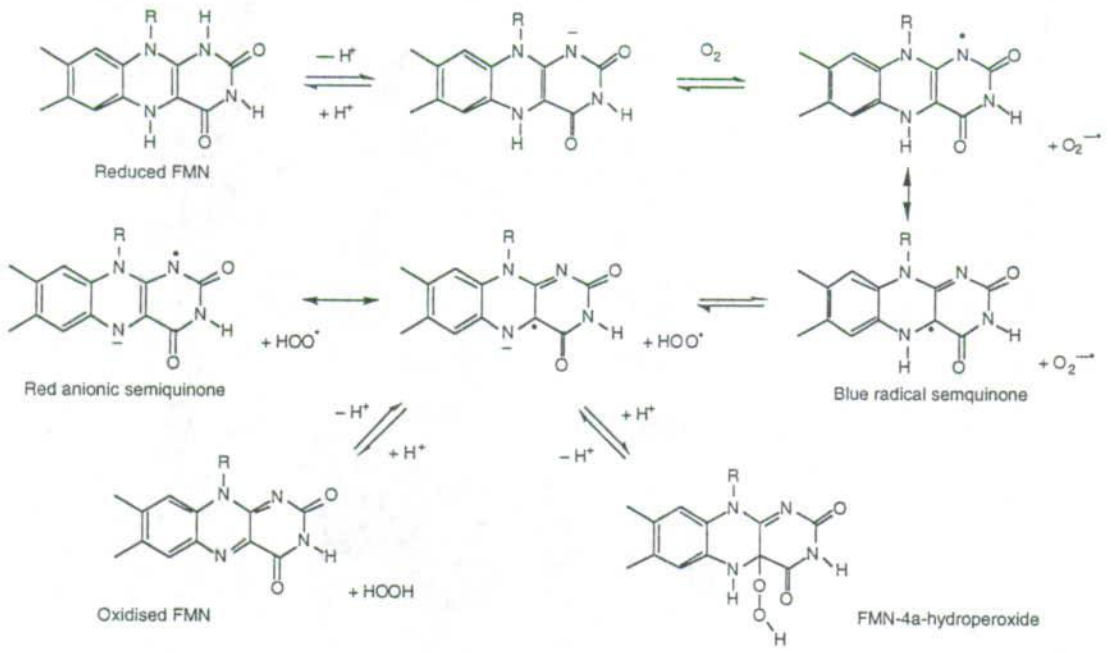

Figure 1.3. Oxidation of free reduced FMN by stepwise one-electron transfers to dioxygen (adapted from Torssell, 1989).

The reactivity of a flavoprotein with molecular oxygen is modulated by the protein environment in which the reduced flavin is located, both in terms of rates and products of the reaction. Modulation of flavin reactivity may be divided into effects on the thermodynamics and those on the kinetics of a possible reaction (Ghisla & Massey, 1989). The thermodynamics of the reaction are modulated by changes in the electron or negative charge density of the enediamine function. Reduced flavin consists of an electron-rich phenylenediamine moiety fused with a (4,5-diamino)-uracil (Figure 1.1). The negative charge is localised and stabilised in the latter. The degree to which this negative charge is stabilised governs the redox potential. A positive charge in the protein around the flavin pyrimidine ring will increase the redox potential, whereas a negative charge or hydrophobic environment will lower it. Indeed, the redox potentials of glycolate oxidase and flavocytochrome b_2 are shifted markedly more positive than that of unbound FMN. Interactions between FMN and the apoproteins thus produce oxidants that can react with substrate in a thermodynamically feasible reaction. The relative free energies may be computed by appropriate combinations of flavin and oxygen half-cells.

$$\Delta G^0 = -nF\Delta E^0$$

Equation 1.1. The relative free energy $\Delta G°$ is given by the above equation, where n is the charge number for the electrochemical reaction, F is the Faraday constant ($9.648x10^4$ C/mol), and ΔE^0 is the change in the standard electromotive force.

Electrode	E^0 / V	Half cell reaction	Reference
$HO_2^{\bullet}\|H_2O_2$	+1.680	$HO_2^{\bullet} + H^+ + e^- \rightarrow H_2O_2$	(Ebsworth *et al.*, 1975)
$O_2^{\bullet-}\|H_2O_2$	+0.940	$O_2^{\bullet-} + 2H^+ + e^- \rightarrow H_2O_2$	(Kemal *et al.*, 1977)
$Fe(CN)_6^{3-}\|Fe(CN)_6^{4-}$	+0.358	$Fe(CN)_6^{3-} + e^- \rightarrow Fe(CN)_6^{4-}$	(Lide, 1993)
$O_2\|H_2O_2$	+0.347	$1/2\ O_2 + H^+ + e^- \rightarrow 1/2\ H_2O_2$	(Lide, 1993)
$FMNH^{\bullet}\|FMNH_2$ (GO†)	-0.038	$FMNH^{\bullet} + H^+ + e^- \rightarrow FMNH_2$	(Pace & Stankovich, 1986)
FMN|$FMNH^{\bullet}$ (FCb2¶)	-0.044	$FMN + H^+ + e^- \rightarrow FMNH^{\bullet}$	(Lederer, 1991)
FMN| $FMNH_2$ (FCb2¶)	-0.051	$1/2\ FMN + H^+ + e^- \rightarrow 1/2\ FMNH_2$	(Lederer, 1991)
$FMNH^{\bullet}\|FMNH_2$ (FCb2¶)	-0.057	$FMNH^{\bullet} + H^+ + e^- \rightarrow FMNH_2$	(Lederer, 1991)
$FMN\|FMNH_2$ (GO†)	-0.068	$1/2\ FMN + H^+ + e^- \rightarrow 1/2\ FMNH_2$	(Pace & Stankovich, 1986)
Glyoxylate|glycolate	-0.086	1/2 glyoxylate + $H^+ + e^- \rightarrow$ 1/2 glycolate	(Pace & Stankovich, 1986)
$FMN\|FMNH^{\bullet}$ (GO†)	-0.096	$FMN + H^+ + e^- \rightarrow FMNH^{\bullet}$	(Pace & Stankovich, 1986)
$O_2\|O_2H^{\bullet}$	-0.130	$O_2 + H^+ + e^- \rightarrow O_2H^{\bullet}$	(Ebsworth *et al.*, 1975)
$O_2\|O_2^{\bullet-}$	-0.160	$O_2 + e^- \rightarrow O_2^{\bullet-}$	(Ingraham & Meyer, 1985)
$FMNH^{\bullet}\|FMNH_2$ (free)	-0.167	$FMNH^{\bullet} + H^+ + e^- \rightarrow FMNH_2$	(Kemal *et al.*, 1977)
Pyruvate|lactate	-0.189	1/2 pyruvate + $H^+ + e^-$ → 1/2 lactate	(Clark, 1960)
FMN| $FMNH_2$ (free)	-0.209	$1/2\ FMN + H^+ + e^- \rightarrow 1/2\ FMNH_2$	(Massey, 1994)
$FMN\|FMNH^{\bullet}$ (free)	-0.231	$FMN + H^+ + e^- \rightarrow FMNH^{\bullet}$	(Kemal *et al.*, 1977)
$SO_4^{2-}\|SO_3^{2-}$	-0.465	$1/2SO_4^{2-} + 1/2H_2O + e^- \rightarrow 1/2SO_3^{2-} + OH^-$	(Lide, 1993)

¶) Glycolate oxidase at pH 7.1 and 10°C.
†) Morton enzyme (flavocytochrome b_2 cleaved by yeast proteases) at pH 7 and 20°C.

Table 1.1. Standard electrode potentials at 25°C.

However, the redox potentials fail to explain why glycolate oxidase reacts efficiently with molecular oxygen, and why flavocytochrome b_2 reacts only slowly. Obviously, the reactions are also kinetically modulated by steric access to the flavin itself or to a specific position, which may lower the rate of a reaction to essentially zero. Indeed, the N3, C4=O, C4a, N5 area of the flavin moiety at the active site in oxidases are often more solvent accessible. Reaction of peroxides with 5-deazaflavin bound to oxidases results in the formation of 5-deazaflavin 4a,5-epoxide (Jorns *et al.*, 1983). This result confirms that these positions of the coenzyme must be accessible to solvent. Furthermore, the oxidase activity is lowered considerably when hindering access of O_2 to the reduced flavin by introduction of iso-FMN (Ghisla & Massey, 1992). The oxygenases also prevent the otherwise rapid decay of flavin C4a-hydroperoxide by insulation of this intermediate from the solvent, either by binding the initial product tightly (Maeda-Yorita *et al.*, 1995), by movement of loop regions (Fisher *et al.*, 1995), or even by moving the flavin ring itself (Gatti *et al.*, 1994).

1.4. Flavin analogues

Valuable information about the nature of the flavin binding site in flavoproteins comes from studies where the native flavin has been replaced by artificial flavins with selective properties specific to the individual flavins (Ghisla & Massey, 1986). Studies on synthetic flavin analogues may be employed to dissect out features which control sites of hydrogen transfer, two-electron versus one-electron pathways, and modes of O_2 reductive activation.

5-Carba-5-deazaflavin (Figure 1.4), with the central dihydropyridine in the reduced state, is competent for rapid two-electron chemistry only (Walsh, 1980). One-electron chemistry is simply not thermodynamically accessible. One consequence of this is that no catalytic reoxidation by dioxygen or by haem cofactors is detectable, and indeed only two-electron oxidants are active. Reconstituted flavocytochrome b_2 is thus reduced by lactate, but no electrons are transferred to the haem and no ferricyanide reductase activity can be measured (Pompon & Lederer, 1979). Furthermore, the carbon site at position 5 is inert to rapid exchange with solvent, unlike the parent flavin, and has been used to demonstrate direct hydride transfer to position 5 from substrate (Brüstlein & Bruice, 1972).

1-Carba-1-deazaflavin (Figure 1.4), with its deazauracil moiety is, in contrast to the parent flavin, purple. It has a redox potential of -280 mV, and is thermodynamically more difficult to reduce than the parent flavin (Spencer *et al.*, 1977). Hence, coenzyme

substition is expected to slow down the flavin-reduction step, but increase the rate of reoxidation. The central ring is still a pyrazine, the dihydro form is reoxidised rapidly by molecular oxygen, and a semiquinone is detectable. 1-deazaflavin-reconstituted oxidases and dehydrogenases are catalytically competent (Walsh, 1980). The only exception appears to be flavocytochrome b_2, which is reported not to bind 1-deazaflavin. A rather speculative hypothesis suggests that this is due to the C1-C2=O area: The binding is supposedly so tight that the protein simply cannot accommodate an extra hydrogen atom on the flavin in that area (Pompon & Lederer, 1979). However, the minor steric difference between the N1 sp^2 free electron pair of normal flavin as compared to the C1-H function of the analogue hardly provides a reasonable explanation as to why flavocytochrome b_2 does not bind this analogue.

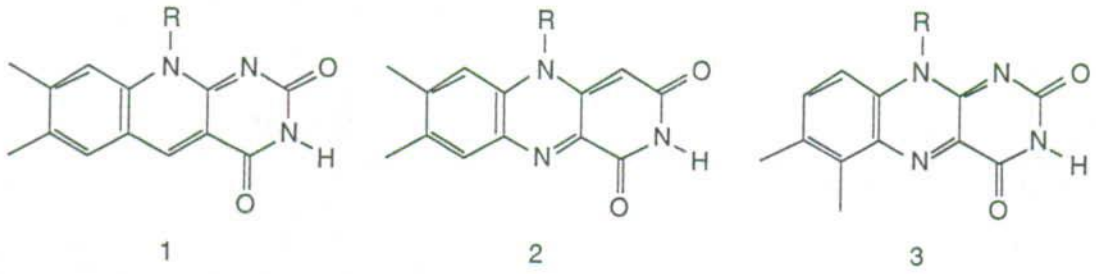

Figure 1.4. The flavin analogues 5-deaza- (1), 1-deaza- (2), and iso-FMN (3).

1.5. The family of 2-hydroxy acid-oxidising FMN-dependent proteins

The flavoprotein enzymes catalysing oxidation of L-2-hydroxy acids share many mechanistic similarities (Ghisla & Massey, 1989). The relationship between the proteins has been confirmed at both DNA and protein sequence level. This makes it likely that they constitute a family of proteins with common structural motifs (Scrutton, 1994). Indeed, the two known three-dimensional structures both contain a TIM-barrel motif (Lindqvist *et al.*, 1991). Each member is thus typified by having a barrel structure which binds a FMN molecule. The isoalloxazine ring of FMN is held at the C-terminal ends of the internal β strands of the barrel domain, where it is surrounded by the catalytic residues present in the loops.

However, the terminal electron acceptor varies among the members. This is partly reflected in the modular complexity of the member proteins. Two members, flavocytochrome b_2 (Lederer, 1991) and L-mandelate dehydrogenase (Smékal *et al.*, 1993), possess cytochrome domains spliced onto the N terminus of the barrel domain. In flavocytochrome b_2, the amino acid sequence of this domain is about 30% identical

with that of the bovine cytochrome b_5. The three-dimensional structures of flavocytochrome b_2 core and beef cytochrome b_5 are also very similar. These accessory domains are not involved in bond making or breaking, but ensure efficient delivery of electrons to the physiological acceptor via the redox centres housed in them. The isolated flavodehydrogenase domain of flavocytochrome b_2 does not interact with the isolated cytochrome domain, and thus demonstrates the importance of a linkage between the two domaines with respect to the enzyme's physiological function.

The family has probably evolved from a common ancestral barrel fold (Scrutton, 1994). Evolution has enabled different chemistries to reside on similarly folded and related core structures. The modular assembly and divergence of recruited core structures has contributed further to the development of some family members. The additional N-terminal domain of flavocytochrome b_2 and mandelate dehydrogenase from *R. graminis* was thus aquired by a process of gene fusion. The two enzymes presumably evolved divergently from a single gene fusion of separate ancestral flavin-binding and cytochrome domains. Furthermore, the fusion event is likely to have occurred late in time, as most of the members contain subunits comprising only a single barrel domain.

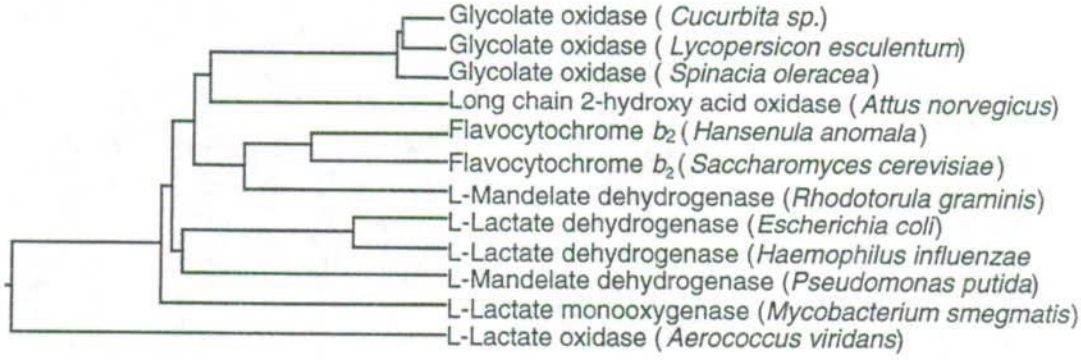

Figure 1.5. Phylogenetic tree of 2-hydroxy acid-oxidising enzymes.

The remaining two lactate dehydrogenases (Dong *et al.*, 1993) and the mandelate dehydrogenase from *P. putida* (Mitra *et al.*, 1993) are all membrane bound enzymes, and hence fall into another branch of the family's phylogenetic tree. Other closely related proteins include the long and short chain 2-hydroxy acid oxidases. A high degree of similarity also exists between members on different branches. The sequences of flavocytochrome b_2 and glycolate oxidase can thus be aligned with a few insertions and deletions starting at residue 121 of the yeast enzyme (Figure 1.6). They show a total of 38.8% identity at the protein sequence level. The similarity between these two enzymes will be even more evident upon comparison of their three-dimensional structures.

Figure 1.6. An amino acid sequence comparison between flavocytochrome b_2 (S. cerevisiae), glycolate oxidase (spinach), long-chain hydroxy acid oxidase (A. norvegicus), and L-lactate oxidase (A. viridans). Identical amino acid residues occuring in three or all four enzymes are boxed, stars above the sequence indicate catalytically active residues, whereas residues in helices and strands of the TIM-barrel are marked below the sequence.

1.6. Flavocytochrome b_2

Flavocytochrome b_2 (L-lactate:cytochrome *c* oxidoreductase, EC 1.1.2.3) from baker's yeast (*Saccharomyces cerevisiae*) couples L-lactate dehydrogenation to cytochrome *c* reduction (Appleby & Morton, 1954). The catalytic cycle consists of five consecutive electron-transfers. L-lactate dehydrogenation results in two-electron reduction of FMN; the two electrons are then individually passed to b_2-haem and finally onto cytochrome *c* (Daff *et al.*, 1996a).

1.6.1. Biological function

Flavocytochrome b_2 is synthesised on free ribosomes in the cytoplasm of *Saccharomyces cerevisiae*. The initial preprotein includes an 80 amino acid residue precursor sequence attached to the N-terminal end. The N-terminal signal sequence directs the protein to the mitochondria. Mitochondria have two bilayer membranes and an intermembrane space. The preprotein is imported across both membranes simultaneously into the interior matrix at a site where the two membranes are in close contact.

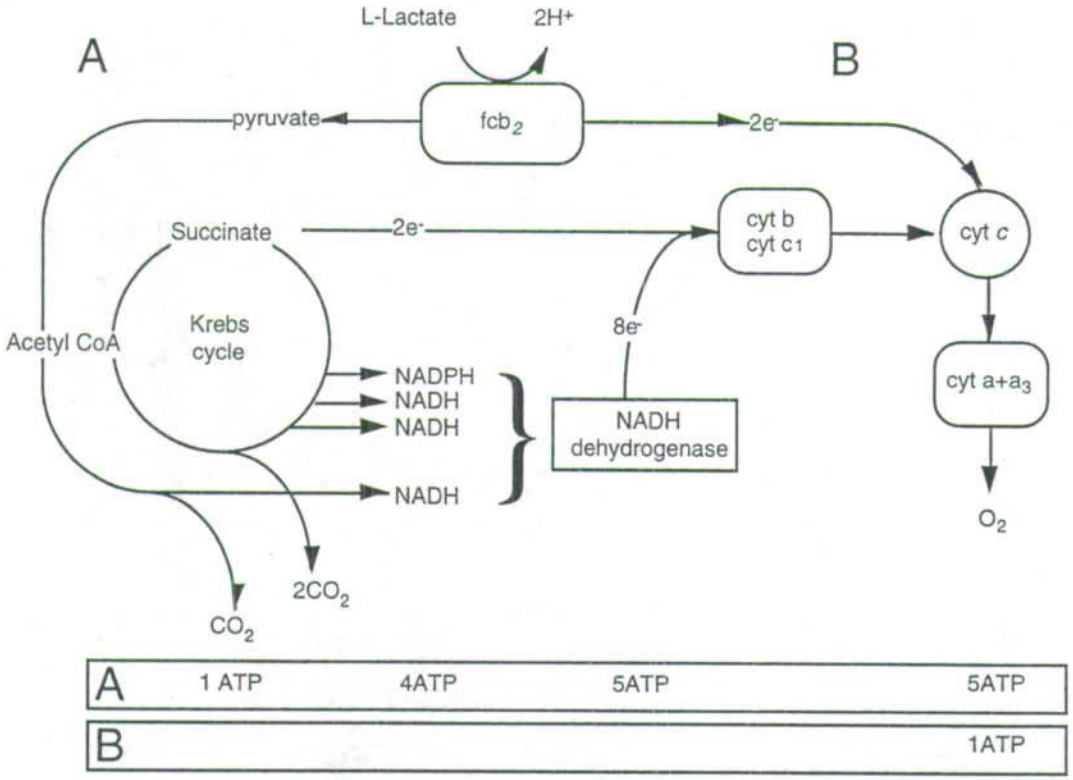

Figure 1.7. Respiration of L-lactate yield 16 equivalents of ATP of which L-lactate dehydrogenation by flavocytochrome b_2 only generates one equivalent (adapted from Daff, 1996).

The protein has a double presequence, and the N-terminal part of this presequence is cleaved by proteolysis after import. The second part of the presequence is similar to the signal sequence for export from the mitochondria. Hence, the protein is exported across the inner membrane into the intermembrane space, where the second part of the presequence is removed. Flavocytochrome b_2 is thus located in the intermembrane space of yeast mitochondria (Daum *et al.*, 1982; Gasser *et al.*, 1982). The synthesis of flavocytochrome b_2 is induced both by oxygen and its substrate L-lactate. Its physiological role is to provide pyruvate for the Krebs cycle during aerobic respiration on L-lactate (Figure 1.7). However, it also forms part of a secondary electron transport chain, along with cytochrome *c* and cytochrome oxidase, to ensure growth of the organism on lactate, even if the rest of the mitochondrial electron transport chain is blocked (Pajot & Claisse, 1974).

1.6.2. Structure

The enzyme is a homotetramer of subunit molecular weight 57,500 Da. The complete amino acid sequence (Lederer *et al.*, 1985) and DNA sequence (Guiard, 1985) of flavocytochrome b_2 from baker's yeast has been determined. The refined crystal structure of flavocytochrome b_2 is available at 2.4 Å resolution (Xia & Mathews, 1990). The molecule possesses pseudo 4-fold symmetry. Each subunit is composed of two discrete domains connected by a peptide hinge (Figure 1.8). The N-terminal cytochrome domain binds a protohaem IX, and consists of residues 1 to 99. The C-terminal domain binds an FMN prosthetic group, and is composed of residues 100 to 486. The four flavin-binding domains pack together about the molecular 4-fold axis to form a disk about 100 Å in diameter and about 60 Å thick. The remaining residues 487-511 form a tail, that wraps around the molecular 4-fold axis and makes contact with each of the other subunits. The cytochrome domains are located on the outer edge of the tetramer protruding away from the 4-fold axis. They form no intersubunit contacts.

Subunits positioned opposite each other with respect to the 4-fold axis behave similarly to each other, but differently from the other pair of subunits upon crystallisation. Two of the cytochrome domains are thus ordered in the crystal structure (subunit 1), while the two others are disordered (subunit 2). The flavin-binding domains behave quite similarly in all four subunits. Residues from position 100 to 299 and from 317 to 511 are ordered in all four subunits. Residues 300 to 311 are disordered in all subunits, while residues 312 to 316 are also disordered in two subunits only (subunit 1). The conformations of two dipeptides, 298 to 299 and 510 to 511 are poorly ordered in all

subunits. Furthermore, two subunits (subunit 2) have a molecule of pyruvate, the product of the catalytic reaction, bound at the active site. In these subunits the flavin is in the semiquinone form. The carboxylate group of pyruvate binds to Arg376 and Tyr143 and the keto group is hydrogen bonded to Tyr254 and His373. The anionic form of the flavin semiquinone, with the negative charge of deprotonated atom N1 distributed over the N1-C2=O locus, is stabilised by ionic interactions to a buried Lys349 near the N1, O2 position (see figure Figure 1.15, p. 23).

Figure 1.8. Model of subunit 1 based on the crystal-structure of flavocytochrome b_2. The cytochrome domain, with a red haem molecule bound, is shown in orange. The rest of the structure belongs to the flavin-binding domain, which has a yellow FMN molecule bound at the C-terminal end of the β-barrel. The components of the barrel, the α-helices and β-strands, are highlighted in green and purple, respectively.

The cytochrome domain consists of a six-stranded mixed β-sheet (5 strands in one direction, 1 in the other), with a single helix lying on one side. On the other side of the sheet are two pairs of antiparallel helices that form the haem-binding pocket. The flavin-binding domain contains a TIM–barrel motif. This barrel motif is contained within the segment of residues 191 to 465. In addition to the $\beta_8\alpha_8$ motif there are eight helices and four short β-strands external to the barrel. A helix is located within the β/α-barrel between elements β8 and α8 and forms dipolar interactions with the phosphate group of FMN. The barrel itself is interrupted between β4 and α4 by the disordered segment described above. The isoalloxazine ring of the enzyme-bound

flavin, which is located at the C-terminal end of the central β-barrel, is mostly sequestered from solvent. The only atoms of FMN with any appreciable exposure to solvent are C4a, N5 and C5a on the edge of the isoalloxazine ring. The remaining atoms of FMN, which are of a polar or hydrogen-binding nature, interact with polar main- or side-chain atoms of the β-strands.

1.7. Glycolate oxidase

Glycolate oxidase (glycolate:oxygen oxidoreductase EC 1.1.3.1) from spinach is a flavoprotein catalysing the oxidation of 2-hydroxy acids to the corresponding 2-keto acids (Frigerio & Harbury, 1958). The highest affinity is for glycolate followed by DL-2-hydroxy butyrate and then L-lactate (Stenberg *et al.*, 1995). Glyoxylate is the product of glycolate oxidation. Glycolate oxidase is found in the peroxisomes, where the enzyme plays a crucial function in photorespiration.

1.7.1. Biological function

The process of photorespiration (Leegood *et al.*, 1995) is initiated by one of the key enzymes in the Calvin cycle of carbon dioxide fixation, ribulose-1,5-bisphosphate carboxylase/oxygenase (Rubisco). Rubisco is a bifunctional enzyme, catalysing both the carboxylation and oxygenation of ribulose-1,5-bisphosphate (RuBP). CO_2 and O_2 compete with one another at the active site of Rubisco. While carboxylation results solely in the formation of glycerate-3-P, oxygenation also leads to production of glycolate-2-P. Glycolate-2-P can not be utilised within the Calvin cycle. Instead, it is salvaged in the photorespiratory pathway (Figure 1.9). Glycolate-2-P is dephosphorylated, a reaction which is catalysed by glycolate-2-P phophatase recycling P_i within the chloroplast. Glycolate is then exported from the chloroplast, enters the peroxisome and is oxidised by glycolate oxidase to glyoxylate. The hydrogen peroxide generated is decomposed by catalase within the peroxisomes. Glyoxylate is then transaminated to form glycine.

Photorespiration is apparently a wasteful process, consuming energy and resulting in loss of fixed carbon. Indeed, C3 plants lose up to 50% of the carbon fixed (Bainbridge *et al.*, 1995). Hence, it is highly desirable to engineer higher plant Rubisco with increased specificity, that favours carboxylation, increases photosynthetic rate and thus plant yield (Gutteridge *et al.*, 1995). However, although some natural variation actually exists among higher plants, there also appear to be a negative correlation between specificity factor and maximum carboxylation rate (Bainbridge *et al.*, 1995).

Instead, nature evolved the C4 plants. In addition to the normal Calvin cycle these plants also have another cycle that is used for the fixation of carbondioxide in these plants. This separation eliminates the factors, such as ratio of CO_2 to O_2 and temperature, that influence the rate of photorespiration in C3 plants. Algae have chosen a different approach (Brändén *et al.*, 1987). Rubisco in algae has also oxygenase activity, but they have been under selective pressure to conserve energy. The competition for light energy is harsh in water, and it would be advantageous to preserve the energy otherwise released in glycolate oxidation. Hence, the degradation of glycolate in algae is initiated by a glycolate dehydrogenase, which channels the energy to cytochrome *c* instead. These findings point in the direction of Rubisco not being maladapted, but misunderstood. Rubisco may indeed already function optimally as a carboxylase, or maybe the oxygenase activity fulfils a role of its own. Photorespiration could also have evolved to consume excess reducing power produced in high light flux (Dey & Harborne, 1997). Engineering dehydrogenase activity into glycolate oxidase might thus be a better approach to increase plant yield.

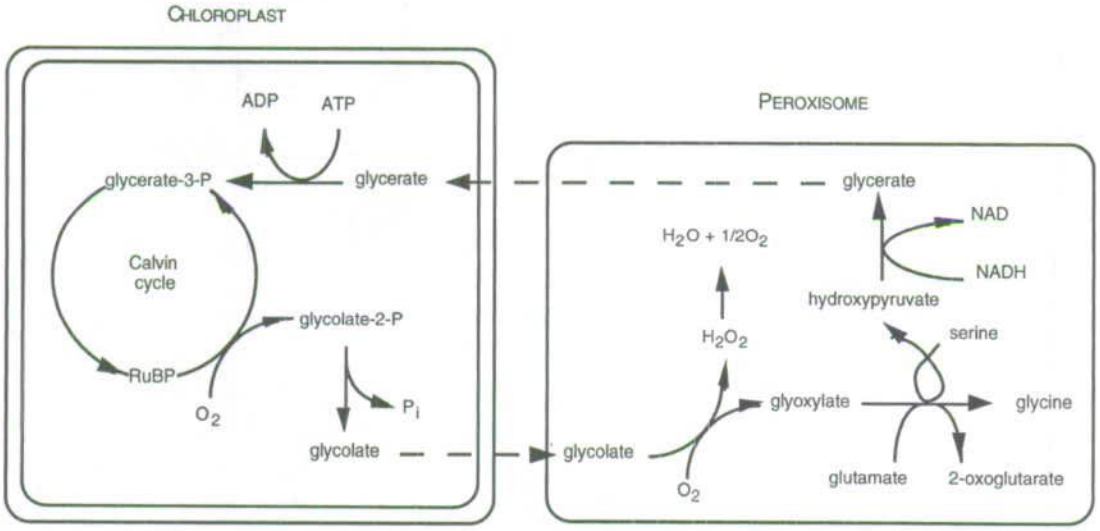

Figure 1.9. The photorespiratory pathway. The final product is here shown as glycine, and is generated by transamination of glyoxylate using either glutamate or serine (adapted from Leegood et al., 1995). However, the produced glycine subsequently enters the mitochondria and is converted into serine and CO_2.

1.7.2. Structure

The primary structure of glycolate oxidase from spinach has been determined by peptide sequencing (Cederlund *et al.*, 1988) and also deduced from the DNA sequence (Volokita & Somerville, 1987) of a cDNA clone. Glycolate oxidase is an octamer of identical subunits. Each subunit consists of 369 amino acid residues with a molecular weight around 43,000 Da. The enzyme is very basic with an isoelectric point above 9

(calculated value of 9.16), which is due to an unusually high number of arginine residues on the surface. The three-dimensional structure at 2.0 Å resolution has been elucidated by X-ray crystallography (Lindqvist, 1989). The model consists of 350 amino acid residues, the cofactor flavinmononucleotide and 298 water molecules (Figure 1.10). The C-terminal ten amino acid residues and a surface loop consisting of residues 189 to 197 are disordered in the electron density map. The octameric glycolate oxidase molecule has a diameter of approximately 100 Å and a strict 422 symmetry in the subunit arrangement. The molecule makes strong interactions around the 4-fold axis forming a tight tetramer, but only weak interactions between the two tetramers forming the octamer.

Figure 1.10. The structure of a subunit of glycolate oxidase. The TIM-barrel motif is shown in green (α-helices) and purple (β-strands) with FMN bound the the C-terminal end of the central β-strands.

The main parts of the subunits are folded into the TIM-barrel motif. The barrel is build up from a core of eight parallel β-strands connected by α-helices on the surface. The remaining residues in glycolate oxidase have been assigned to two regions. The first region comprises 70 residues at the N-terminal. The second region is part of a long peptide segment of 45 residues between strand four and helix four of the barrel. Most of the structure not belonging to the barrel is located outside the carboxyl end of the β-strands of the barrel and forms a lid on the barrel, which partly shields the active site.

As is common in soluble α/β-proteins, the α-helices in glycolate oxidase are exposed to the solvent and are thus amphiphilic. The exception is an almost buried α-helix, which binds the phosphate group of FMN. The FMN molecule is bound at the carboxy end of the β-strands. Almost the entire coenzyme is buried in the interior of the enzyme. The exception is a region around the N5 position of the isoalloxazine ring that is accessible to solution. Multiple interactions are made between FMN and the loops connecting the carboxy end of the eight strands with the amino end of the helices. The specificity is determined by the length and the sequence of these loop regions. The barrel itself constitutes the scaffold for these loop residues participating in catalysis.

1.8. Comparison of three-dimensional structures

Glycolate oxidase and the flavin-binding domain of flavocytochrome b_2 have the same structural motif, the 8-fold β/α-barrel. The FMN-binding site is at the carboxyl-terminal end of the eight β-strands of the barrel, where the active site is invariably located in this type of domain structure. The similarity of the structures extends to the loop regions and even outside the β/α-barrels with a root mean square deviation of 0.93 Å for 311 superimposed C^{α}-atoms (Lindqvist *et al.*, 1991). This implies that the general architecture of each of the two structures is virtually identical (Figure 1.11).

The only large difference between the superimposed structures is that the loop in glycolate oxidase between strand four and helix four of the barrel, involving 29 residues which cover the active site, is moved away from the active site in flavocytochrome b_2 and is replaced by the cytochrome domain. Also, the extended tail of about 25 residues at the C-terminal end of flavocytochrome b_2 does not exist in glycolate oxidase. Other minor differences between the two structures are variations in the length of loops. However, the affected loops are in both structures facing the solvent and are of no obvious functional significance.

Despite the strong similarity in the backbone structure, the FMN orientation and binding mode, although similar, are significantly different (Figure 1.12). The differences are due to different conformations of residues in the end of strand one. Amino acid residue Pro77 in glycolate oxidase is equivalent to Ala196 in flavocytochrome b_2, and might have some effect although the main chain conformations of these residues are the same. One important difference in FMN binding is a hydrogen bond from the side chain of Ser195 to the ribityl side chain in flavocytochrome b_2, which is not present in glycolate oxidase where the corresponding

residue is Ala76. Another difference is the main chain conformation of Thr78/197. The side chain conformations of these threonines are different in the two structures. This might be caused by Leu436 in flavocytochrome b_2, which corresponds to Val312 in glycolate oxidase. This residue could restrain the position of methyl group of Thr197 in flavocytochrome b_2. The different conformation of Thr197 gives rise to a hydrogen bond between NH-198 and N5 of FMN in flavocytochrome b_2, and probably influence the orientations of the flavin ring.

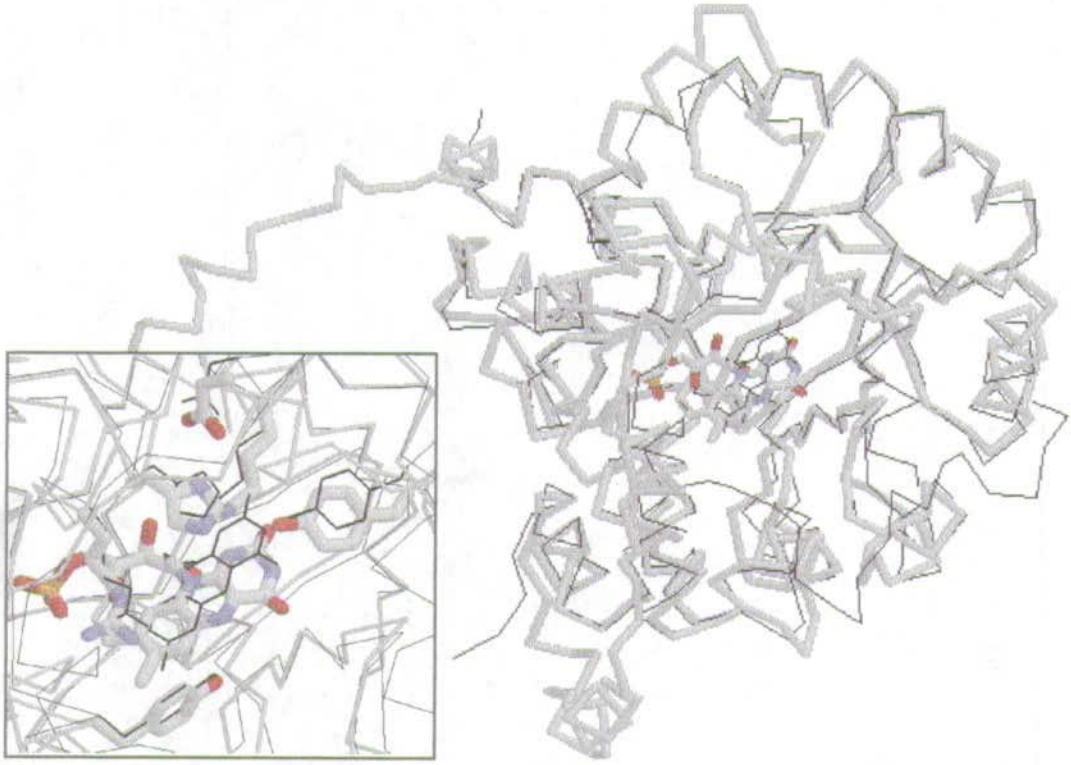

Figure 1.11. The C^{α}-backbone of the glycolate oxidase (black) superimposed upon that of the flavin-binding domain (fat grey). The insert shows a close-up of the active sites, where the catalytic active residues are highlighted.

A major difference in the active site is a water molecule close to the O4, C4 positions on the *re*-side of the isoalloxazine ring in glycolate oxidase. In flavocytochrome b_2, where the FMN ring system lies closer to strand one, the main chain amide of Ala198 form a hydrogen bond to the FMN N5 position, and there is thus no space for a water molecule. Furthermore, solvent access to the *re*-side is prohibited by the hydrogen bonds from the side chains of Gln252 and Ser228 to FMN N3 and O4, respectively. Molecular graphics have shown that the water molecule in glycolate oxidase could be replaced by oxygen, which would be suitable located for receiving electrons from $FMNH_2$ and forming a covalent bond at position C4a. However, recent three-dimensional structures of glycolate oxidase with bound active site inhibitors show the isoalloxazine ring tilted towards Thr78 leaving no room for a water molecule (Stenberg

& Lindqvist, 1997). Unless an artefact of the bulky inhibitors, it demonstrates mobility of FMN in glycolate oxidase upon substrate binding, or alternatively the orientation of FMN is determined by the redox state of the cofactor. The water pocket would then be occupied by the O4 of FMN, and oxygen would instead attack on the *si*-face. The hypothetical C4a-hydroperoxide would thus be orientated on the *si*-face of the flavin toward His254. Hydrogen peroxide would be formed by acceptance of a proton from the histidine, and thereby complete the catalytic cycle (Lindqvist & Brändén, 1989).

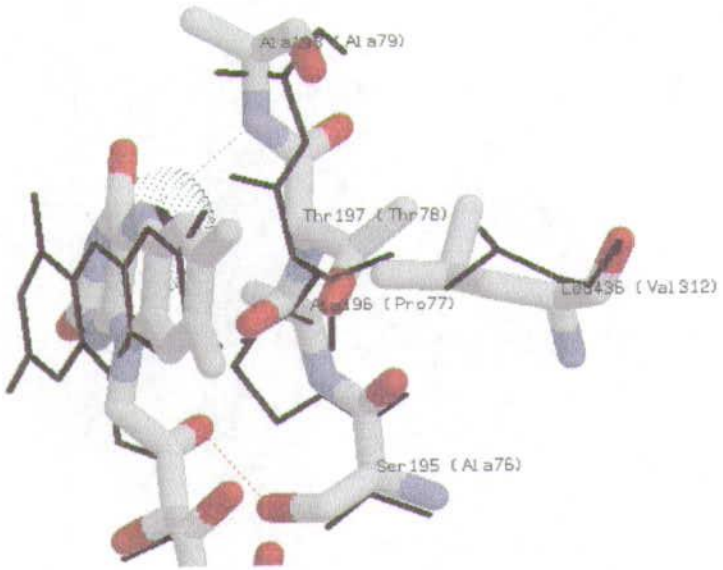

Figure 1.12. The illustration shows the area on the re-side of FMN in flavocytochrome b_2 (coloured) and glycolate oxidase (black), including a part of strand one with Thr197 and residue Leu436. The position of the water molecule, only found in glycolate oxidase, is indicated as a black ball surrounded by a dotted sphere. The dotted lines represent hydrogen bonds, which only exist in flavocytochrome b_2.

1.9. Catalysis in L-2-hydroxy acid-oxidising FMN-dependent proteins

The first event in catalysis is the rupture of a substrate-H bond, with concomitant transfer of two electrons to the FMN acceptor molecule. A second substrate serves to reoxidise the reduced flavin to complete the catalytic cycle (Figure 1.13). Thus catalysis by flavoprotein enzymes always involves a reductive half-reaction, where the enzyme-bound flavin is reduced, and an oxidative half-reaction, where the reduced flavin is reoxidised (Singer & Edmondson, 1978). In most cases it is possible to study the two half-reactions separately, a feature which has permitted the detailed analysis of catalytic events.

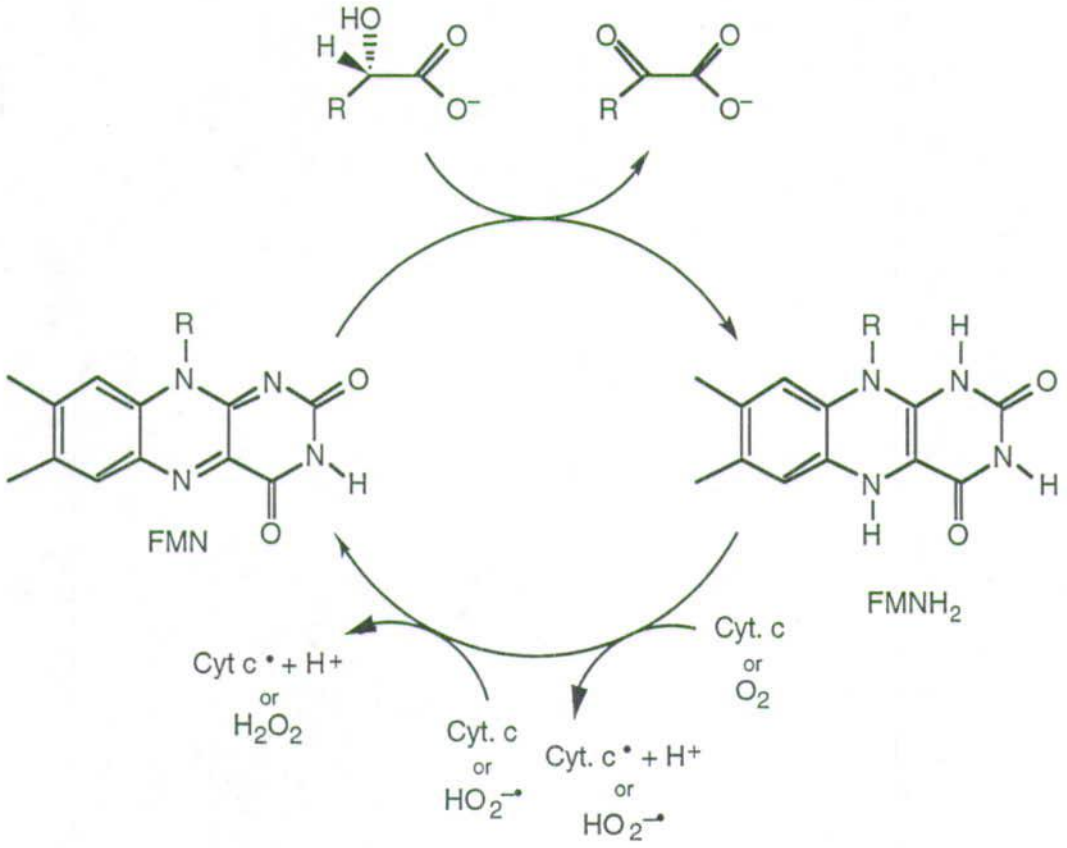

Figure 1.13. Scematic representation of the catalytic cycle of flavocytochrome b_2 (reoxidised by cytochrome c) and glycolate oxidase (reoxidised by dioxygen).

The three dimensional structures of flavocytochrome b_2 and glycolate oxidase have been solved. In addition to similar folding patterns, both enzymes possess a set of conserved amino acid residues with a very similar spatial positioning around the flavin (Lindqvist et al., 1991). Although the structures of the remaining enzymes in the family are as yet unknown, these same six residues are conserved in their amino acid sequences (except for long chain 2-hydroxy acid oxidase, where a phenylalanine residue is found instead of an otherwise conserved tyrosine; Diêp Lê & Lederer, 1991). Specific catalytic roles have been assigned to these conserved residues, and confirmed by site-directed mutagenesis studies.

1.9.1. Substrate binding and specificity

The topology of the active centre of flavocytochrome b_2 shows the substrate (or rather product) bound to the *si*-side of the flavin (Figure 1.14). The carboxylate function of the substrate makes both a hydrogen bond and an ionic interaction with the guanido group of Arg376, while the other oxygen is hydrogen bonded to the phenolic hydroxyl of Tyr143. A third substrate attachment point is that of the C2 hydroxyl to Tyr254 phenolate. Only one side-chain in the active site is not conserved. The amino acid

residue at this position, Leu230 in flavocytochrome b_2 and Trp108 in glycolate oxidase, is involved in determining the substrate specificity. The size of the α-carbon side chain of the substrate correlates with the size of the amino acid side chain.

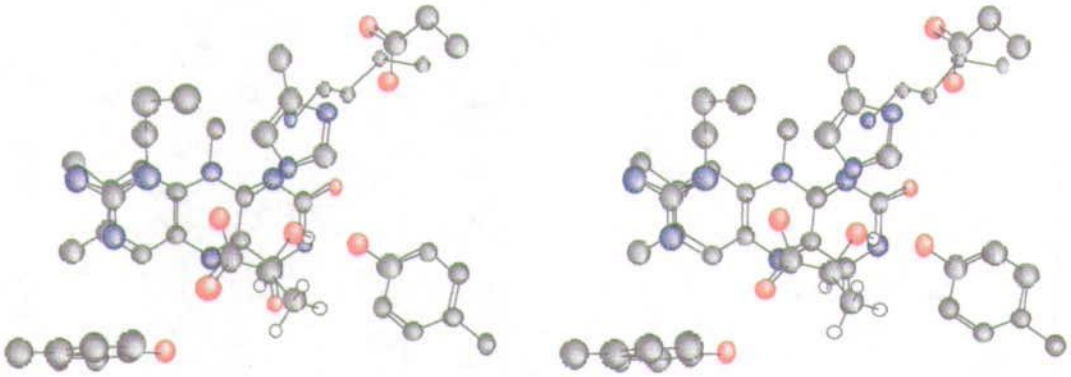

Figure 1.14. Stereo structure of the active site of flavocytochrome b_2 with L-lactate modelled in place of pyruvate. Only the hydrogen atoms of L-lactate are shown (see Figure 1.15 for labelling of the amino acid residues).

1.9.2. Reductive half reaction

The catalytic cycle is initiated by substrate dehydrogenation. The first event is a proton abstraction by His373, which plays an essential role in catalysis as a general base. The cleavage of the C^{α}-H bond of an 2-hydroxy acid can be formulated either as hydride transfer or as a two-electron transfer (Ghisla & Massey, 1989). The proton abstracted in the hydride mechanism would be that of the hydroxyl group, whereas in the carbanion mechanism it would be the proton of the α-carbon (Figure 1.15). Site-directed mutagenesis of His373 to a glutamine results in an essentially inactive enzyme (Müh *et al.*, 1994). The mutation is a semiconservative replacement, as it has similar spatial requirements to the histidine and may be able to substitute for some of the original function by its capacity to form hydrogen bonds (Fersht *et al.*, 1987). However, it lacks the ability to be protonated, and thus proves the histidine's role as a base. The imidazole side chain of His residues possesses several special properties that make it extremely effective as a nucleophilic catalyst. It is a tertiary amine, which is much more reactive than hydroxide ion in terms of its basicity. Imidazole has a pK_a value near 7, so it is one of the strongest bases that can exist at neutral pH. Simultaneously deprotonation of both imidazole nitrogen atoms give an aromatic anion with an apparent pK_a of about 14.4 (Creighton, 1993). Indeed, the proton abstraction is facilitated by electrostatic stabilisation of the incipient imidazolium ion thanks to its interaction with the carboxylate of Asp282.

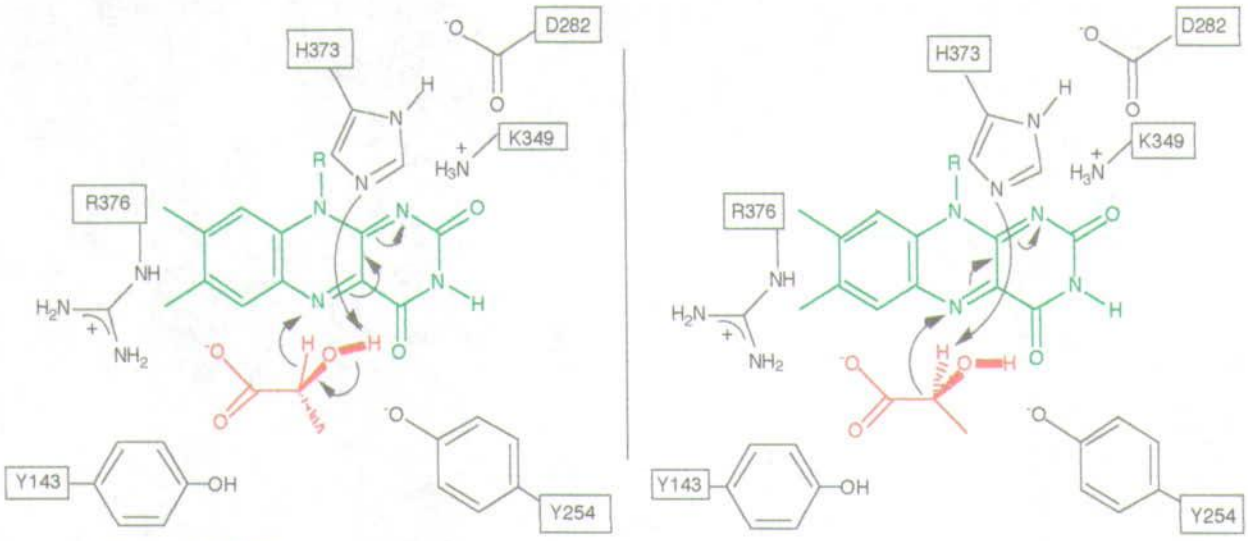

Figure 1.15 The mechanism of L-lactate dehydrogenation is either a hydride transfer to flavin N5 (left), or generation of a carbanion intermediate with subsequent formation of a covalent adduct to N5 (right).

The second step in the hydride mechanism would simply be transfer of hydride to the flavin N5, and would happen concerted with abstraction of the hydroxyl proton . In contrast, the anion generated in the carbanion mechanism would be likely to form a covalent adduct at the flavin N5 by a direct nucleophilic attack. The reaction with the normal substrate L-lactate is fast and proceeds to the product pyruvate without observable intermediates, but the reduced flavin is most unlikely to exist as a dianion with negative charges both at N1 and N5 (Ghisla & Massey, 1989). Tyr254 would subsequently have to act as a second general base by pulling away the substrate hydroxyl proton. This would contribute to expulsion of the electrons toward the flavin, and generate the product and reduced flavin (Lederer, 1991). Whatever the mechanism, the positive charge of Lys349 constitutes an electron sink by interaction with N1-C2=O of the flavin, and facilitates flavin reduction thermodynamically.

The hydride mechanism is supported by several observations. The carboxyl group of the substrate is likely to be ionised, as it interacts with a positively charged side chain. It would thus not be favourable to form a carbanion adjacent to the carboxylate due to the high pK of the C^{α}-H bond (Lederer, 1991; Stenberg *et al.*, 1995). Halogeno substrates have been employed to provide evidence for the carbanion mechanism, and these substrates are indeed processed by abstraction of C^{α}-H abstraction (Urban & Lederer, 1984). However, an electrophilic halide placed right next to the α-carbon is bound to make the hydrogen more acidic, and makes the comparison to normal substrate somewhat invalid. Replacement of the native flavin with 5-carba-5-deazaflavin has provided further proof of direct hydride transfer to position 5 from cosubstrates (Pompon & Lederer, 1979; Ghisla & Massey, 1986). Site-directed mutagenesis also favours the hydride mechanism, as mutation of the proposed second

base Tyr254 to phenylalanine fails to inactivate the enzyme (Reid *et al.*, 1988). The structure itself, with the α-hydrogen of L-lactate positioned optimally for direct transfer to the N5 of FMN (Figure 1.14), also suggest the hydride transfer as the mechanism of catalysis. Kinetic and structural studies of other flavoproteins offer further support for this mechanism. D-amino acid oxidase, although structurally unrelated, exhibits a curious similarity to flavocytochrome b_2. The active site residues superimpose those of the mirror image of flavocytochrome b_2, and reduction of its bound flavin is likely to occur via a hydride transfer (Mattevi *et al.*, 1996). The reaction catalysed by a distant relative, dihydroorotate dehydrogenase, also involves a hydride transfer (Rowland *et al.*, 1997).

1.9.3. Oxidative half reaction

Reduced flavoproteins complete their catalytic cycle in the oxidative half-reaction. Reoxidation of reduced flavin in flavocytochrome b_2 happens in two sequential step (Daff *et al.*, 1996a). The electrons are individually passed to the haem and then onto cytochrome *c*, as the haem groups are obligate one-electron acceptors. The active-site residue Tyr143, lying between the two domains, plays a key role in facilitating electron transfer between FMN and haem (Miles *et al.*, 1992). The interdomain electron transfer is also dependent on an essential hinge peptide connecting the two domains (Sharp *et al.*, 1994). Indeed, electron transfer from the flavin-binding domain to the separately expressed cytochrome domain is undetectable (Pallister *et al.*, 1990). Furthermore, the isolated flavin-binding domain is uncapable of interacting efficiently with cytochrome *c*. However, it is still a good L-lactate dehydrogenase, when using ferricyanide as an artificial electron acceptor (Balme *et al.*, 1995).

The oxidative half-reaction in glycolate oxidase is also generally thought to proceed via one-electron oxidoreduction steps. No catalytic reoxidation by dioxygen is observed in oxidases, when substituting native FMN with 5-carba-5-deazaflavin (Walsh, 1980). The crossover between two-electron transfer and one-electron transfer is a phenomenon largely restricted to flavoproteins and is due to their favourable redox potentials and thermodynamic stabilisation of the key intermediate semiquinone form. The red anionic semiquinone, generally found in oxidases, is stabilised by hydrogen bonding from a H-bond donor of the protein to the radical anion, with its negative charge localised in the N1-C2=O position. Another generalisation, which appears to hold, is that the flavin N5-C4=O locus is exposed to solvent (Ghisla & Massey, 1986). This allows oxygen access to the FMN bound at the active site. The subsequent rapid second order reaction of reduced enzymes with O_2 is initiated by a one-

electron transfer. The generated superoxide then recombines with FMN to form a C4a-hydroperoxide, or alternatively simply accepts a second electron as previously described for the reaction between dioxygen and free FMN (Section 1.3, p. 4).

1.10.The project

The objective of this Ph.D. project has been to elucidate the way in which flavoproteins control their reactivity towards molecular oxygen. Conversion of a dehydrogenase into an oxidase would provide important information about the regulation. This great challenge was pursued using both conventional protein engineering and random mutagenesis combined with selection for the desired reactivity.

The study is based on the dehydrogenase flavocytochrome b_2 and the oxidase glycolate oxidase. These enzymes both belong to the family of 2-hydroxy acid oxidising FMN-dependent proteins. The members share remarkable enzymatic properties, but the terminal electron acceptor varies within the family. The FMN in flavocytochrome b_2 is reoxidised by a cytochrome, whereas glycolate oxidase use molecular oxygen as electron acceptor. The reactivity is obviously modulated by protein-FMN interactions. The flavin-binding domain of flavocytochrome b_2 is very similar in sequence to glycolate oxidase. The architecture of both enzymes is also very similar (Lindqvist *et al.*, 1991). It is thus likely that oxygen reactivity is controlled by access of oxygen, and not by influences on the chemistry of the reduced flavin. A few mutations in, and close to the active site have fine tuned these enzymes to exert their specific functions as an oxidase or a dehydrogenase.

1.10.1.Protein-engineering

Glycolate oxidase was used as a template upon which mutants of the flavin-binding domain of flavocytochrome b_2 were modeled. The redesigns were constructed in the isolated flavin-binding domain of flavocytochrome b_2, because the cytochrome domain is an electron sink and its presence would make direct comparison with glycolate oxidase void. Furthermore, it is possible that the cytochrome domain would restrict O_2 access to the flavin. A detailed analysis shows that the binding of FMN in the active sites of flavocytochrome b_2 and glycolate oxidase is significantly different. The isoalloxazine ring in glycolate oxidase is tilted, which creates a pocket on the opposite side of the ring compared with the substrate binding site. This pocket does not exist in flavocytochrome b_2, where the ring lies closer to β-strand one. The site could bind

either substrate oxygen or O4 of FMN, and thus facilitate accessibility of oxygen to C4a and formation of a C4a-hydroperoxide intermediate. Indeed, access to the flavin bound at the active site generally seems to be a hallmark of oxidases.

Another area of interest has been the disordered loop region between strand β4 and helix α4. The amino acid composition and the length of this loop varies among the members of the family (Figure 1.16). There is no detectable homology in the region, and the alignment is hence somewhat arbitrary. The region is quite basic in flavocytochrome b_2 from *S. cerevisiae* (net charge +4), whereas the corresponding region in *H. anomala* is two residues shorter and very acidic with a net charge of -6 (Haumont *et al.*, 1987). Long chain 2-hydroxy acid oxidase exists in two isoforms (Belmouden *et al.*, 1993), and the loop is either one residue shorter or two longer compared to flavocytochrome b_2. The loop is 6 residues longer in glycolate oxidase, 9 residues longer in L-mandelate dehydrogenase from *R. graminis* (Smékal *et al.*, 1993), 19 residues longer in lactate monooxygenase (Giegel *et al.*, 1990), the same length in lactate oxidase (Maeda-Yorita *et al.*, 1995), and 25 residues longer in L-mandelate dehydrogenase from *P. putida* (Tsou *et al.*, 1990). It is unknown whether this region plays an important role in the structure or function of the enzymes. However, the loop of *P. putida* L-mandelate dehydrogenase seems to be responsible for its membrane association, as shown by replacement with the analogous segment of the soluble glycolate oxidase (Mitra *et al.*, 1993).

```
FCb2 (H.a.)     REKDMKMKFEADSD-------------------------VQGDDEDIDRSQGASRALSSFIDPSLSWKD
HAO (A.n.)      RRRDKRNQLNLEANI------------------------LLKDLRALKEEKPTQSVPVSFPKASFCWND
FCb2 (S.c.)     REKDMKLKFSNTKAGP-----------------------KAMKKTNVEESQGASRALSKFIDPSLTWKD
isoHAO (A.n.)   RRRDKRNQLNLEANILLK---------------------DLRALKEVRKEKPTQSVPVSFPKASFCWND
GO (C.s)        READIKNRFVLPPFLTLKNFEG-----------------IDLGKMDKANDSGLSSYVAGQIDRSLSWKD
Lmdh (R.g.)     RERDLKLKARSQNYEHPIAAQWKAA---------------GSKVEETIAKRGVSDIPDTAHIDANLNWDD
LMO (M.s.)      RPRDLTISNFPFLRGLCLTNYVTDPVFQKKFKAHS------GVEAEGLRDNPRLAADFWHGLFGHSVTWED
Lmdh (P.p.)     RERDLHNRFKIPMSYSAKVVLDGCLHPRWSLDFVRHGMPQLANFVSSQTSSLEMQAALMSRQMDASFNWEA
```

Figure 1.16. Sequence alignment of the hypervariable loop region from members of the family of 2-hydroxy acid-oxidising enzymes.

The visible parts of this loop has a significantly different conformation in the three-dimensional structures of flavocytochrome b_2 and glycolate oxidase. This flexible segment of flavocytochrome b_2 corresponds to protease hypersensitive regions of the molecule. The cleavage alters the kinetic parameters, which indicates some interaction between the disordered region and the active site (Ghrir & Lederer, 1981). The crystal structure of another flavoprotein, dihydroorotate dehydrogenase A from *Lactococcus lactis*, has a flexible loop at the same position of its β/α-barrel (Rowland *et al.*, 1997). This loop covers a cavity above the flavin ring system, and access to or from this cavity require some significant movement of the β4-α4 surface loop. Likewise, a loop

in lactate dehydrogenase from *Bacillus stearothermophillus* undergoes a large conformational change to form its internal catalytic vacuole (El Hawrani *et al.*, 1994). In the apo-protein the loop is fully exposed to solvent, but becomes buried in the catalytically competent ternary complex, where the internal vacuole is filled with substrate, cofactor and low-mobility water molecules. Furthermore, many new substrate specificities have been obtained by varying the sequence of this mobile loop.

Precedent thus points to varying the sequence of solvated loops to obtain new enzymatic specificity and catalysis, with little danger of inducing instability in the protein framework itself. Indeed, the region of the disordered loop may have been a hot spot for evolutionary changes in the protein family. Naturally, its role in catalysis is impossible to deduce from structural information. Hence, the possible function of this loop in controlling oxygen reactivity and other parameters has been studied by construction and characterisation of several loop mutant enzymes.

1.10.2. Random mutagenesis

Classical protein engineering study localised regions of the sequence space, and is a powerful tool for the analysis of structure and function of proteins. The current methods for site-directed mutagenesis are highly efficient and quite effective when some idea of where to make the specific mutations are available. However, if the structure and function of the protein of interest is not well defined, it is often difficult to predict which mutations to make in order to bring about the desired change. Random mutagenesis of the DNA region of interest coupled with a screening or selection system is then generally the chosen method. The great advantage of this approach is that it is able to pick up even subtle changes in the protein structure remote from the active site and combination of non-additive individual mutations resulting in oxidase activity.

Several methods have been developed for the random mutagenesis within a targeted region of DNA. A battery of different methods are available for generation of random mutations in large DNA segments. These include use of mutagenic chemicals, mutagenic *E. coli* strains, and all shades in between. Another simple and efficient method for generation random mutations within a defined DNA segment is the error-prone polymerase chain reaction (Leung *et al.*, 1989). This method makes it possible to limit mutations to a particular regions of the DNA. The concept of the polymerase chain reaction is also applied in DNA shuffling (Stemmer, 1994b). DNA shuffling (sexual PCR) is a method for *in vitro* homologous recombination of pools of mutant genes by random fragmentation and polymerase chain reaction reassembly. The

potential application of the method includes recombination of a pool of mutants, backcroosing with parental DNA to eliminate non-essential mutation, and creation of a library of chimeras of two related genes. Indeed, sexual recombination of blocks is even applied in the evolution, and DNA shuffling thus mimics the natural design process.

The major disadvantage of random mutagenesis is that it requires large number of clones be screened. For the flavin domain of flavocytochrome b_2, with 1, 2 and 3 amino acid changes, the number of possible variants are 7809, 30,416,055 and 78,787,721,000 respectively (Equation 1.2). Thus, it is only feasible to screen variants with a small number of amino acid changes unless selection is possible. Furthermore, degeneracy of genetic code means that only about 30% of the sequence space is explored. Hence, more than two-thirds of the introduced mutations will unfortunately not encode other amino acids than those already encountered.

$$\frac{19^m \times n!}{(n-m)!m!}$$

Equation 1.2. The number of possible variants of a protein with n amino acid residues when introducing m substitutions.

Selection of an L-lactate oxidase in *E. coli* is theoretically possible, if the strain is only able to grow when expressing mutant enzymes with the desired oxidase activity. A L-lactate oxidase converts L-lactate to pyruvate by reducing molecular oxygen to hydrogen peroxide. Hence, the strain should be able to metabolise pyruvate but not L-lactate. Furthermore, it should not provide a terminal electron acceptor for expressed mutant enzymes with dehydrogenase activity. Bacteria grown aerobically are indeed able to oxidise pyruvate that is formed from carbohydrates. However, they are also able to metabolise L-lactate (Anraku & Gennis, 1987). This ability is due to a L-lactate dehydrogenase on the inner surface of the cytoplasmic membrane, which feeds electron into the respiratory system (Figure 1.17). Respiration involves proton-translocating electron transport pathways in which energy is generated by coupling substrate oxidation to the reduction of oxygen. *E. coli* has no cytochrome *c*, and no equivalent to the mitochondrial cytochrome *c* oxidase. Instead, two enzymes in the cytoplasmic membrane, the cytochrome bo_3 and *bd* complexes, oxidise the generated ubiquinol-8 and directly reduce molecular oxygen to water, concomitantly generating an electrochemical proton gradient across the membrane. Hence, an *E. coli* strain, without the ability to metabolise L-lactate, is made by a genetic knock-out the L-lactate dehydrogenase. Furthermore, the mutant enzymes expressed in this strain will most likely have to rely on oxygen as terminal electron acceptor, as the respiratory chain in

E. coli is unrelated to the equivalent in yeast. In principle, selection is thus possible by expressing the mutant enzymes in this strain, supplied only L-lactate as sole source of carbon and grown in the presence of oxygen. The selection system may be combined with a colourmetric screen for oxidase activity (Maeda-Yorita *et al.*, 1995), and would enable distinction between various level of activity. A positive control is naturally essential, but luckily readily available. Expression of glycolate oxidase, which is also able to oxidise L-lactate, should be able to sustain growth under the same conditions.

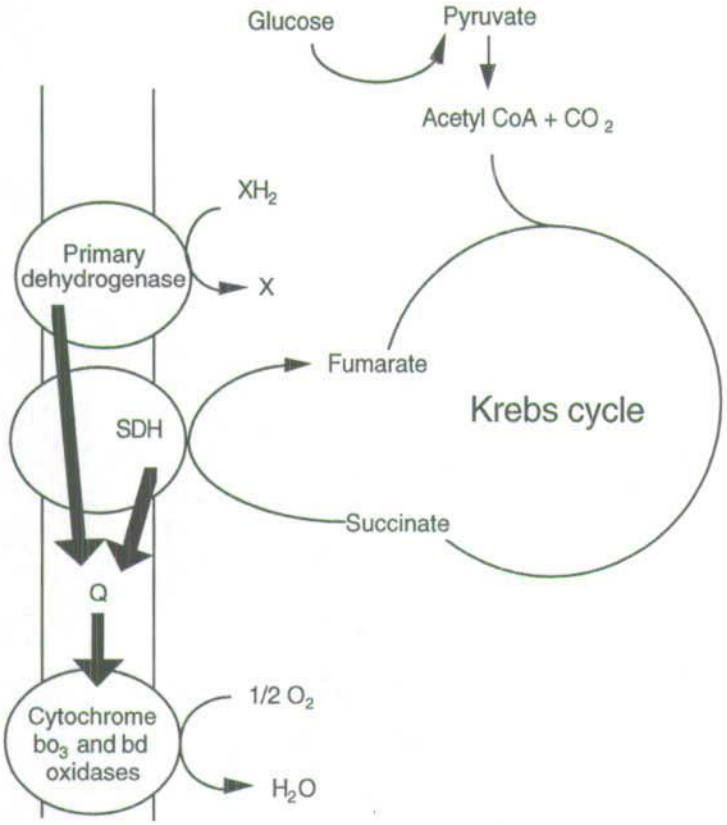

Figure 1.17. Respiratory system in E. coli growing under aerobic condition (adapted from Spiro & Guest, 1991). A series of dehydrogenases reduce ubiquinone-8, the product (ubiquinol-8) diffuses within the bilayer and is oxidised by either terminal oxidase. Q denotes ubiquinone-8.

2. Methods & Materials

2.1. Molecular Biology Techniques

All media, buffers and salts used in the handling of bacteria and phages were prepared according to recipes given by Sambrook *et al.* (1989a).

2.1.1. Mutagenesis

2.1.1.1. Site-specific mutagenesis

Site-specific mutations were introduced into the gene for flavocytochrome b_2 by the Kunkel method (Kunkel, 1985; Kunkel *et al.*, 1987). This "classical" oligonucleotide-directed generation of site-specific mutations is based on the utilisation of a mutagenising oligonucleotide spanning the region of the desired mutation and containing the specific base alterations. These alterations represented exchanges of one or a few specific bases, as well as small deletions or insertions at defined positions.

The single-stranded template DNA used was isolated from a *dut⁻ ung⁻* mutant strain (BW313), and hence contained uracil residues in place of thymine. The single-stranded DNA was produced upon infection of BW313/pGR401 in the mid-log phase with M13K03 helper phage (multiplicity of infection around 10). The incubation was continued for one hour at 37°C in presence of ampicillin only. A 1:25 dilution of this culture was grown overnight with good aeration under ampicillin and kanamycin selection. The single-stranded DNA was extracted as described by Sambrook *et al.* (1989b).

Phosphorylated oligonucleotide was then annealed to the single-stranded DNA tagged with uracil. The oligonucleotide was phosphorylated by incubation of 100 pmol oligonucleotide with 5 units of T4 polynucleotide kinase for 30 minutes at 37°C in 25 µl phosphorylation buffer (50 mM Tris-HCl pH 7.5, 10 mM $MgCl_2$, 5 mM DTT, 0.1 mM spermidine, 1 mM ATP). The reaction was stopped by heating to 70°C for 10 minutes, and the mixture was used immediately. Around 1.25 pmol of the phosphorylated oligo was mixed with 0.05 pmol single-stranded DNA in 20 µl annealing buffer (20 mM Tris-HCl pH 7.5, 10 mM $MgCl_2$, 50 mM NaCl), heated to 70°C for 5 minutes and then allowed to cool to 37°C over a period of 30 minutes.

The annealed oligonucleotide served as a primer for *in vitro* synthesis of the second strand. The annealed primer was extended by incubation of the synthesis reaction mixture for at least 45 minutes at 37°C. This mixture simply consisted of the annealing

reaction added 10 units of T4 DNA polymerase, 0.5 unit of T4 DNA ligase and 1/5 volume of 5x synthesis buffer (50 mM Tris-HCl pH 7.5, 2.5 mM of each dNTP, 5 mM ATP, 10 mM DTT) in a final volume of 30 µl. The resulting double stranded plasmid was transformed into an *ung*$^+$ strain (TG1), and the strand of wild-type sequence was thus eliminated after transformation.

2.1.1.2. Random mutagenesis

The approach of generating random mutations by PCR was based on the technique described by Leung *et al.* (1989). Low concentration of $MnCl_2$ were simply added to normal PCR reactions. The reaction mixture thus consisted of about 50-100 ng plasmid template DNA, 10 pmol of each primer, 0.2 mM of each dNTP, 3.4 mM $MgCl_2$, 0.1 mM $MnCl_2$, and 1 unit *Taq* DNA polymerase in a total of 50 µl reaction buffer. The mixture was overlaid with 40 µl mineral oil in a 0.5 ml microcentrifuge tube, placed in the thermal cycler and heated to 95°C for 40 seconds. The mixture was then subjected to 35 thermal cycles made up of a denaturing step at 94°C for 20 seconds, a primer annealing step at 50°C for 30 seconds, and 1.5 minute of primer extension at 72°C. The cycles were followed by a final extension step for 10 minutes to ensure most product are of full length, before stopping the reaction by cooling the mixture to 4°C.

2.1.2. DNA amplification

2.1.2.1. Polymerase chain reaction

The polymerase chain reactions (Mullis, 1990; Doyle, 1996) were typically performed on 50-100 ng plasmid DNA added 10 pmol of each primer, 1.5 mM $MgCl_2$, 0.2 mM of each dNTP, and 1 unit *Taq* DNA polymerase (Promega) in the supplied reaction buffer (10 mM Tris-HCl pH 9.0, 50 mM KCl, 0.1% Triton® X-100). The plasmid DNA was prepared using the QIAprep kit from QIAGEN. The reaction mixture had a total volume of 50 µl and was overlayed with 40 µl mineral oil in a 0.5 ml microcentrifuge tube. The tube was placed in the thermal cycler (Techne PHC-2), and heated to 95°C for 40 seconds. The reaction mixture was then exposed to 35 cycles of a thermal profile, a 10 minutes extension step at 72°C, and finally cooled to 4°C. The thermal profile generally used consisted of a 20 seconds denaturation step at 94°C, followed by annealing of the primers at 50°C for 30 seconds, and finally a one-and-a-half minute primer extension step at 72°C.

The reaction conditions were occasionally changed slightly depending on the nature of the primer and product. The optimal annealing temperature was estimated by the computer programmes "Amplify" (Engels, 1996) and "Oligo®" (Rychlik, 1992), which were also employed in the design of primers.

2.1.2.2. DNA shuffling

The technique of DNA shuffling (Stemmer, 1994a; Stemmer, 1994b; Crameri *et al.*, 1996) is closely related to PCR, and may be divided into three distinct steps: DNase I digestion, "PCR without primers", and PCR with primers (Figure 2.1). The gene to be shuffled was amplified by PCR as described above, and the product of the reaction was cleaned to free remove primers. About 3 µg of cleaned product was then digested with 0.15 unit of DNase I (Gibco) in 100 µl 50 mM Tris-HCl pH 7.5, 1 mM $MgCl_2$ for 15 minutes at 20°C. The 100-300 bp cleavage fragments were isolated by electrophoresis in a 2% agarose gel. The fragments were cleaned with GENECLEAN®, and then subjected to a PCR-like reaction without primers. Briefly, 25 ng DNA fragments, 0.2 mM of each dNTP, 1.5 mM $MgCl_2$ and 1 unit *Taq* DNA polymerase in 50 µl of the supplied buffer was mixed in a 0.5 ml microcentrifuge tube. The mixture was overlayed with 40 µl mineral oil and heated to 94°C in the thermal cycler for 30 seconds. The mixture was then subjected to 35 cycles, including a 30 seconds denaturing step at 94°C, a 30 seconds annealing step at 50°C, and an primer extension step at 72°C for 45 seconds. The tube was exposed to a final primer extension step of 7 minutes at 72°C, before the reaction was stopped by cooling to 4°C. This primerless PCR product was either stored at 4°C until use, or used immediately as template in the next PCR reaction. A 1:40 dilution of this product was used as template in a normal PCR reaction as described above.

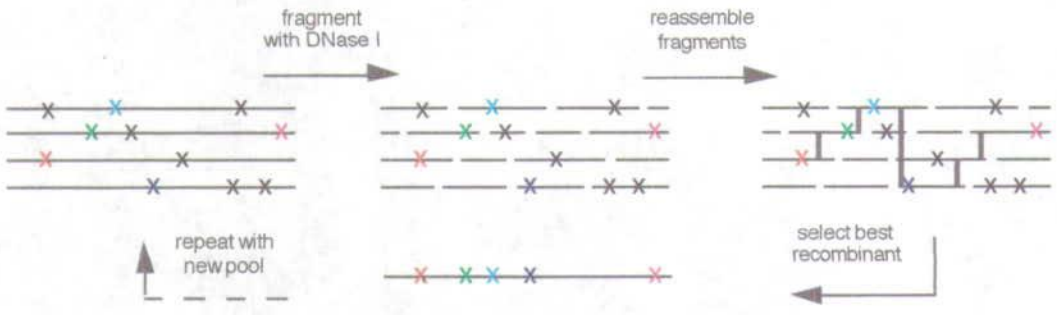

Figure 2.1. Principle of DNA shuffling by random fragmentation and reassembly (adapted from Stemmer, 1994a).

A couple of concluding remarks must include the finding that sufficient dilution of the fragments appeared to be crucial for the success of the technique. Furthermore, the

reaction without primers did not generate enough product to be visualised by EtBr on an agarose gel, but the next reaction with added primer did. Finally, multiple successive shuffles required cloning in between each shuffle, or loss of a uniform product resulted.

2.1.3. DNA sequencing

2.1.3.1. Manual DNA sequencing

All constructed single mutations and hybrid enzymes were sequenced manually to confirm the mutations and to ensure that no secondary mutations had occurred. The "Sequenase™ Version 2.0 DNA Sequencing Kit" from United States Biochemical was employed to determine the DNA sequences. Single stranded pGR401 plasmid DNA was used as template in the reaction and was essentially prepared as already described in section 2.1.1.1 (p. 31), the only differences being that TG1 was used as host cell instead. The sequencing reaction consisted of an initial annealing reaction, followed by the [^{35}S]-labelling reaction, and finally the termination reaction. All steps were performed as recommended in the 9th edition of the protocol for Sequenase. The reaction products were separated by denaturing gel electrophoresis. The gel was 6% in acrylamide (stock solution was 30:0.8), contained 7 M urea, and was run at 60 mA for 1.5-3 hours. The run gel was washed 15 minutes to remove urea, dried completely in a geldryer, and then exposed with direct contact between film and gel.

2.1.3.2. Automatic DNA sequencing

Automatic DNA sequencing was used to determine the level of mutation generated by random mutagenesis by PCR. The samples for sequencing analysis on an ABI377 instrument (Perkin Elmer) was basically performed as described in revision A (August 1995) of the protocol for "ABI PRISM™ Dye Terminator Cycle Sequencing Ready Reaction Kit". The cycle sequencing reaction demanded highly pure plasmid DNA, and this was prepared using the "QIAprep kit" from QIAGEN. The reaction mixture included 8 µl Terminator Mix, 400 ng DNA, and 3.2 pmol primer in a total volume of 20 µl overlayed with 40 µl mineral oil in a 0.5 ml microcentrifuge tube. The tube was placed in the thermal cycler, which was programmed to heat the mixture to 96°C for 30 seconds, then cool it to 50°C for 15 seconds and finally heat it to 60°C for 4 minutes. The programme was repeated 25 times, before cooling the sample to 4°C. The extension products were then purified according to the protocol. Briefly, the reaction mixture was transferred to another tube, added 2 µl 3 M NaOAc pH 4.6, and 50 µl

95% EtOH. The tube was vortexed, placed on ice for 10 minutes, and centrifuged at maximum speed in a microcentrifuge for 15 minutes. The supernatant was carefully removed, the pellet was then washed with 0.5 ml 70% EtOH, and finally dried in a vacuum centrifuge. The dried pellet was stored in the dark at -20°C until analysed by Ms. N. Preston.

2.1.4. Cloning in plasmid vectors

2.1.4.1. Preparation of plasmid DNA

The plasmid DNA used for most cloning purposes was prepared by the standard SDS-alkaline lysis method as described by Sambrook *et al.* (1989c). The DNA purified from a 5 ml overnight culture was generally redissolved in 50 µl water, and used without removal of RNA prior to restriction enzyme cleavage. The plasmid DNA used as template in the polymerase chain reaction (including the reaction for automatic fluorescent sequencing) demanded highly pure DNA as template, and this plasmid DNA was instead prepared using the "QIAprep kit" from QIAGEN. Occasionally, when larger quantities of plasmid DNA were needed, either for partial digests or because of low copy numbers, this was prepared by the caesium chloride - ethidium bromide gradient technique (Sambrook *et al.*, 1989c).

2.1.4.2. Restriction enzyme digest

The digestion of DNA with restriction enzymes was performed according to manufacturers instructions (Doyle, 1996). The restriction enzymes were supplied by Promega, New England Biolabs, Northumbria Biologicals Ltd. or GIBCO BRL. The RNA present in the plasmid preparations was removed by addition of minute amounts of DNase-free RNase (Sambrook *et al.*, 1989a) to the restriction enzyme reaction. The PCR products were always purified prior to restriction using the "GENECLEAN® III Kit" from BIO 101.

Double digests, involving two restriction enzymes, were often done by adding the enzymes simultaneously to the reaction mixture. However, the two enzymes would occasionally only work in incompatible buffers, and the digests were then done in a stepwise manner, purifying the DNA using the "GENECLEAN® III Kit" in between.

Partial digests were optimised in time course experiments with diluted enzyme. The results were analysed by gel electrophoresis and then scaled up accordingly.

2.1.4.3. Addition of bases to 3'-hydroxyl terminus

The site of a restriction enzyme generating 5'-overhang was removed by filling-in and re-ligating the DNA. The DNA was first digested with the enzyme in question, isolated and cleaned. The DNA was then added bases to the 3'-hydroxyl terminus by incubating 1 µg DNA with 0.08 mM of each dNTP and 2 unit Klenow fragment in 25 µl nick translation buffer (0.5 M Tris-HCl pH 7.5, 0.1 M $MgSO_4$, 1 mM DTT and 500 µg/ml BSA) for 45 minutes at 37°C. The reaction was stopped by heating the mixture to 70°C for 5 minutes. The DNA with blunt ends was finally used in a ligation reaction as described below.

2.1.4.4. Conversion of restriction sites

Restriction sites were converted into alternative sites by the use of adapters. Briefly, the DNA was digested with the restriction enzyme in question, phosphorylated oligonucleotides were then added, and annealed to the DNA. The product of the annealing reaction was ligated and transformed into *E. coli*. The conversion was confirmed by appropriate restriction reactions.

2.1.4.5. Ligation

The DNA fragments were ligated together using T4 DNA ligase from Boehringer Mannheim, and performed according manufacturers recommendations. Briefly, the DNA fragments were isolated by gel electrophoresis. The fragments were then purified using GENECLEAN® and eluted into water. The molar ratio of vector DNA to insert DNA was generally 1:3. The reaction was performed in 10 µl of the supplied reaction buffer, incubated overnight at 16°C or a couple of hours at room temperature, and then transformed into *E. coli*.

2.1.4.6. Transformation

The plasmid DNA was transformed into competent cells of *E. coli*. The competent cells were prepared either by the calcium chloride procedure as described by Sambrook *et al.* (1989c) or according to Doyle (1996) using rubidium chloride. The cells were preferably prepared fresh, but any surplus was stored at -80°C in 15% glycerol for later use. The competent cells were mixed with about 10 ng DNA (up to 5 µl DNA solution per 100 µl cells) in an eppendorf tube, and incubated on ice for 30 minutes or longer. The tube was then heated to 42°C in a waterbath for one minute, and placed back on ice to cool for 3 minutes. One ml Luria broth was added, before incubating the

tube with shaking for one hour at 37°C. Finally, the transformation mixture was plated onto selection plates.

2.1.5. Genetic manipulation of *E. coli*

2.1.5.1. Deletion and gene replacement

The mutation in the gene encoding L-lactate dehydrogenase in *E. coli* was performed as described by Hamilton *et al.* (1989). The constructed derivative of suicide plasmid pMAK705 is described in the results section (Section 6.2.1, p. 102). Basically, a kanamycin cassette was inserted into the *lctD* gene, which was then cloned in the suicide plasmid. This plasmid contained a thermosensitive origin of replication, and thus replicated at 30°C but not at 44°C. It was hence forced to recombine with the chromosome, when transformants were grown at 44°C under selection for the chloramphenicol resistance encoded on the plasmid. The cointegrates were subsequently resolved by a second recombination event taking place after growth at 30°C. Depending on the site of the second recombination event, the kanamycin resistance casette had either been inserted into the chromosome or reappeared on the plasmid (Figure 2.2).

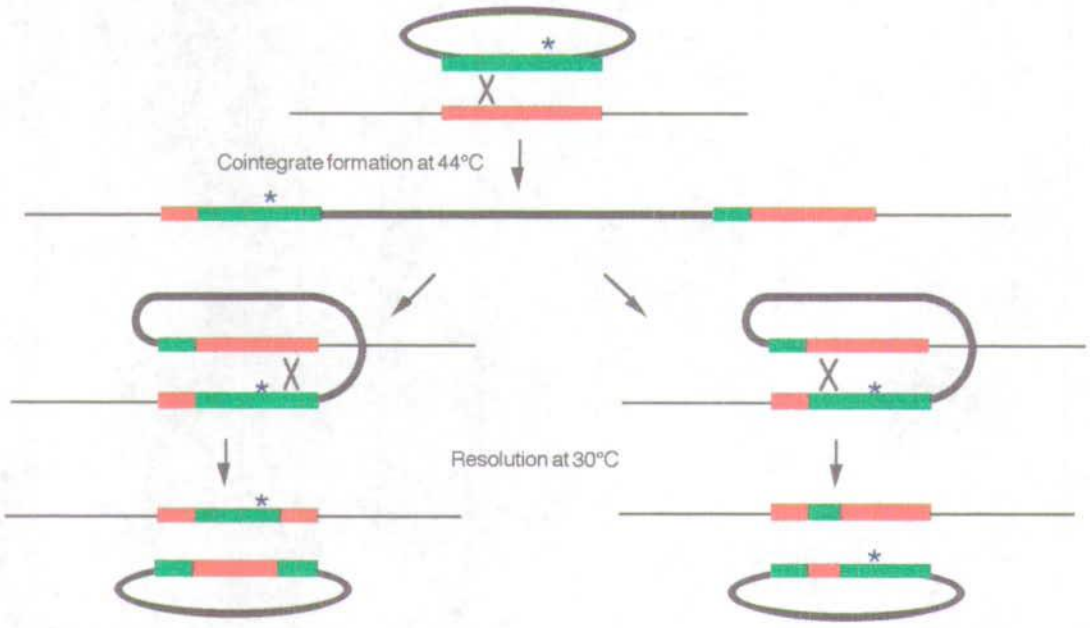

Figure 2.2. General strategy for the gene replacement method. The marker (*) will either remain in the chromosome or reappear on the plasmid depending on the second recombination event.

The plasmid was easily cured from the strain by growing the cells at 44°C with kanamycin but without chloramphemicol. The addition of kanamycin to the culture resulted in growth of the null strain only, and naturally made the identification of these very easy. The genotype of the strain was confirmed by Southern blotting (Southern, 1975).

2.1.5.2. Southern blotting

Genomic DNA was prepared from cell of a 5 ml overnight culture resuspended in 400 µl of 10 mM EDTA pH 8.0 (Mejean *et al.*, 1994). The cells were lysed by addition of 8 µl of 10%(w/v) SDS. The DNA was then purified by extraction with equal volumes of phenol, followed by phenol:chloroform:isoamylalcohol (25:24:1), and finally chloroform. The aqueous phase was treated with RNase, before precipitation from 0.3 M NaOAc with isopropylalcohol. The DNA was redissolved in 50 µl water, and then digested with appropriate restriction enzymes. The DNA fragments were separated by gel-electrophoresis and transferred to nitro-cellulose by capillary transfer (Sambrook *et al.*, 1989b). The DNA was subsequently cross-linked to the membrane in a UV-cross-linker.

The hybridisation reaction itself was performed as described by (Sambrook *et al.*, 1989c) in a hybridisation oven (Techne Hybridiser HB-1D). The probe used for hybridisation was radio-labelled with [α-^{32}P]dCTP using the random primers DNA labeling system from Life-Technologies. The recommended protocol was essentially followed. About 75 ng DNA was denatured by boiling for 5 minutes, and then added of 2 µl of each dNTP (except dCTP), 15 µl random primer buffer mix (0.67 M HEPES, 0.17 M Tris-HCl, 17 mM $MgCl_2$, 33 mM 2-mercaptoethanol, 1.33 mg/ml BSA), 5 µl [α-^{32}P]dCTP (about 50 µCi) and 3 U Klenow fragment in a total volume of 50 µL. The mixture was incubated for one hour at 25°C. The labelling reaction was stopped by addition of 5 µl stop buffer (0.2 M Na_2EDTA pH 7.5).

2.1.5.3. Transduction with P1

Tranduction using P1*kc* was achieved in two stages (Miller, 1992). A P1 lysate was made on the donor strain, resulting in the packaging of host DNA in a small proportion of phage heads. Briefly, the lysate was made by mixing 1 ml of donor strain at OD_{600} = 1 with 10^5-10^6 P1, and incubating this mixture at 37°C for 15 minutes. The cell are added 3 ml Luria broth and 3 ml LC top agar. All solutions were 25 mM in $CaCl_2$. The cells were then poured onto a Luria broth agar plate, and incubated non-inverted overnight at 37°C. The top agar was scraped off, added 0.5 ml chloroform,

and left shaking for 20 minutes at 30°C. The lysate was subsequently separated from the agar by centrifugation and stored at 4°C.

The recipient was then transduced by growth with the phage and selection for recombinants. The transduction was performed on a recipient strain at OD_{600} = 1. The cells were isolated by centrifugation and resuspended in 0.1 volume of Luria broth including 2.5 mM $CaCl_2$. Aliquots of 0.1 ml cells were incubated with several different amounts of P1 lysate (0, 1, 10, and 100 µl) at 37°C for 15 minutes. The cells were then added 1 ml phage buffer, pelleted in a centrifuge, and resuspended in 100-200 µl of the supernatant. Finally, the cells were spread onto appropriate plates.

2.1.5.4. Preparation of λDE3 lysogens

Phage λDE3 (Studier & Moffatt, 1986) contains the T7 gene *1*, encoding T7 RNA polymerase, inserted in the *int* gene of the phage λD69 vector. Hence, λDE3 needs a helper for either integration into or excision from the chromosome. λDE3 was isolated from a culture of BL21(DE3) by Dr. G. King in the laboratory of professor N. Murray (King & Murray, 1995). Lysogens of λDE3 were prepared by co-infecting 200 µl plating cells with λDE3 (imm^{21}) and λNM75 ($\lambda imm^{21} int^{+} xis^{+}$) in the top layer of BBL-agar at a moi ~10. Lysogens were then selected by streaking on L-agar seeded with two homo-immune λ*c*I phages of different host ranges (~10^9 pfu λNM507 and a derivative with the host range ϕ80 (λNM508; λ*imm21c*I). Lysogens were re-streaked to purify and the immunity confirmed by their sensitivity to λ*vir*, but not λimm^{21} phages. Monolysogens were confirmed by their sensitivity to λ*c*I, and these imm^{21} hosts were presumed to have been lysogenised by λDE3. All phages were most kindly provided by Professor N. Murray.

2.2. Protein Chemistry Techniques

2.2.1. Purification of glycolate oxidase

2.2.1.1. Expression in E. coli

The *E. coli* strain BL21(DE3)/pLysS transformed with the plasmid pPM1 was used for expression of glycolate oxidase (Macheroux *et al.*, 1992). The plasmid pPM1 is derived from pET-3d (Studier *et al.*, 1990), and expression is thus under control of the T7 RNA polymerase promoter. Active T7 RNA polymerase is delivered by induction

of a chromosomal copy of gene *1* under control of the *lac*UV5 promoter. Furthermore, BL21 is deficient in the lon protease, and also lacks the ompT outer membrane protease. The plasmid pLysS express low levels of T7 lysozyme, which binds to T7 RNA polymerase and essentially inhibits transcription until induction with IPTG. The presence of pLysS also has the advantage of facilitating preparation of cell extracts, as the resident lysozyme lyses the cells upon freezing and thawing.

A starter culture of 5 ml Luria broth, containing 100 µg/ml ampicillin and 50 µg/ml chloramphenicol, was inoculated from a single colony on Luria agar plates and grown overnight at 37°C. This culture was used to inoculate five 2 litre flasks, each containing 1 litre of Luria broth, 100 µg/ml ampicillin and 50 µg/ml chloramphenicol, and grown to an OD_{600} of 0.9. The expression of glycolate oxidase was then induced by addition of 50 µM IPTG, and growth continued overnight. The cells were harvested by centrifugation at 8,000 rpm for 20 minutes using a GS3 rotor head, and the pellets were stored at -80°C until used for purification. The yield was typically around 20 g cells wet mass per 5 litre cell culture.

2.2.1.2. Preparation of cell lysate

The thawed cells were resuspended in 100 ml of 100 mM Tris-HCl buffer pH 8.3, containing 1 mM EDTA, 10 µM PMSF and 20 µM FMN, using a homogeniser. Aliquots of 25 ml cell extract were then sonicated for three times 20 seconds with 30 second intervals to allow cooling of the suspension using bath of mixed ice, ethanol and sodium chloride. This step reduced the viscosity of the suspension due to DNA, and eased the subsequent handling greatly. The cell debris was removed by centrifugation at 18,000 rpm for 20 minutes at 4°C using a SS34 rotor head. All subsequent steps in the purification of glycolate oxidase were also conducted at 4°C.

2.2.1.3. Ammonium sulphate fractionation

The proteins in the supernatant were fractionated by precipitation with ammonium sulphate added to 50% saturation. The soluble fraction was separated from the precipitate by centrifugation at 18,000 rpm for 20 minutes. Glycolate oxidase was present in the pellet, which was redissolved in a minimum volume of 10 mM Tris-HCl buffer pH 8.3 containing 1 mM EDTA, 10 µM PMSF and 5 µM FMN. The solution was then dialysed overnight at 4°C against 2 litres of the same buffer to remove ammonium sulphate and other small contaminants. The dialysate was finally centrifuged at 18,000 rpm for 20 minutes using a SS34 rotor head before being subjected to further purification.

2.2.1.4. Anion exchange chromatography

The principle of anion exchange chromatography is based on electrostatic forces between proteins' surface charges and charged groups on the exchanger. The anion exchanger used is diethylaminoethyl-cellulose (Whatman® DE52), which is positively charged when equilibrated at pH 8.3. Glycolate oxidase has an isoelectric point of 9.16, and will thus be positively charged at pH 8.3 as well. However, the majority of contaminating proteins will be negatively charged and hence stick to the exchanger. The anion exchange column (2.5 cm x 25.0 cm) was prepared by equilibrating the material with 10 mM Tris-HCl buffer pH 8.3. The dialysate was then loaded on the column, and glycolate oxidase was eluted by continuing to wash the column with 10 mM Tris-HCl buffer pH 8.3. The active fractions were pooled and loaded directly onto a column of hydroxyapatite. The column material was recycled several times by treatment with 100 ml of 0.5 M HCl, followed by 100 ml of 0.5 M NaOH, and finally neutralised with Tris-HCl buffer pH 8.3.

2.2.1.5. Hydroxyapatite chromatography

Hydroxyapatite (BIO-RAD), consisting of crystalline particles of $Ca_{10}(PO_4)_6(OH)_2$, was used for selectively adsorbing glycolate oxidase. Basic proteins bind through PO_4^{n-} sites, whereas acidic proteins are adsorbed by Ca^{2+} sites on the crystal surfaces (Scopes, 1987). The column (2.5 cm x 10 cm) was equilibrated with 10 mM phosphate buffer pH 8.3, and then the pooled fractions from the anion exchange chromatography were loaded. The bound proteins were eluted by a linear gradient of phosphate buffer pH 8.3 from 10 mM to 300 mM in a total volume of 400 ml. Glycolate oxidase eluted at about 150 mM phosphate buffer. Fractions were considered pure and pooled, if the ratio of A_{274}/A_{448} was less than 8.8. The purified glycolate oxidase was concentrated by precipitation with ammonium sulphate at 80% saturation, redissolved in a minimal volume of 10 mM Tris-HCl buffer pH 8.3 (I = 0.1M), and gelfiltred on a column (1 cm x 30 cm) of Sephadex G-25 to remove the ammonium sulphate. The pure protein was stored in liquid nitrogen (-194°C) until used. The yield was typically around 7.5 mg from 20 g of cells. The concentration of enzyme was determined by the absorbance at 448 nm (ε = 9,200 $M^{-1}cm^{-1}$ for oxidised glycolate oxidase; Macheroux *et al.*, 1991).

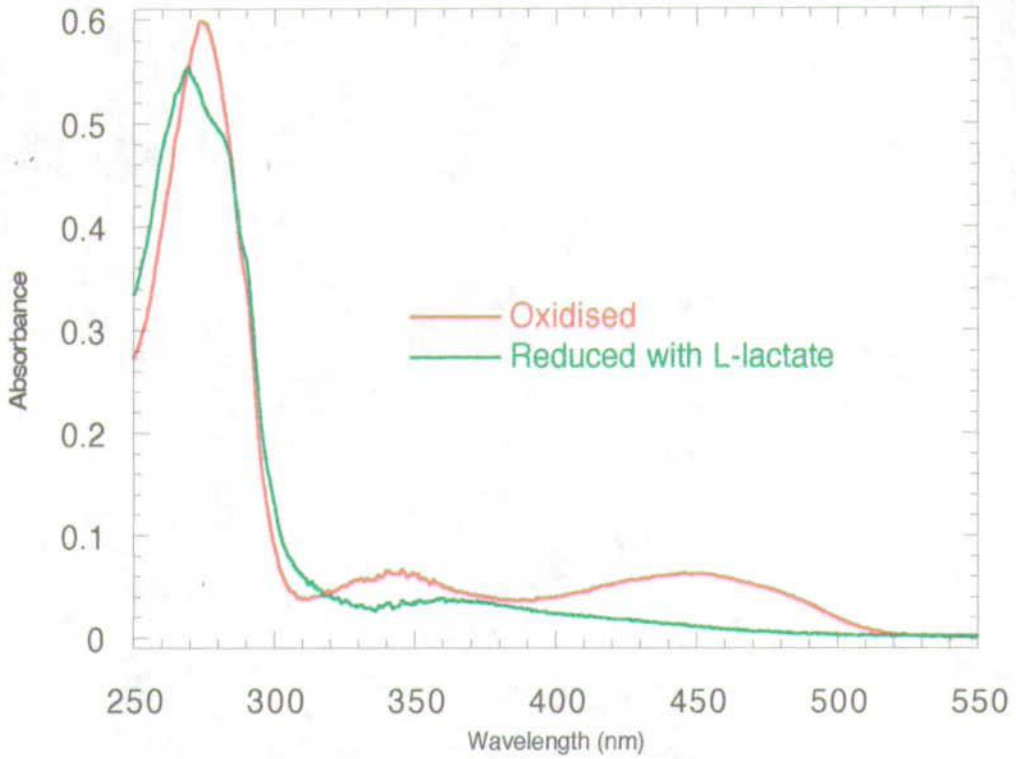

Figure 2.3. Absorption spectrum of 6.7 μM glycolate oxidase in 10 mM Tris-HCl buffer pH 7.5 (I = 0.1M) recorded at 25°C in a 1 cm cuvette.

2.2.2. Purification of the flavin-binding domain of flavocytochrome b_2

2.2.2.1. Expression in E. coli

The flavin-binding domain had already been cloned into expression vector pRC23 (Crowl *et al.*, 1985) by introducing an initiation codon and an *Eco*RI cleavage site immediately upstream of the sequence encoding residues 101-511 of flavocytochrome b_2 (Pallister *et al.*, 1990). The expression vector, pRC23, is based on the P_L promoter of bacteriophage λ. The host, pop2136 or NF1, contains the thermosensitive *cI*857 allele of the lambda repressor and allows induction by shifting to high temperatures. However, the levels of expression were quite low with yields around 1-5 mg pure enzyme per litre cell culture. This problem was partly due to difficulties in controlling the temperature, but also the nature of the mutant enzyme influenced the expression level. The level of expression was improved significantly by cloning the flavin-binding domain into the expression vector pJF118EH (Fürste *et al.*, 1986), and transforming the plasmid into TG1 for expression. This vector is based on the hybrid *tac* promoter, and is even more efficient than the *trp* promoter itself. The expression plasmid has the gene for the lac repressor (*lac*I^q) inserted to ensure tight regulation of expression. The

yields of pure enzyme observed were in the range 50-100 mg per litre, all mutant enzymes were compatible with the expression vector and expressed a lot more consistently.

A 5 ml starter culture of Luria broth, containing 100 µg/ml ampicillin, was inoculated from a single colony of pop2136/pRC23 on Luria agar plates and grown overnight at 30°C. The starter culture was used to inoculate five 2 litre flasks each containing 1 litre of Luria broth and 100 µg/ml ampicillin. The cultures were grown at 30°C until an OD_{600} of 0.6, when the temperature was shifted to 41°C. Growth was continued overnight and the cells were then harvested by centrifugation at 8,000 rpm for 20 minutes using a GS3 rotor. The typical yield was around 20 g cells (wet mass). The cell were stored as pellets at -80°C until used. Cell cultures transformed with the pJF118EH expression vector were prepared as above, but grown in Terrific broth at 37°C and induced in the mid-log phase with 1 mM IPTG instead. Furthermore, the cell cultures were grown in 500 ml broth per 2 litre flask to ensure sufficient aeration. Only two litres were prepared of these cell cultures, thus adjusting the amount of protein expressed to the capacity of the columns used. The yield of cells was generally around 10 g wet weight per litre culture

2.2.2.2. Preparation of cell lysate

The thawed cells were resuspended in 100 ml of 10 mM phosphate buffer pH 7.0 containing 10 µM PMSF using a homogeniser. Aliquots of 25 ml cell extract were then sonicated three times for 20 seconds, and allowed to cool in the 30 second interval on a bath of mixed ice, ethanol and sodium chloride. The lysate finally was centrifuged at 18,000 rpm for 20 minutes using a SS34 rotor head. The supernatant contained the soluble proteins and also the ferricyanide reductase activity. All subsequent operations were conducted at 4°C, and the purification was generally done in less than 6 hours from this point in order to minimise the loss of flavin co-factor.

2.2.2.3. Anion exchange chromatography

The DEAE column (2.5 cm x 25.0 cm) was prepared by equilibrating the column material with 10 mM phosphate buffer pH 7.0. The flavin-binding domain has an isoelectric point of 6.28 and will be negatively charged at pH 7.0. Hence, the flavin-binding domain binds the exchanger and has to be eluted by increasing salt concentrations. The cell lysate was diluted two-fold with 10 mM phosphate buffer pH 7.0 containing 10%(w/v) glycerol, thus lowering the ionic strength to ensure binding of flavin-binding domain to the exchanger. The addition of glycerol stabilised the

enzyme (Figure 2.4) by reducing the water activity, and thus mimicking the conditions in the cell cytoplasm. The column was washed with 100 ml of 10 mM phosphate buffer pH 7.0 containing 10%(w/v) glycerol. The bound proteins were eluted by a step-gradient of phosphate buffers. The buffer concentration was increased successively by adding 50 ml of 25, 50, 62.5, 75, 87.5 and finally 100 mM buffer containing 10%(w/v) glycerol to the column. The mutant enzymes of the flavin-binding domain generally began to elute at 75 mM. The protein was visible due to the bright yellow colour of oxidised FMN. However, the absorption spectra of the catalytically active fractions were always recorded to avoid haem-binding proteins. The ferricyanide reductase active fractions were pooled, if they contained significant amounts of flavin but no haem.

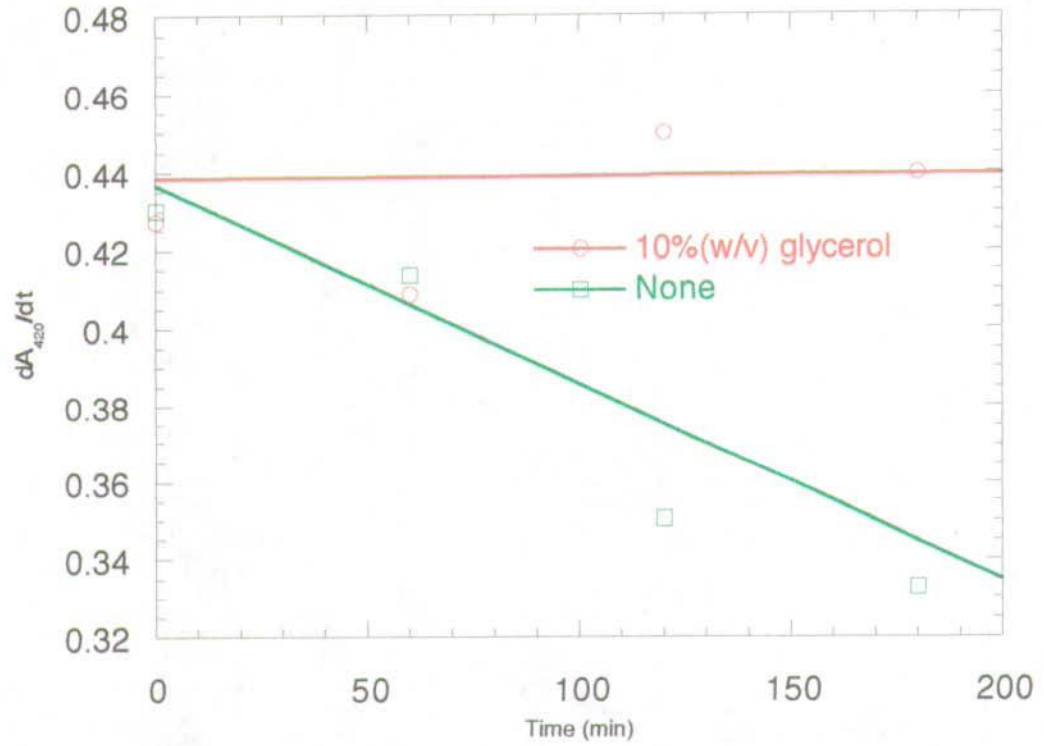

Figure 2.4. Effect on activity of incubating enzyme on ice in buffer with or without 10%(w/v) glycerol. Assays were performed by addition of 0.08 μM enzyme to 10 mM Tris-HCl buffer pH 7.5 (I = 0.1 M) including 10 mM L-lactate and 2 mM ferricyanide. The change in absorbance at 420 nm was monitored using a 1 cm cuvette.

2.2.2.4. Hydroxyapatite chromatography

A column (2.5 cm x 10.0 cm) of hydroxyapatite was prepared as described previously. The pooled fraction from above was diluted two-fold with 10 mM phosphate buffer pH 7.0 containing 10%(w/v) glycerol and then loaded on the column. The column was washed with 10 mM phosphate buffer pH 7.0 containing 10%(w/v) glycerol until all unbound protein had been removed. The flavin-binding domain was eluted by adding

25 ml of each 100, 150, 200 and 400 mM phosphate buffer pH 7.0 containing 10%(w/v) glycerol. The active fractions with a ratio of A_{280}/A_{460} = 8.56 were considered pure and pooled. The pooled fractions were precipitated by addition of ammonium sulphate to 80% saturation, stirred until the ammonium sulphate was dissolved, and then centrifuged for 10 minutes at 18,000 rpm using a SS34 rotor head. The supernatant was discharged, while the yellow pellet was redissolved in a minimum volume of 10 mM Tris-HCl buffer pH 7.5 (I = 0.1M) containing 10%(w/v) glycerol. The solution was gel filtered on G25 Sephadex to remove the ammonium sulphate, and finally stored in liquid nitrogen until use. The protein concentration was estimated by the change in absorption at 454 nm upon reduction with L-lactate (ε^{ox}=11,100 $M^{-1}cm^{-1}$, ε^{red}=1,100 $M^{-1}cm^{-1}$, and $\Delta\varepsilon^{(ox-red)}$=10,000 $M^{-1}cm^{-1}$; Iwatsubo *et al.*, 1977).

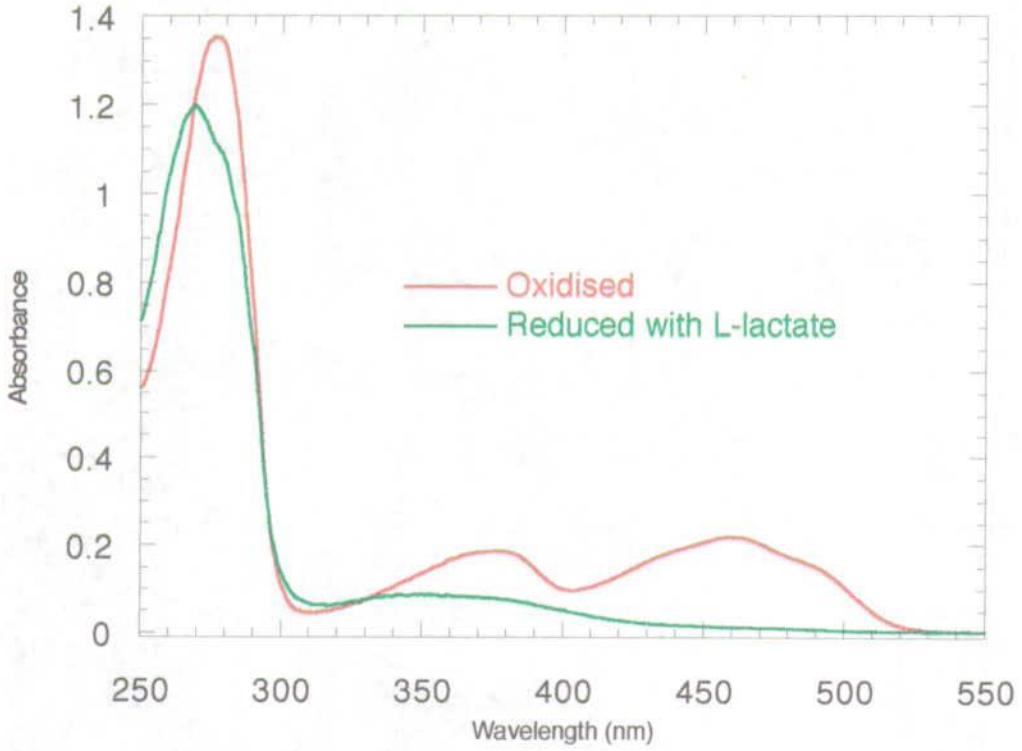

Figure 2.5. Absorption spectrum of 20 μM flavin-binding domain of flavocytochrome b_2 in 10 mM Tris-HCl buffer pH 7.5 (I = 0.1 M) recorded at 25°C using a 1 cm cuvette.

2.2.3. Purification of flavocytochrome b_2

2.2.3.1. Expression in E. coli

Flavocytochrome b_2 was expressed in the *E. coli* strain TG1 using the expression vector pDSb2 (Black *et al.*, 1989). A 5 ml starter culture of Luria broth, containing 100 μg/ml ampicillin, was inoculated from a single colony on Luria agar plates and grown overnight at 37°C. Five 2 litre flasks, each containing 1 litre of Luria broth and

100 µg/ml ampicillin, were inoculated from the starter culture. The cultures were grown overnight at 37°C, and then harvested by centrifugation at 8,000 rpm for 20 minutes using a GS3 rotor head. The typical yield was around 20 g cells (wet mass). The cell were stored as pellets at -80°C until used.

2.2.3.2. Preparation of cell lysate

The cell lysate was prepared as when purifying the flavin-binding domain. The resulting lysate was visibly coloured red by the flavocytochrome b_2 in solution.

2.2.3.3. Anion exchange chromatography

The lysate was loaded directly on a column (2.5 cm x 25.0 cm) of DEAE pre-equilibrated in 10 mM phosphate buffer pH 7.0. Flavocytochrome b_2 has an isoelectric point of 6.38 and therefore sticks to the anion exchanger. The column was washed with 100 ml of 10 mM phosphate buffer pH 7.0. The bound proteins were eluted by successively adding 25 ml phosphate buffers of increasing concentration. The concentration of the buffer was increased in steps of 25 mM starting at 25 mM. Flavocytochrome b_2 was eluting around 75 mM. The fractions with ferricyanide reductase activity were pooled, if they contained significant amounts of flavocytochrome b_2 as judged by the absorption at 412 nm.

2.2.3.4. Hydroxyapatite chromatography

The pooled fractions were diluted two-fold and loaded onto a column (2.5 cm x 10.0 cm) of hydroxyapatite equilibrated in 10 mM phosphate buffer pH 7.0. The column had been prepared as described previously. The loaded column was washed with 10 mM phosphate buffer pH 7.0. The bound proteins were eluted by a step-gradient. The salt concentration was increased by addition of ammonium sulphate, thus increasing the level of saturation by 1% in the 12.5 ml of phosphate buffer pH 7.0 successively added. Flavocytochrome b_2 began eluting at 4% saturation. The pooled pure fractions of flavocytochrome b_2 were added ammonium sulphate to 80% saturation, stirred until the ammonium sulphate was dissolved, and then centrifuged for 10 minutes at 18,000 rpm using a SS34 rotor head. The supernatant was discarded, while the red pellet was redissolved in a minimum volume of 10 mM Tris-HCl buffer pH 7.5 (I = 0.1M). The solution was gel filtered on G25 Sephadex to remove the ammonium sulphate, and finally stored in liquid nitrogen until use. The concentration of enzyme was determined by the aborbance of the Soret peak at 423 nm (ε_{423}=183,000 $M^{-1}cm^{-1}$ for reduced flavocytochrome b_2; Pajot & Groudinsky, 1970).

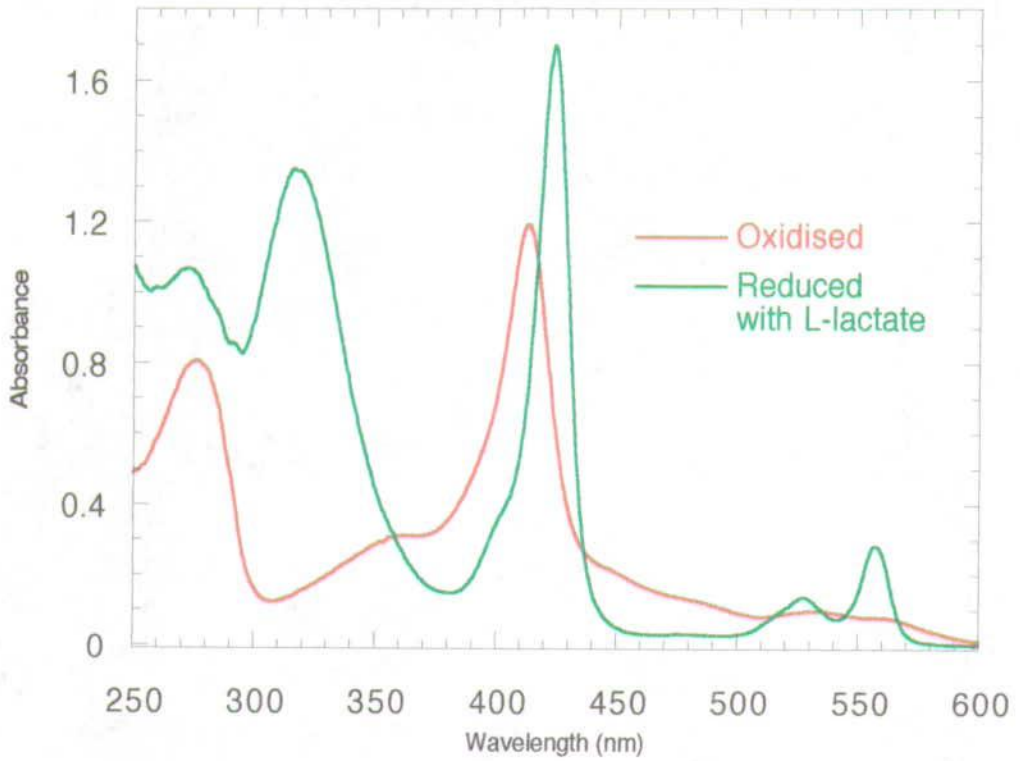

Figure 2.6. Absorption spectrum of 9.2 μM flavocytochrome b_2 in 10 mM Tris-HCl buffer pH 7.5 (I = 0.1 M) recorded at 25°C using a 1 cm cuvette.

2.2.4. Steady-state kinetics

The Michaelis-Menten equation applies for enzyme-catalysed reactions in steady-state and may be written as:

$$v = \frac{k_{cat}[E_0][S]}{K_m + [S]}$$

$$= \frac{V_{max}[S]}{K_m + [S]}$$

where

v	rate
k_{cat}	limiting rate constant
$[E_0]$	enzyme molarity
$[S]$	substrate concentration
K_m	Michaelis constant
V_{max}	limiting rate

Equation 2.1. The Michaelis-Menten equation.

The constant k_{cat} has the properties of a first-order rate constant and defines the capacity of the enzyme-substrate complex, once formed, to form product. The specificity constant is given by $k_A = k_{cat}/K_m$. Its value is the apparent rate constant for combination of a substrate with the free enzyme and is the most critical parameter in

determining the specificity of an enzyme for a substrate. It cannot be greater than the diffusion limit of about 10^9 $s^{-1}M^{-1}$. The value relates directly to the free energy of the enzyme transition state relative to that of free substrate and enzyme (Creighton, 1993). The effect of a mutation on the energy of transition state may thus be expressed as:

$$\Delta\Delta G^{\neq} = -RT\ln\left(\frac{k_A(\text{mutant enzyme})}{k_A(\text{WT enzyme})}\right)$$

where $R = 8.31441\ JK^{-1}mol^{-1}$
$T = 298.15\ K\ (25°C)$

Equation 2.2. Effect of a mutation on the energy of transition state.

The enzyme assays, used for determination of the steady-state kinetic parameters, were conducted on a Shimadzu 2101PC spectrophotometer. All experiments were performed at 25°C in 10 mM Tris-HCl buffer pH 7.5 adjusted to $I = 0.1$ M by addition of NaCl, unless otherwise stated. The observed initial rate data, dA/dt (min^{-1}), were converted into moles of electron acceptor reduced by one mole enzyme per second according to Equation 2.3.

$$k_{obs}(\text{moles acceptor/mole enzyme/sec}) = \frac{dA/dt(min^{-1}) \times v_t(l)}{60(sec/min) \times \varepsilon(M^{-1}cm^{-1}) \times l(cm) \times v_E(l) \times c_E(M)}$$

where
- k_{obs} rate constant
- dA/dt observed rate
- v_t total volume in cuvette
- ε molar absorption coefficient
- l cuvette pathlength
- v_E volume of enzyme stock solution added
- c_E concentration of enzyme stock solution

Equation 2.3. Formula used for calculation of the initial rate constant during steady-state turn-over. The units used are given in brackets.

The calculated values were fitted by non-linear least squares regression to the theoretical hyperbolic curve of the Michaelis-Menten equation. The curve fitting was performed using the Macintosh platform based software KaleidaGraph™ from Abelbeck Software. The deviation from the theoretical curve was checked by plotting the residuals of y against x. These were randomly distributed around the x-axis, and it was thus evident that the data fitted the chosen Michaelis-Menten equation. The errors in K_m given are the standard deviations from least squares fitting, and errors in k_{cat} are standard deviations from multiple assays at saturating substrate concentration ($10xK_m$).

2.2.4.1. Oxidase activity

2.2.4.1.1. Pyruvate production

The oxidation of L-lactate was accompanied by a change in absorbance and could be followed directly in a spectrophotometer. The oxidation of lactate converts the alcohol to a carbonyl group in pyruvate. This carbonyl function is capable of electronic transition, whereby electrons are excited by light in the ultraviolet region (Streitwieser & Heathcock, 1985). The lone-pair electrons on oxygen are excited to anti-bonding π^*-molecular orbitals by light with a wavelength of 315 nm (Figure 2.7). The absorption in the region around 200 nm results from the excitation of an electron from the bonding π-molecular orbital to the antibonding π^*-molecular orbital. These two transitions occur at relatively long wavelength (low energy), because the π-system is extended by conjugated double bonds in pyruvate. L-Lactate itself absorbs little light and only in the ultraviolet region with a maximum around 200 nm.

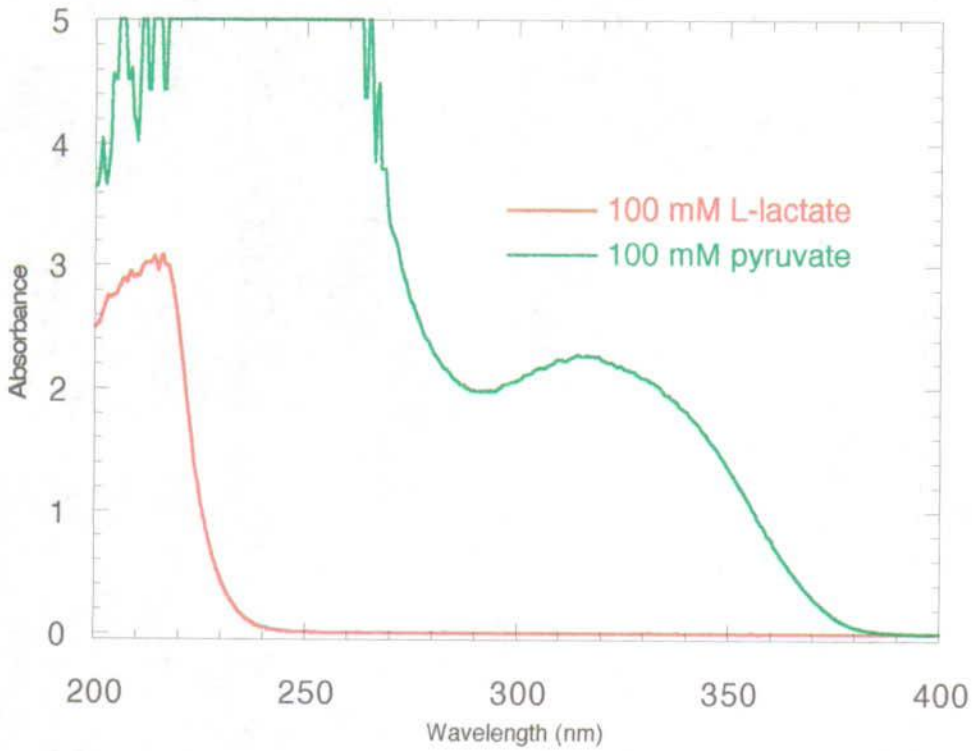

Figure 2.7. Absorption spectra of L-lacate and pyruvate dissolved in 10 mM Tris-HCl pH 7.5 (I = 0.1 M) recorded at 25°C using a 1 cm cuvette.

The absorption at 315 nm is far too low (ε_{315} = 22.6 $M^{-1}cm^{-1}$) for observing minute changes in the concentration of pyruvate. Instead, the absorption around 200 nm was used. The maximum change in absorption upon oxidation of lactate to pyruvate is observed at 205 nm ($\Delta\varepsilon$ = 1712.2 $M^{-1}cm^{-1}$). Wavelengths of light above 200 nm are

not absorbed by the oxygen in air, but the absorbance of the produced hydrogen peroxide had to be taken into account ($\varepsilon_{205} = 51.4\ M^{-1}cm^{-1}$).

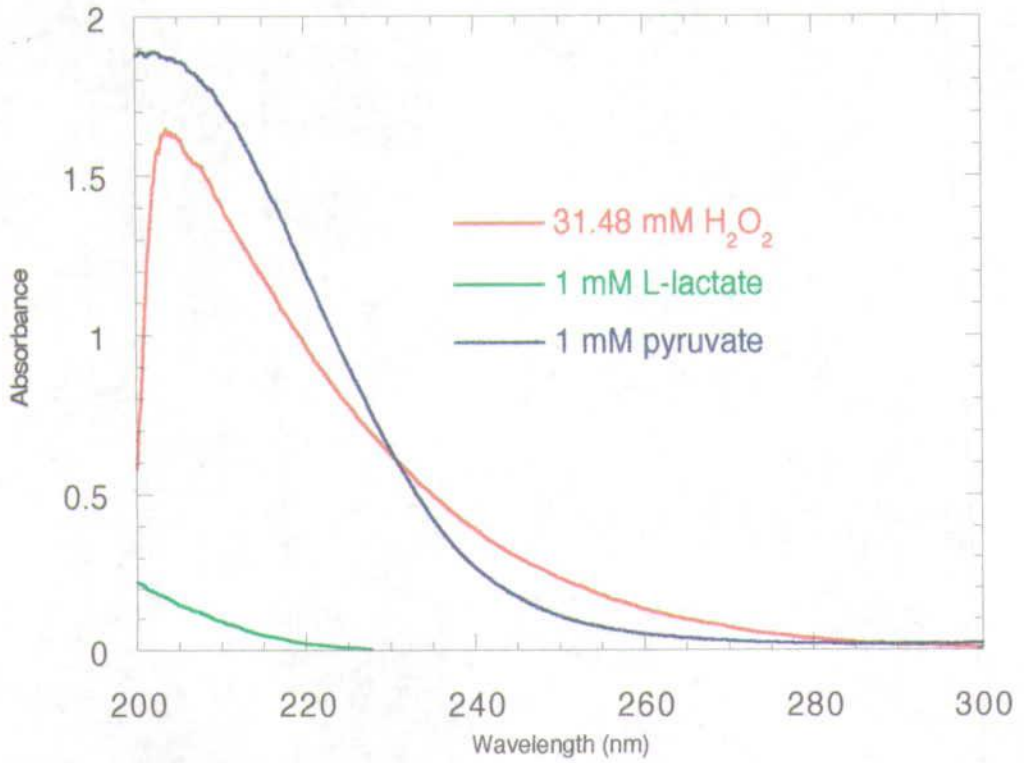

Figure 2.8. Absorption spectra of hydrogen peroxide, L-lactate and pyruvate in 10 mM Tris-HCl buffer pH 7.5 (I = 0.1 M) recorded at 25°C using a 1 cm cuvette.

2.2.4.1.2. Hydrogen peroxide production

Direct observation of the reaction catalysed by a poor oxidase would require large amounts of enzyme. The change in absorbance upon oxidation of lactate is simply too small to be of any practical use in such cases. The sensitivity may be increased considerably by following the production of hydrogen peroxide indirectly by coupling it to the reaction catalysed by horse radish peroxidase (Macheroux *et al.*, 1991).

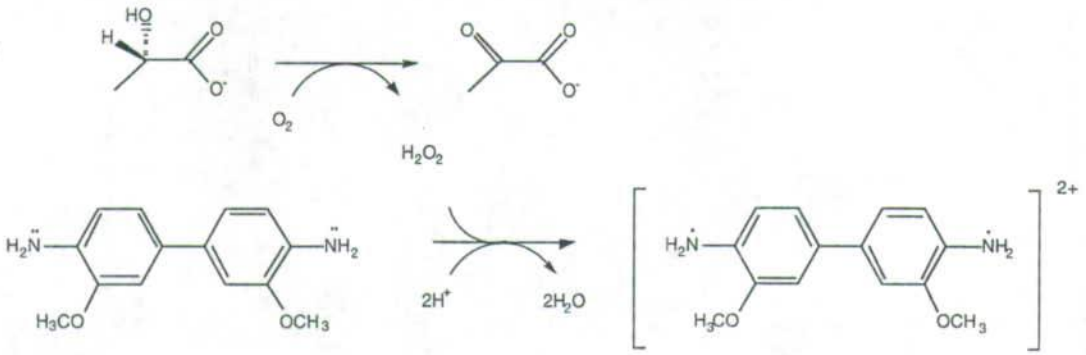

Figure 2.9. Coupling of 2-hydroxy acid-oxidation to the reaction catalysed by horse radish peroxidase.

The reaction was monitored by the formation of the *o*-dianisidine radical cation (Figure 2.9), which was followed by the change in absorbance at 440 nm (ε_{440} = 11,600 $M^{-1}cm^{-1}$). Provided that the activity of the coupling enzyme is high enough for the hydrogen peroxide to be reduced as fast as it is produced, the rate of *o*-dianisidine oxidation recorded in the spectrophotometer will correspond exactly to the rate of glycolate oxidation. The k_{cat} for horse radish peroxidase was found to be 735±21 s^{-1}, while K_m had a value of 0.15±0.01 mM. The amount of coupling enzyme, needed to result in a coupling rate after 0.5 minutes that is 98% of the true rate, was calculated according to Equation 2.4. This equation (Scopes, 1987) is based on the assumption that the concentration of hydrogen peroxide is much lower than the Michaelis constant of horse radish peroxidase for hydrogen peroxide. The calculated value is thus an approximation, and appropriate measures were taken to account for this. The actual concentration of coupling enzyme used was thus nearly ten-fold higher (0.25 µM), and the concentration of *o*-dianisidine was 0.4 mM. These theoretical considerations were naturally confirmed experimentally before application of the coupled assay for determination of kinetic parameters.

$$[E_{HRP}] = \frac{3.9 \times K_m^{HRP}}{30\ s \times k_{cat}^{HRP}} = \frac{3.9 \times 0.15\ mM}{30\ s \times 734.7\ s^{-1}} = 26.54\ nM$$

Equation 2.4. The concentration of coupling enzyme needed to obtain a rate after 30 s that is 98% of the true rate is given by the calculated value of $[E_{HRP}]$.

2.2.4.2. Dehydrogenase activity

2.2.4.2.1. Ferricyanide reduction

The flavin-binding domain does not transfer electrons to cytochrome *c* efficiently (Balme *et al.*, 1995). Hence, its L-lactate dehydrogenase activity was only measured using the artificial electron acceptor, ferricyanide (Figure 2.10). The reduction of ferricyanide was followed by the change in absorbance at 420 nm (ε_{420} = 1010 $M^{-1}cm^{-1}$). Since two electrons are produced per substrate molecule, the rates should be halved if required in terms of substrate. The concentration of ferricyanide used in the L-lactate dehydrogenase assay was ten-fold higher (or the highest feasible) than the value of the Michaelis-Menten constant for ferricyanide determined at saturating L-lactate levels. The rate would thus be 91% of the theoretical rate at infinite concentration of ferricyanide. Furthermore, consumption of ferricyanide during the assay or slight variation from one set of assay to another would make very little difference. The assay conditions ensured that the progress curves were virtually straight during the period of measurement. This was arranged by using lower enzyme

and higher initial substrate concentration so that less than 1% of the complete reaction was followed. The substrate concentrations used for measuring the initial steady-state rates generally fell in the range from $0.2xK_m$ to $10xK_m$.

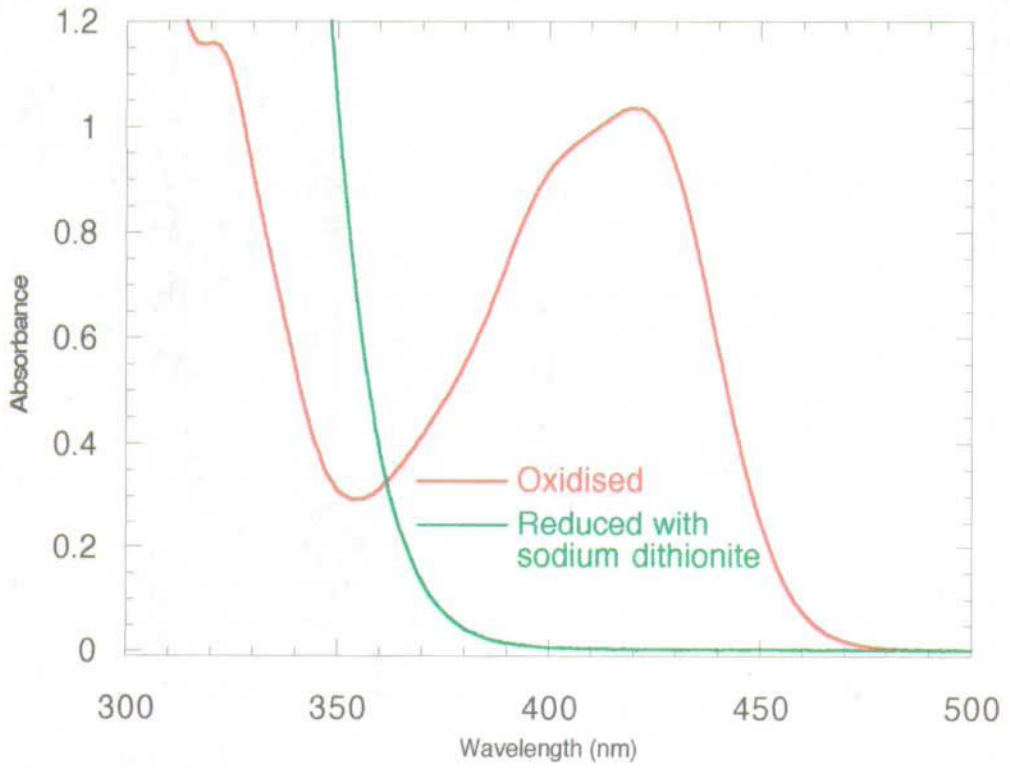

Figure 2.10. Absorption spectrum of 1 mM ferricyanide dissolved in 10 mM Tris-HCl buffer pH 7.5 (I = 0.1 M) and recorded at 25°C using a 1 cm cuvette.

2.2.4.2.2. Cytochrome c reduction

The dehydrogenase activity of intact flavocytochrome b_2 was also measured using its natural redox partner cytochrome *c*. The electrons are also individually passed onto cytochrome *c*, and the mechanism of this reaction is identical to that of ferricyanide. The reduction of cytochrome *c* was observed by the change in absorbance at 550 nm ($\Delta\varepsilon^{(red\text{-}ox)}$ = 22,640 $M^{-1}cm^{-1}$). The concentration of cytochrome *c* itself was determined by its absorbance at 550 nm (ε^{red} = 30,800 $M^{-1}cm^{-1}$; Hazzard *et al.*, 1986).

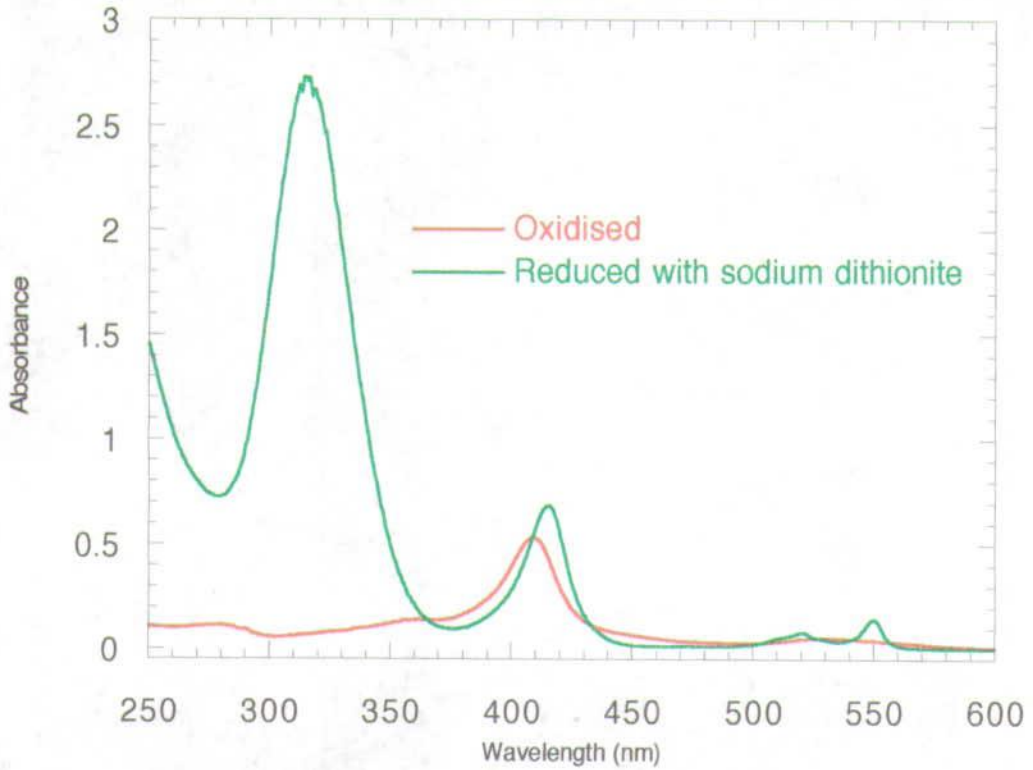

Figure 2.11. Absorption spectrum of 9.2 μM cytochrome c dissolved in 10 mM Tris-HCl buffer pH 7.5 (I = 0.1 M) and recorded at 25°C using a 0.5 cm cuvette.

2.2.5. Stopped-flow spectrophotometry

Stopped-flow spectrometry is based on observing the reaction between two reactants after their rapid mixing. The method is used for studying fast reactions, as the dead time between mixing and observation is of the order of 1 ms. The course of the reaction is followed on a spectrophotometer, and method thus requires a reaction that produce a large change in absorbance.

The experiments were conducted on an Applied Photophysics SF-17 Micro Volume stopped flow spectroflourimeter in a 1 cm cuvette at a single wavelength. All experiment were performed in 10 mM Tris-HCl buffer pH 7.5 adjusted to I = 0.1M by addition of NaCl at 25°C. The data were analysed on the software supplied with the stopped flow apparatus and KaleidaGraph™.

2.2.5.1. Glycolate oxidase

The reduction of FMN was monitored at 448 nm after mixing 20 μM enzyme with various concentrations of glycolate. The experiments were conducted in absence of dioxygen, as the rate of oxidation was comparable to that of reduction. The solutions were hence flushed with nitrogen to drive out the dissolved dioxygen. The traces from the stopped-flow experiments were fitted to a single exponential function. The

calculated rates were then plotted versus the substrate concentration, and finally fitted to the Michaelis-Menten equation in order to determine the kinetic parameters.

2.2.5.2. Flavin-binding domain

Enzyme reduction with L-lactate was monitored by observing the FMN reduction at 454 nm. The traces were fitted to a double exponential function, and the rates were then plotted against the substrate concentrations to determine the kinetic parameters. The experiments were performed in presence of dissolved atmospheric air. The rate of reoxidation by molecular oxygen was simply too low to cause any interference. The reoxidation of FMN by dioxygen could also be monitored at 454 nm, but on a completely different time-scale (minutes as opposed to milliseconds).

2.2.5.3. Flavocytochrome b_2

The reduction of FMN by L-lactate was monitored at the isosbestic point of 438.3 nm after mixing equal volumes of 20 μM enzyme and 20 mM L-lactate. The rate of haem reduction by electron transfer from reduced FMN to haem was measured in a similar but separate experiment. However, the change in absorbance was instead monitored at 557 nm, where the FMN absorbance is essentially zero.

The haem was also followed during its rapid oxidation by cytochrome *c*. Various amounts of flavocytochrome b_2, in the range from 5 μM to 20 μM, was pre-reduced with 20 mM L-lactate and then mixed with 2 μM oxidised cytochrome *c*. The reaction was followed by monitoring the change in absorbance of cytochrome *c* at 416.5 nm. The observed rates were then plotted against the concentrations of flavocytochrome b_2. The second order rate constant was determined as the slope of the fitted linear function.

3. Characteristics of the Wild-Type Enzymes

3.1. Introduction

It was established in chapter 1, that flavocytochrome b_2's physiological function is to serve as a L-lactate dehydrogenase within the intermembrane space of baker's yeast. The enzyme is closely related to glycolate oxidase from spinach, which is involved in the process of photorespiration taking place in the peroxisomes. Both enzymes catalyse oxidation of small 2-hydroxy carboxylic acids to the corresponding 2-keto acids. The crystal structures of both enzymes are available, and the C^{α}-atoms of the flavin-binding domain of flavocytochrome b_2 and glycolate oxidase superimpose with a root mean square deviation of only 0.93 Å (Lindqvist *et al.*, 1991). A number of amino acid residues around the isoalloxazine ring of the flavin are conserved and have a similar spatial position in the two enzymes. The mechanism of catalysis is thus likely to be similar, and indeed conserved residues have been assigned specific roles in the reductive half-reaction. The bound FMN is, in both glycolate oxidase and flavocytochrome b_2, likely to be reduced via a hydride transfer. The catalytic cycle is completed by reoxidation of the cofactor by two one-electron transfers. However, this half-reaction is remarkably different between the two enzymes despite the high degree of similarity in their three-dimensional structures. The flavin cofactor of glycolate oxidase is reoxidised by transfer of the electrons to oxygen producing hydrogen peroxide. Flavocytochrome b_2 has practically eliminated this reaction, and its reduced cofactor even has a considerably lower reactivity towards oxygen than has free FMN. Instead, the electrons are transferred to cytochrome *c* via the haem-binding domain. The obvious explanation of this phenomenon is that the cytochrome domain constitutes an electron sink. However, removal of this domain by expression of the flavin-binding domain in *E. coli* does not make an oxidase. The resulting enzyme is still an efficient L-lactate dehydrogenase though, when using ferricyanide as an artificial electron acceptor (Balme *et al.*, 1995). The reactivity towards oxygen is controlled by the protein moiety around the active site. These differences in the environment around the co-factor are clearly illustrated by absorption spectra of the bound flavin (Figure 3.1). It is the nature of these environmental differences which are sought in this study.

However, prior to attempting to elucidate the structural features differentiating an oxidase from a dehydrogenase, it is appropriate to describe the two enzymes employed in this venture. The isolated flavin-binding domain of flavocytochrome b_2 and glycolate oxidase, expressed in *E. coli*, have both been studied and characterised already (Balme *et al.*, 1995; Macheroux *et al.*, 1992). Unfortunately, the experimental conditions, such as choice of buffer and pH, used in these studies differ. Furthermore,

the residual oxidase activity of the dehydrogenase, though very small, has until now been given little attention. This chapter is devoted to establishing techniques and setting reference values, which may be used in the assessment of the efficiency of a mutant enzyme when it functions as a dehydrogenase or as an oxidase. The mutant enzymes will be characterised by stopped-flow spectrophotometry and standard kinetic methods to determine the effects of the mutations especially on their reactivity with substrates and O_2. A biochemical and biophysical characterisation is essential in the judgement of success in an ongoing design process. The oxidase activity is presumably not the result of a single mutations, but the effect of a number of additive mutations. Only the final combination of these will result in an optimised oxidase with high levels of activity. Hence, it is of the utmost importance to be able to detect mutant enzymes with even just minor improvement in the oxidase activity.

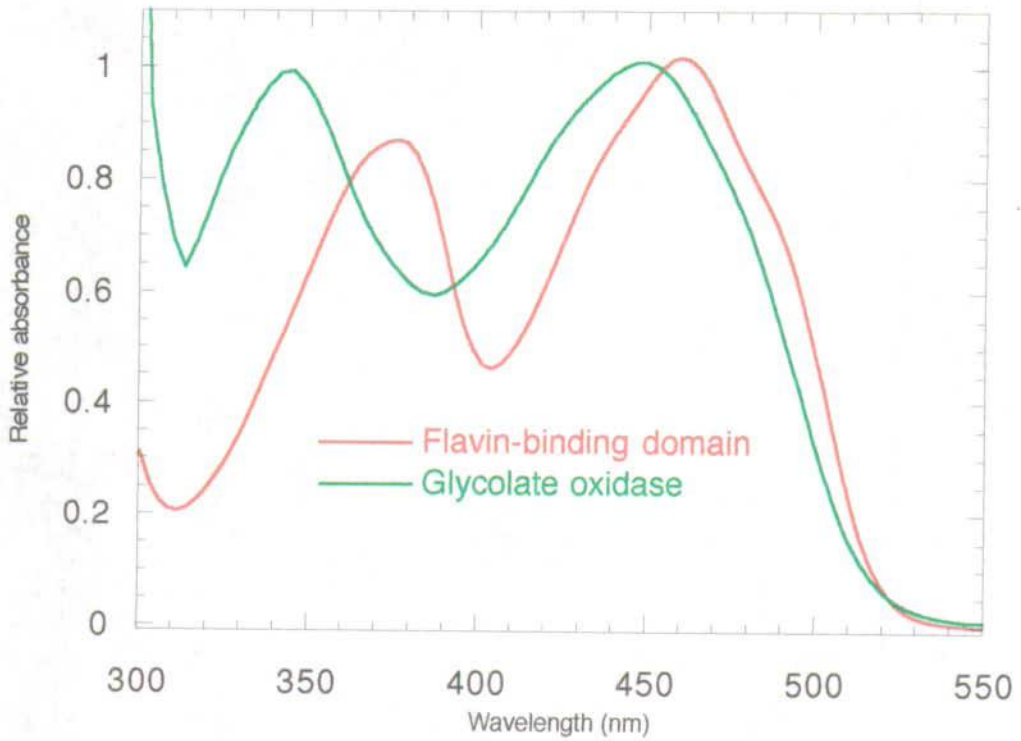

Figure 3.1. Absorption spectra of the FMN-binding domain and glycolate oxidase normalised at λ = 454 nm. The original spectra were recorded in 10 mM Tris-HCl pH 7.5 (I = 0.1 M) at 25°C using a 1 cm cuvette.

3.2. Results and discussion

3.2.1. The flavin-binding domain of flavocytochrome b_2

The isolated flavin-binding domain is unable to communicate with either the isolated haem-binding domain or the physiological oxidant of flavocytochrome b_2, cytochrome *c* (Brunt *et al.*, 1992). However, it is an efficient L-lactate dehydrogenase when using ferricyanide as an artificial electron acceptor. The mechanism for reduction of oxidised enzyme by L-lactate and subsequent reoxidation of reduced enzyme by ferricyanide is given by the scheme below:

$$E\sim FMN + S \underset{k_{-1}}{\overset{k_1}{\rightleftharpoons}} E\sim FMN-S \xrightarrow{k_2} E\sim FMNH_2 + P$$

$$E\sim FMNH_2 + Fe(CN)_6^{3-} \xrightarrow{k_3} E\sim FMNH^{\bullet} + Fe(CN)_6^{4-} + H^+$$

$$E\sim FMNH^{\bullet} + Fe(CN)_6^{3-} \xrightarrow{k_4} E\sim FMN + Fe(CN)_6^{4-} + H^+$$

The initial rate equation for this mechanism is:

$$v = \frac{V_{max}}{1 + K_m^S/[S] + K_m^{Fe(CN)_6^{3-}}/[Fe(CN)_6^{3-}]}$$

where

$$V_{max} = [E_0]2k_2$$
$$= [E_0]k_{cat}$$
$$K_m^{Fe(CN)_6^{3-}} = k_2(1/k_3 + 1/k_4)$$
$$K_m^S = (k_{-1} + k_2)/k_1$$

Equation 3.1. Rate equation for the flavin-binding domain using ferricyanide as electron acceptor (adapted from Morton et al., 1961; Iwatsubo et al., 1977).

The steady-state kinetic behaviour of the purified enzyme was analysed by monitoring the reduction of ferricyanide in the presence of substrate. The enzyme exhibits saturation kinetics with a K_m for ferricyanide of 0.46±0.04 mM. Hence, a concentration of 4 mM ferricyanide (8.5xK_m) was used for determination of the steady-state parameters, which was a convenient concentration to use along with 0.5 cm cuvettes. The observed rate would thus be 89.5% of the theoretical rate at infinite ferricyanide concentration. Figure 3.2 shows a plot of the steady-state data obtained for the flavin-binding domain of flavocytochrome b_2 and fitted to the Michaelis-Menten equation. It represents a typical plot of values determined as described in section

2.2.4.2.1 (p. 51). The catalytic rate constant was determined as 279±5 s^{-1}, and the Michaelis constant as 0.34±0.02 mM (Table 3.1). The enzyme thus has a specificity constant, k_{cat}/K_m, of 820,000±70,000 $M^{-1}s^{-1}$. The kinetic parameters for the reductive half-reaction has previously been determined by stopped-flow spectrophotometry (Balme *et al.*, 1995). The reported value of k_{cat} is 400±40 moles of L-lactate oxidised by one mole enzyme in a second and 0.26±0.07 mM L-lactate for the value of K_m. Hence, the reduction of FMN is faster than the reoxidation by ferricyanide, as only about 140 moles L-lactate are oxidised by one mole of the isolated flavin-binding domain per second during steady-state with ferricyanide as terminal electron acceptor. The kinetic parameters of the isolated flavin-binding domain differ from those of the intact protein (Table 3.1). The limiting rate and the Michaelis constant are both only decreased slightly though. Indeed, removal of the cytochrome domain seems to have little effect on catalysis at the active site of the flavin-binding domain. The mutant enzyme thus appears to provide the ideal starting material for conversion of a dehydrogenase into an oxidase. The flavin-binding domain is still active as a dehydrogenase, and shares great structural resemblance with the model oxidase.

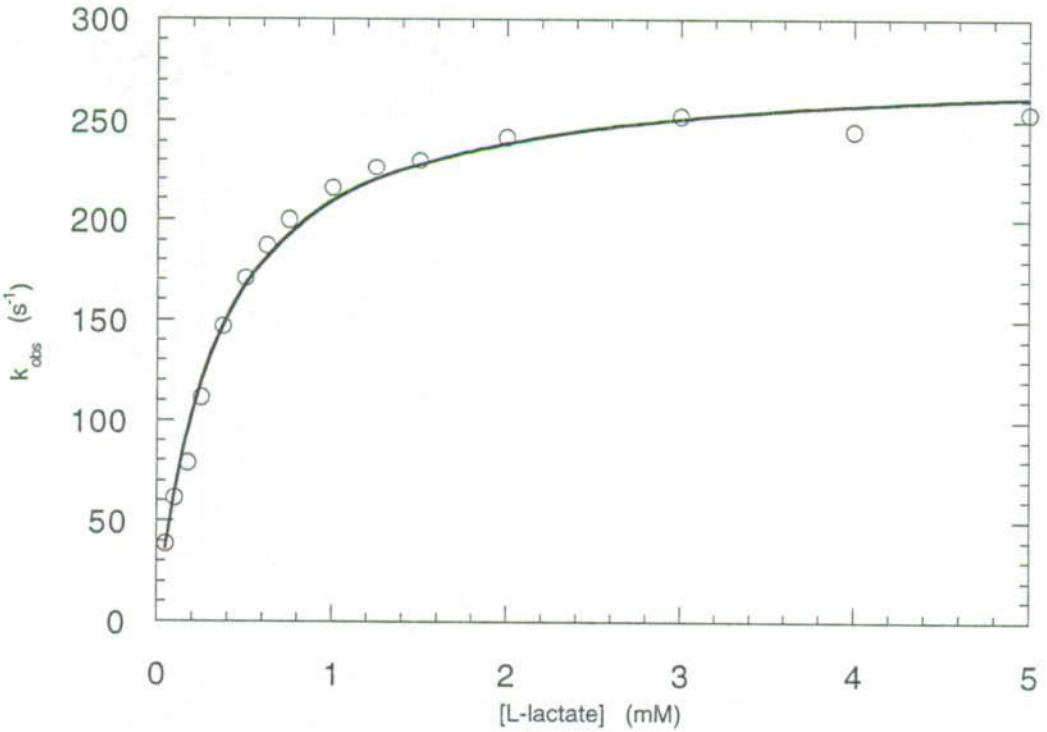

Figure 3.2. Plot of the steady-state data for the flavin-binding domain fitted to the Michaelis-Menten equation. The assays were performed in Tris-HCl buffer pH 7.5 (I = 10 mM) at 25°C and using ferricyanide as the electron acceptor.

	k_{cat} s^{-1}	K_m mM	k_{cat}/K_m $x10^6$ $M^{-1}s^{-1}$
Flavin-binding domain	279±5	0.34±0.02	0.82±0.07
Intact flavocytochrome b_2 †	400±10	0.49±0.05	0.82±0.12

Table 3.1. Steady-state kinetic parameters for the flavin-binding domain and the intact enzyme (†taken from Miles et al., 1992).

The rate of reoxidation of FMN by dioxygen has been determined to be 0.012 s^{-1} by mixing 20 μM enzyme with an equal concentration of L-lactate in buffer containing oxygen at atmospheric pressure (Figure 3.3). The change in absorbance at 454 nm was observed by stopped-flow spectrophotometry, and the trace was fitted to a double exponential curve. However, this very low oxidase activity was not detectable when using a coupled assay with horse radish peroxidase, and this observation possibly implies that superoxide is produced rather than hydrogen peroxide. Production of superoxide would also explain the low level of cytochrome *c* reduction observed upon L-lactate oxidation catalysed by the isolated flavin-binding domain (Balme *et al.*, 1995).

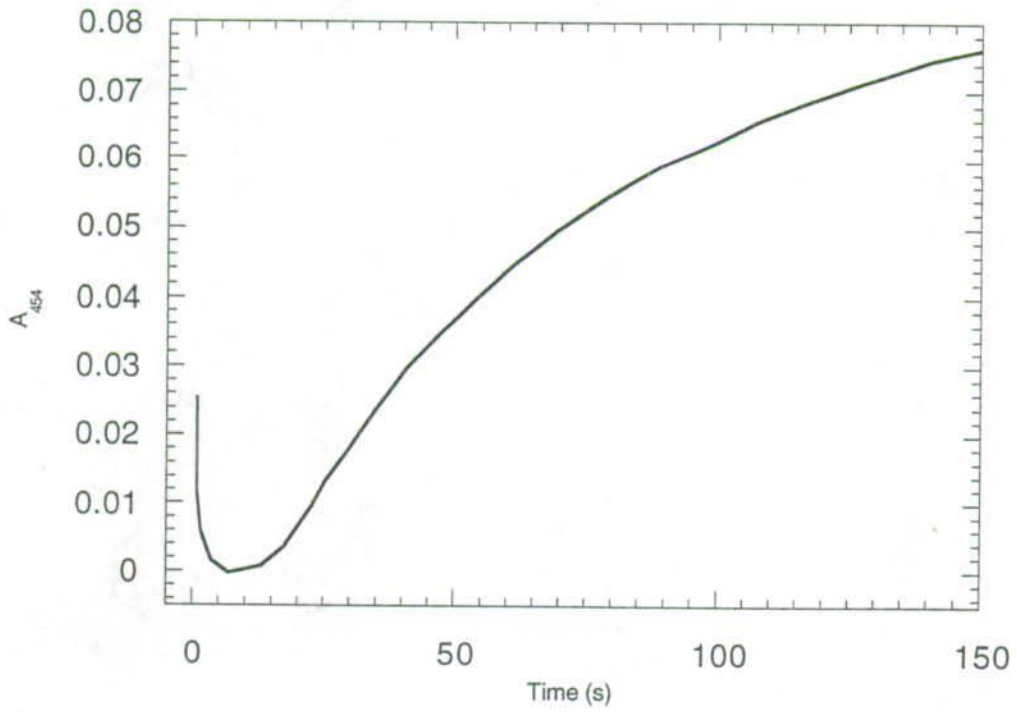

Figure 3.3. The stopped-flow trace for FMN-reoxidation was generated on mixing 20 μM reduced enzyme with an equal concentration of L-lactate containing oxygen at atmospheric pressure and recording the change in absorbance at 454 nm.

The above described method of stopped-flow spectrophotometry may be used for estimation of the relative rate of reoxidation at atmospheric oxygen pressure, but this reaction is really of second order and determination of the rate constant requires

measurement of the rate at several different dioxygen concentrations. However, the method of directly observing FMN-reoxidation by stopped-flow spectrophotometry at atmospheric oxygen pressure, as well as the previously described methods for determining the oxidase activity by steady-state kinetics (section 2.2.4.1, p. 49), will suffice for assessing whether a mutation has generated oxidase activity or if the mutant enzyme simply remains a dehydrogenase.

3.2.2. Glycolate oxidase

Glycolate oxidase is rapidly reduced by substrate, either glycolate or L-lactate, under anaerobic conditions, showing saturation at high substrate concentrations. The reduction step, preceding the reversible equilibrium formation of a complex between oxidised enzyme and substrate, is hence essentially irreversible. The oxidative half-reaction is a second order reaction, in which reduced enzyme reacts with molecular oxygen. The general mechanism for the reaction catalysed by glycolate oxidase is thus given by the scheme below:

$$E\sim FMN + S \underset{k_{-1}}{\overset{k_1}{\rightleftharpoons}} E\sim FMN-S \xrightarrow{k_2} E\sim FMNH_2 + P$$

$$E\sim FMNH_2 + O_2 \xrightarrow{k_3} E\sim FMN + H_2O_2$$

The initial rate equation for this simple mechanism is

$$v = \frac{V_{max}}{1+K_m^S/[S]+K_m^{O_2}/[O_2]}$$

where

$$\begin{aligned} V_{max} &= [E_0]k_2 \\ &= [E_0]k_{cat} \\ K_m^S &= (k_{-1}+k_2)/k_1 \\ K_m^{O_2} &= k_2/k_3 \end{aligned}$$

Equation 3.2. Mechanism and rate equation for the reaction catalysed by glycolate oxidase (adapted from Macheroux et al., 1991).

The enzyme was studied during steady-state turnover using the techniques described in the previous chapter. The limiting rate and the Michaelis constant depended on the substrate, the buffer and the technique used. The limiting rates determined for L-lactate and glycolate oxidation by the coupled assay with horse radish peroxidase were in reasonable agreement with published results (Stenberg *et al.*, 1995). The rate for L-

lactate oxidation was about half of the rate with glycolate as substrate. However, the published results were determined using a different approach and in another buffer with a higher ionic strength and pH value altogether. The observed results are thus not directly comparable to the published data. Even the two techniques employed for determination of the steady-state kinetic parameters in this study gave different results. The limiting rate was higher when monitoring the production of pyruvate as compared to when measuring the amount of hydrogen peroxide produced (Figure 3.4 & Table 3.2). The Michaelis constants were identical within the experimental error though. The direct measurement of pyruvate is arguably the more accurate, as this technique avoids the complication of coupling two enzymatic reactions. The coupling enzyme may not pick up all hydrogen peroxide produced, maybe as a result of a secondary reaction occurring before encounter between peroxidase and H_2O_2. Another, less plausible explanation is that the production of pyruvate does not correspond with the amount of hydrogen peroxide produced. However, the methods of coupling the oxidase reaction to hydrogen peroxide detection is much more sensitive, and the observed data ideally relate to the actual production of hydrogen peroxide. Besides, the measurement of change in absorbance at 205 nm is close to the useful limit of routine spectrophotometers, it also requires very clean cuvettes and a relatively new deuterium lamp. Hence, the coupled assay technique generally was employed for screening mutant enzymes for oxidase activity. The much higher sensitivity combined with the visible colour change simply made it invaluable for fast and easy detection of oxidase activity. Indeed, the same principle was adapted for screening thousands of mutant enzymes simultaneously after random mutagenesis.

	k_{cat} s^{-1}	k_{red} (k_2) s^{-1}	k_{ox} (k_3) $x10^6$ $M^{-1}s^{-1}$	K_m^{O2} (k_2/k_3) mM	K_m^{S} ($[k_{-1}+k_2]/k_1$) mM
GO (G/H_2O_2)	19.3±0.2	106±3			0.25±0.01
GO (G)[¶]	20	25	0.085	0.21	1
GO (L/H_2O_2)	10.1±0.2				2.1±0.2
GO (L/pyr.)	17.5±0.4				1.9±0.2
GO (L)[#]	11				11.5
LOX (L)[¥]	280	500	1.9	0.16	0.94
Free FMN[§]			0.00025		

Table 3.2. Steady-state kinetic parameters for glycolate oxidase (GO) turning-over glycolate (G) or L-lactate (L). The data were obtained by monitoring the production of either hydrogen peroxide (H_2O_2) or pyruvate (pyr). The published data for glycolate oxidase, L-lactate oxidase (LOX) and free FMN are listed for comparison. Taken from [¶](Macheroux et al., 1991),[#](Stenberg et al., 1995),[¥] (Maeda-Yorita et al., 1995), [§](Kemal et al., 1977).

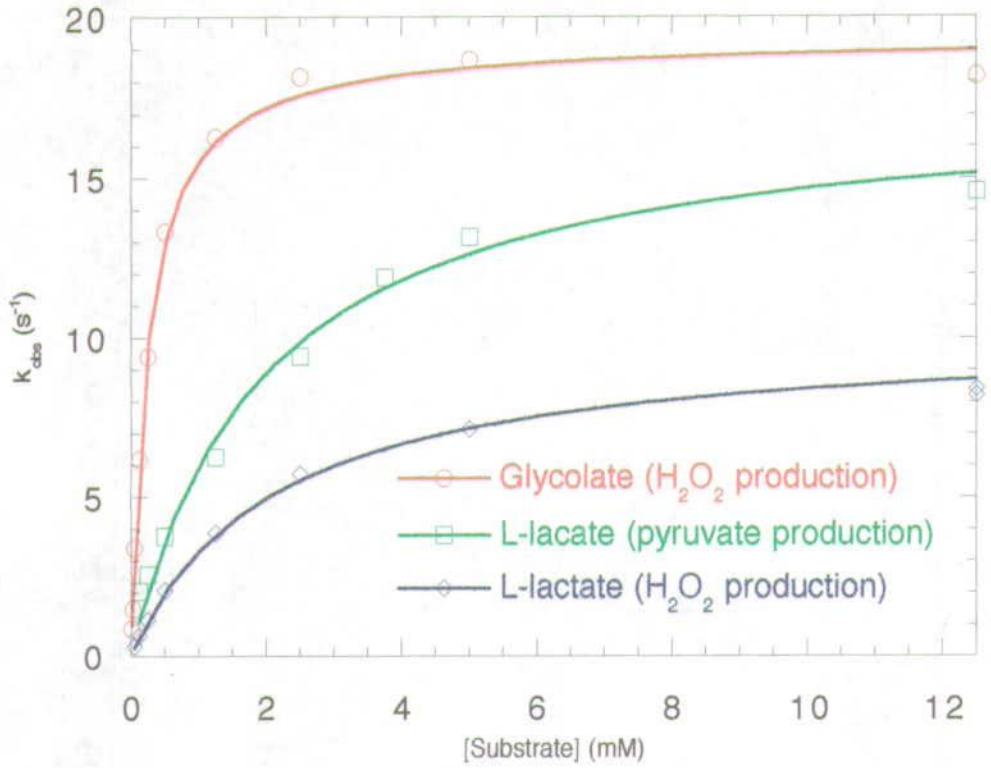

Figure 3.4. Plot of steady-state data obtained by monitoring the production of either hydrogen peroxide or pyruvate. The data were fitted to the Michaelis-Menten equation and the results are listed in Table 3.2.

The published values for the steady-state kinetic parameters were obtained by measuring the change in absorbance at 448 nm in a stopped-flow apparatus after mixing oxidised enzyme with various concentrations of glycolate in presence of O_2. This technique would give rise to traces as those illustrated in Figure 3.5, which were obtained by mixing a solution of 25 μM glycolate oxidase with an equal volume of buffer containing glycolate. Each trace displayed a quickly established steady-state phase, which persisted for varying lengths of time depending on the concentration of reducing substrate used. Finally, the change in absorbance ceased when dioxygen became depleted. The same technique, but with varying oxygen concentrations, was used for determining the published steady-state parameters for dioxygen. The stopped-flow apparatus was used because it offers an environment insulated from its surroundings, and hence eliminates exchange of oxygen with the air. However, the data obtained are somewhat an approximation to real steady-state turn-over, as the oxygen concentration changes considerably as the reaction progresses.

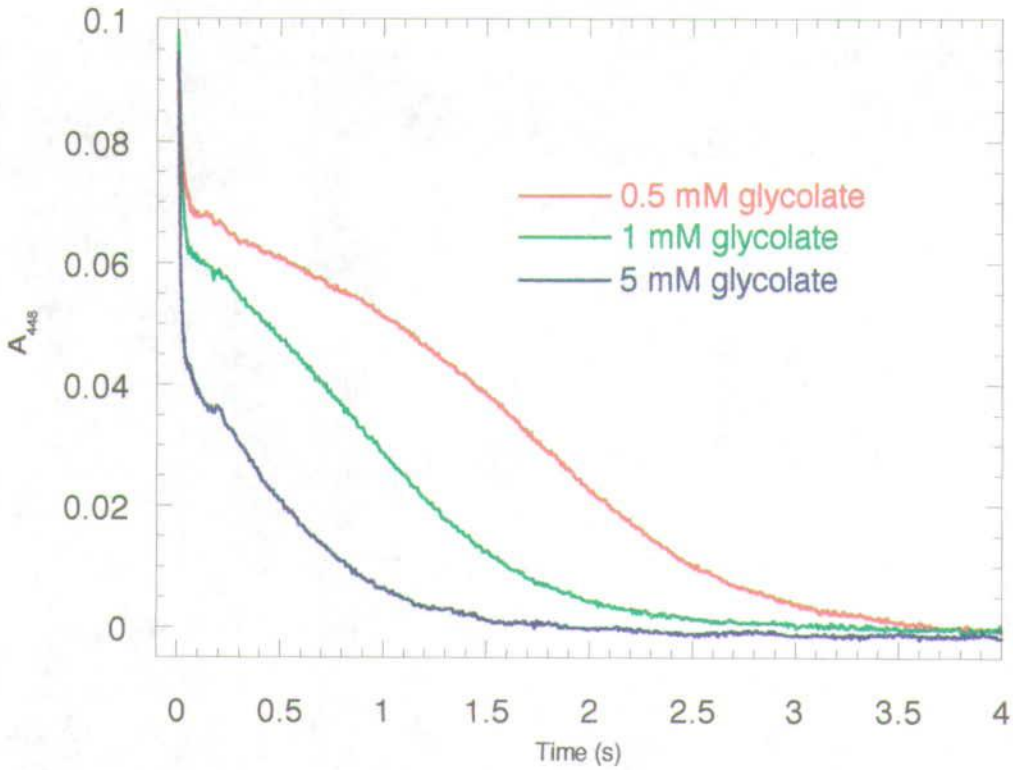

Figure 3.5. Stopped-flow traces generated by mixing 25 μM oxidised enzyme with glycolate solutions containing oxygen at atmospheric air pressure (about 0.41 mM O_2; Macheroux et al., 1993).

Furthermore, the published experiments were performed in 0.1 M potassium phosphate buffer pH 8.3 and 4°C. The argument for using phosphate buffer was that Tris-HCl buffer is a competitive inhibitor, as the K_m for glycolate was much higher (K_m = 5.2 mM) in 0.1 M Tris buffer (Macheroux *et al.*, 1991). However, repeating these experiments albeit at a lower buffer concentration did not confirm these findings (Figure 3.6 & Table 3.3). The K_m was not particularly affected by the buffer used. The observed changes were just as dependent upon a shift in pH. This dependence on pH was actually even greater for phosphate buffer than for Tris. The lower Michaelis constant for glycolate oxidase in Tris-HCl buffer at pH 7.5 seemed to be a direct result of a decrease in the limiting rate. Glycolate oxidase simply has a higher pH optimum than pH 7.5. However, the Michaelis constant dropped considerably more when using phosphate buffer, and this decrease was not merely the result of working at a sub-optimal pH value. Indeed, phosphate must interact with the active site. The published effects of Tris-HCl buffer are thus likely to be a result of the abnormally high buffer concentration used, possibly combined with the lower temperature used. The argument for using phosphate over Tris-HCl buffer is hence rather unjustified, and Tris-HCl buffer was used in all subsequent experiments.

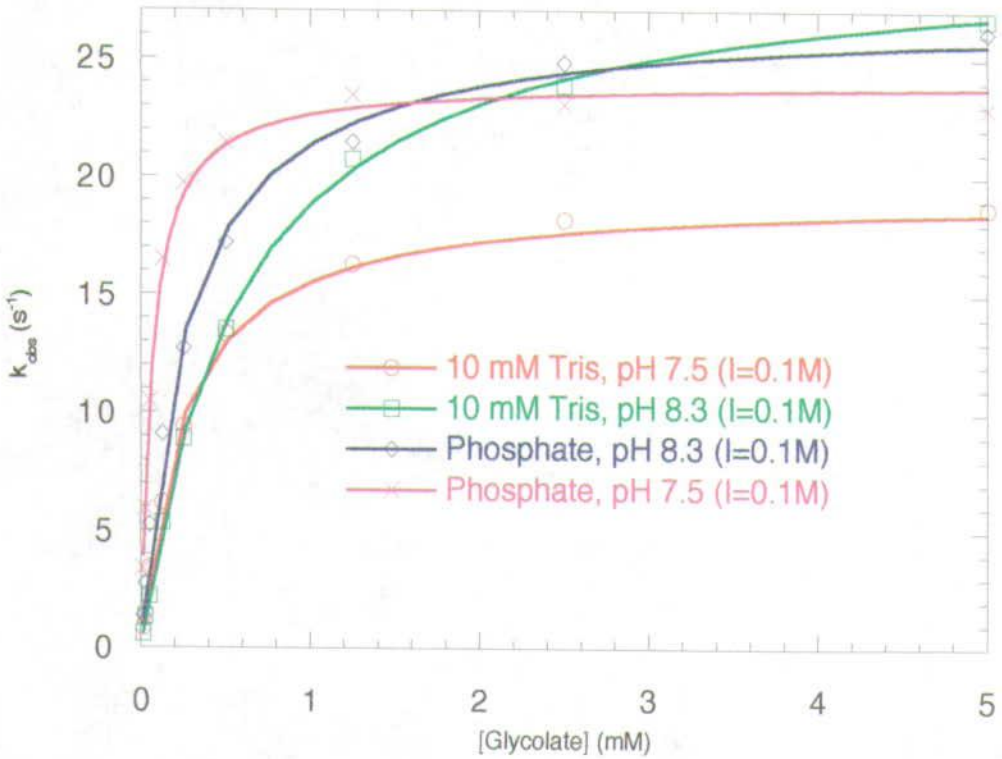

Figure 3.6. Plot of steady-state data for glycolate oxidase from experiments performed in various buffers and at different pH values. The data were fitted to the Michaelis-Menten equation and the resulting parameters are listed in Table 3.3.

	k_{cat} s^{-1}	K_m mM	k_{cat}/K_m x10^6 $M^{-1}s^{-1}$
Phosphate, pH 7.5	24.0±0.4	0.064±0.005	0.38±0.04
Phosphate, pH 8.3	27.0±0.3	0.27±0.01	0.10±0.01
Tris-HCl, pH 7.5	19.3±0.2	0.25±0.01	0.077±0.004
Tris-HCl, pH 8.3	29.8±0.1	0.59±0.01	0.051±0.001

Table 3.3. Steady state parameters for glycolate oxidase calculated from the data plotted in Figure 3.6. All data were obtained by monitoring the hydrogen peroxide production using the coupled assay.

Finally, the reduction of glycolate oxidase with glycolate under anaerobic conditions was monitored at 448 nm using a stopped-flow apparatus. The traces obtained were fitted to a single exponential function. The calculated rates were then plotted versus the concentration of glycolate (Figure 3.7). The limiting rate and Michaelis constant were determined as 106±3 s^{-1} and 1.2±0.1 mM, respectively. This result is in conflict with the reported rate of 25 s^{-1}, which was used to argue that the rate-limiting step was oxidation of substrate (Macheroux *et al.*, 1991). The present result on the contrary indicates that the limiting step is the reoxidation of FMN by dioxygen, as the overall reaction otherwise would be expected to proceed at a higher rate. Furthermore, this is not contradicted by the reported second order rate constant for the reaction between O_2 and FMN of 85,000 $M^{-1}s^{-1}$, given that the concentration of dioxygen dissolved in

buffer at atmospheric air pressure is about 0.41 mM. The rate of reoxidation of FMN would thus be around 35 s^{-1} when oxygen is present at atmospheric air pressure, which makes this step a very suitable candidate for the rate-limiting step indeed. Again, the experimental data and published results are not directly comparable due to variation in choice of buffer, pH and temperature. However, the result seemed to be confirmed when studying the trace recorded in the stopped-flow apparatus after rapid mixing oxidised enzyme and glycolate in the presence of oxygen (Figure 3.5). There was a clear burst of enzyme reduction before steady-state was established. Reoxidation would only be considered faster than reduction of the FMN, if the equilibrium establishes rapidly with a majority of the FMN-population in the oxidised form. Instead, the rate of reduction seems likely to be of the same order of magnitude if not even faster than the rate of reoxidation, as the steady-state occurs late and with a high proportion of the reduced form of FMN.

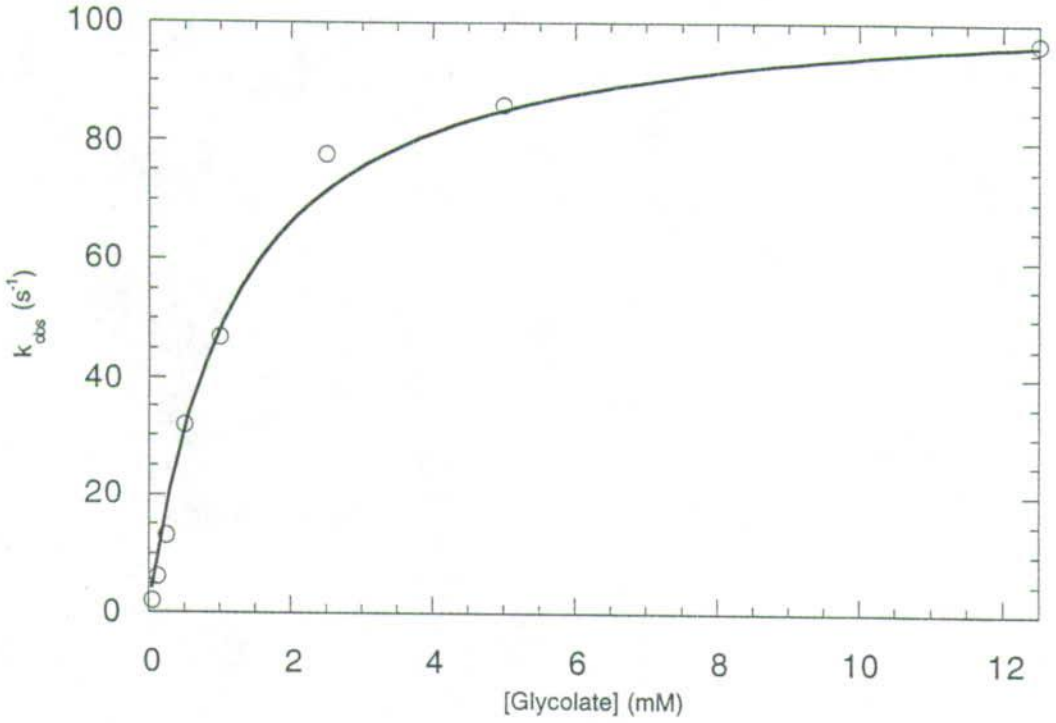

Figure 3.7. Rates calculated from stopped-flow traces plotted against the substrate concentration and fitted to the Michaelis-Menten equation. Each trace was generated by mixing 20 µM enzyme with glycolate in 10 mM Tris-HCl buffer pH 7.5 (I=0.1M) at 25°C.

3.3. Conclusion

The two enzymes providing the basis for this work clearly differ with respect to the reaction catalysed. The flavin-binding domain is a good L-lactate dehydrogenase as

demonstrated by monitoring the reduction of ferricyanide. Glycolate oxidase is unable to reduce ferricyanide, and passes the electrons onto dioxygen instead. This observation is slightly puzzling as free reduced FMN is oxidised very efficiently by ferricyanide with a rate constant of the order 10^8 $M^{-1}s^{-1}$ (Gibson & Hastings, 1962). Glycolate oxidase could possibly have eliminated the reaction with ferricyanide by rendering the active site more hydrophobic. Preliminary results suggest that the ferricyanide reductase activity is linked to the C-terminal end of the flavin-binding domain. Recently constructed hybrid enzymes of glycolate oxidase, where the last 100 amino acid residues were replaced with those of the flavin-binding domain, displayed both oxidase and ferricyanide reductase activity. The flavin-binding domain in contrast excludes oxygen from its active site. These catalytic differences, despite the high degree of structural similarity, makes the flavin-binding domain and glycolate oxidase ideal as starting point and model for the mutant enzymes, respectively.

A number of useful assays have been established in this chapter to allow differentiation between a mutant enzyme with dehydrogenase and one with oxidase activity. Microscopic increases in the reactivity towards molecular oxygen may be detected by a stopped-flow approach, where reduced enzyme is mixed with buffer containing oxygen. Other methods, used to determine the steady-state kinetic parameters, offer quicker and easier detection of oxidase activity though. The production of pyruvate may be followed directly by the change in absorbance at 205 nm. However, this assay is not as sensitive as the assay coupled with a peroxidase for detection of hydrogen peroxide. Furthermore, the coupled assay involves a visual colour change, which makes it a valuable tool for screening large quantities of mutant enzymes. Thus, in general this steady-state approach will suffice. A complete characterisation by stopped-flow methods will only be of interest for a mutant enzyme with significantly improved oxidase activity.

Glycolate oxidase leaves some room for improvement itself. The enzyme is not a particularly efficient oxidase, as shown by comparison with its distant relative L-lactate oxidase from *Aerococcus viridans* (Table 3.2). The L-lactate oxidase enhances the second order rate constant between reduced FMN and dioxygen by more than a 7,500-fold, as compared to the reaction of free flavin. Glycolate oxidase increase the rate constant little more than 300 times, and thus does not appear to be fully optimised by the evolutionary process. However, the objective of this study is to engineer oxidase activity into flavocytochrome b_2, and merely raising the reactivity to the level of free flavin would be an immense improvement with regards to this enzyme. The reoxidation of reduced FMN by molecular oxygen is negligible, and has probably been

achieved by excluding oxygen from the active site of flavocytochrome b_2. The following chapters will give a detailed description of the many and varied approaches taken to obtain the desired oxidase activity. Success would not only solve one of the greatest mysteries in the world of flavoproteins, but might also provide clues to a rational design of new catalysts for O_2 reactions in chemistry.

4. Engineering Oxidase Activity in a Dehydrogenase

4.1. Introduction

The difference in reactivity towards dioxygen between flavocytochrome b_2 and glycolate oxidase has been considered in chapter one. Since both enzymes have the same flavin prosthetic group, it was established that the difference must be due to the protein moiety itself. Indeed, interactions between the protein and FMN shift the redox potentials to significantly more positive values than those of unbound FMN (Pace & Stankovich, 1986), making the reaction with substrate thermodynamically possible, but provide no explanation as to why the two proteins differ with respect to O_2. Hence, the reactivity towards oxygen is probably modulated by steric access to the FMN instead. This chapter will explore protein engineering as an approach to convert the flavin-binding domain of flavocytochrome b_2 into an oxidase. Such a conversion would allow identification of the exact molecular features determining the reactivity. The flavin-binding domain is used as a scaffold to avoid interference from the haem-binding domain and also to allow direct comparison with glycolate oxidase. Indeed, the high degree of similarity between the two makes glycolate oxidase an ideal model for the design of mutant enzymes. The three-dimensional structure of the isolated flavin-binding domain is not available, but is assumed to be identical to its structure within flavocytochrome b_2. This assumption is justified by the observation of L-lactate dehydrogenase activity in the isolated flavin-binding domain (Pallister *et al.*, 1990). Furthermore, the haem-binding domain is located on the outer edge of the tetramer and forms no intersubunit contacts (Xia & Mathews, 1990). The haem-binding domain does however occupy a spatial position, where the loop between strand four and helix four is found in glycolate oxidase (Lindqvist *et al.*, 1991). This position is located in close proximity to the active site, and it is thus possible that the loop region in glycolate oxidase interacts with the active site. Removal of the cytochrome domain would potentially allow similar interactions to take place in flavin-binding domain of flavocytochrome b_2. Unfortunately, the flavin-binding domain expressed independently in *E. coli* possess no oxidase activity, yet the loop region may still fulfill a function in controlling the activity. Indeed, the nature of the loop itself could be of great importance, and has been subjected to further investigations as described in the next chapter.

A more detailed analysis of flavocytochrome b_2 and glycolate oxidase using molecular graphics revealed only minor differences between the active sites. Nevertheless, these may provide important clues to the functional differences of the two enzymes. Only a single residue in the active site is not conserved. The position equivalent to Trp108 in

glycolate oxidase is occupied by a leucine residue in flavocytochrome b_2 (Figure 4.8, p. 80). This residue is involved in determining the substrate specificity of the enzymes. Substitution of the tryptophan in glycolate oxidase with a serine residue is reported to affect the Michaelis constant as expected, but it surprisingly also decreased the rate of catalysis (Stenberg *et al.*, 1995). The residue thus has another important function in the catalytic process apart from determination of substrate specificity. The indole ring nitrogen hydrogen-bonds to a water molecule in the active site. Part of the volume of the large aromatic indole ring is occupied by the propionate side chain of haem in flavocytochrome b_2, but this is naturally not the case in the flavin-binding domain. It would thus be interesting to study the effect of introducing this tryptophan residue in the flavin-binding domain. Another striking difference is the presence of a hydrogen bond from the side chain of Ser195 in β-strand one to the ribityl side chain, which is not present in glycolate oxidase where the corresponding residue is Ala76. However, this residue merely contributes to the strength of the FMN binding, and does not modulate the reactivity towards dioxygen (Lindqvist *et al.*, 1991). The neighbour at the C-terminal end of this residue is conserved as a proline in all family members, except in flavocytochrome b_2 where it is an alanine (Ala196). The cyclic five-membered ring imposes rigid constraints on rotation about the N-C^{α} bond of the backbone. However, these two corresponding residues appear to have the same structural main chain conformation, and the constraints imposed on the proline residue may thus of little importance in this particular instance (Figure 4.6, p. 78). The slightly more bulky proline could induce other changes elsewhere in the neighbourhood though. Indeed, the orientation of FMN differs significantly in the two structures due to different conformations of residues at the end of strand one. Both the main chain and side chain conformations of Thr78/197 differ in the two structures. These differences could be caused by residue Leu436, which corresponds to Val312 in glycolate oxidase, constraining the position of the methyl group of Thr197 in flavocytochrome b_2 (Figure 4.2, p. 74). The close proximity of strand one and the FMN ring system enables formation of a hydrogen bond between FMN N5 position and the main chain amide of Ala198. In glycolate oxidase, where the ring system in contrast is tilted away from the strand, a pocket with a water molecule is found near the *re*-face of the FMN ring. This pocket is believed to be very important for oxidase activity, either as a binding site for dioxygen or to accommodate the O4 oxygen of FMN. Recent structures of glycolate oxidase, with inhibitors bound at the active site, show the FMN in the same orientation as in flavocytochrome b_2 (Stenberg & Lindqvist, 1997). This observation implies some degree of mobility of FMN in glycolate oxidase. The isoalloxazine ring in flavocytochrome b_2 has the same

orientation with or without bound pyruvate, which indicates a less mobile flavin molecule. The importance of FMN mobility in the oxidase becomes obvious when considering that the formation of C4a-hydroperoxide imposes bending of the isoalloxazine ring system (Walsh, 1980).

4.2. Results and discussion

A number of single mutations have been introduced into the flavin-binding domain of flavocytochrome b_2 with the purpose of engineering oxidase activity into it. The design of the mutant enzymes was based on the structural differences between the flavin-binding domain and glycolate oxidase considered above. The protein moiety apparently modulates the reactivity with dioxygen by controlling access to the active site. Hence, many of the mutations were designed with the purpose of generating space around FMN, making the FMN more mobile, and creating a binding site for oxygen. Other mutant enzymes were constructed to study the importance of conserved residues, and include both residues conserved among the oxidases as well as catalytically active residues. All mutations involved residues close to the active site and were expected to have some effect on the catalysis.

The reactivity towards dioxygen was assessed by measuring the production of hydrogen peroxide using the coupled assay with horse radish peroxidase. The production of hydrogen peroxide was detectable for the mutant enzymes as opposed to the wild type enzyme. The limiting rates observed (0.002 s^{-1}) were about 5000-times lower than the rate for glycolate oxidase, and were unfortunately too low to allow determination of the Michaelis constant. However, some interesting observations were done with respect to the L-lactate dehydrogenase activity. All mutants was analysed by steady-state kinetics using ferricyanide as electron acceptor. The observed parameters are tabulated in the table below, and the results are discussed in the relevant sections.

	k_{cat} s^{-1}	K_m (L-lactate) mM	k_{cat}/K_m (L-lactate) $x10^6$ $M^{-1}s^{-1}$	K_m ($Fe(CN)_6^{3-}$) mM
WT	279±5	0.34±0.02	0.82±0.07	0.46±0.04 (4)
A196P	298±3	0.31±0.01	0.96±0.04	0.23±0.01 (2.5)
T197A	95±3	1.9±0.2	0.050±0.008	0.10±0.02 (1)
A198P	-	-	-	-
L230W	92±3	6.1±0.6	0.015±0.002	0.34±0.02 (3)
D282N	1.69±0.01	0.45±0.01	0.0038±0.0001	0.07±0.01 (2)
A283T	50±1	2.5±0.2	0.020±0.002	0.31±0.02 (2.5)
L436A	96±3	0.85±0.10	0.11±0.02	0.13±0.03 (2)

Table 4.1. Steady-state kinetic parameters for mutant enzymes. The concentration of acceptor used is given in brackets after the K_m value obtained for ferricyanide.

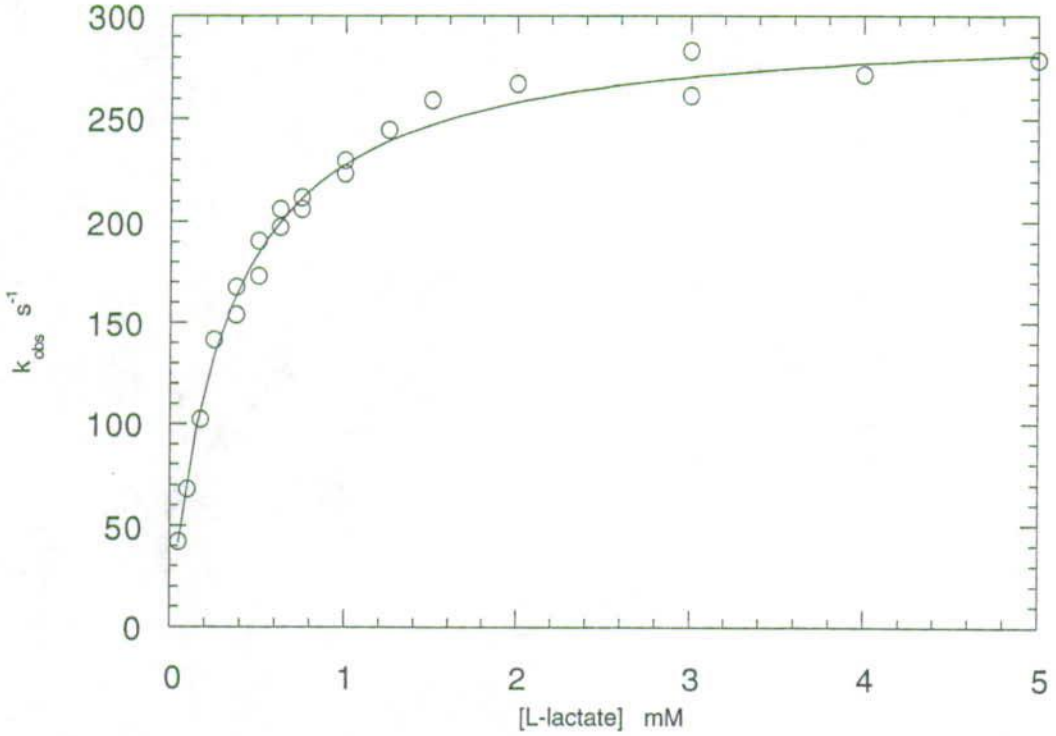

Figure 4.1. Plot of steady-state data obtained for mutant enzyme A196P, and fitted by least squares to the function for the Michaelis-Menten equation. The plot represents a typical set of data from steady-state assays using ferricyanide as the electron acceptor. The assays were performed in 10 mM Tris-HCl pH 7.5 (I = 0.1 M) at 25°C.

4.2.1. The T197A and L436A mutations

The two residues Leu436 and Thr197 were each mutated to alanine in an attempt to create a pocket on the *re*-side of the isoalloxazine ring of FMN. It is apparent from the crystal structures that this position is much more spacious in glycolate oxidase than in flavocytochrome b_2. This primarily seems to be an effect of the different orientations of FMN. However, changing amino acid residues could possibly generate more space in this area as well. Indeed, the introduction of less bulky residues at positions Leu436 or Thr197 would possibly change the course of strand one and create the desired pocket (Figure 4.2). Unfortunately, the changes did not make an oxidase. The mutant enzymes displayed significant changes in the steady-state kinetic parameters using ferricyanide as electron acceptor though (Table 4.1). The limiting rate went down by a factor of three for both mutant enzymes, whereas the Michaelis constant was increased nearly a three-fold for L436A and a six-fold for T197A. The mutations thus surprisingly influenced the apparent rate constant for the combination of substrate with free enzyme, even though they were located on the opposite site of the isoalloxazine ring with respect to the L-lactate binding site. Presumably, they are actually changing the position of the flavin relative to the bound L-lactate. The strength of the observed

effect on substrate binding was determined by the location of the mutation with respect to the flavin. Mutation T197A, being the closest, had the strongest effect, while L436A was positioned more distantly and had less effect. Once the complex was formed, both mutant enzymes formed product with the same rate.

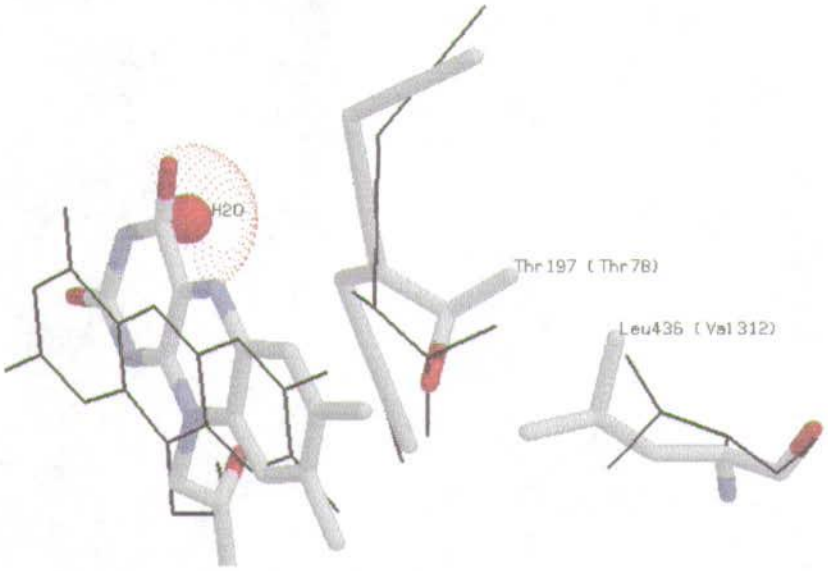

Figure 4.2. The area on the re-side of FMN in flavocytochrome b_2 (coloured) and glycolate oxidase (black), including residue Leu436 (Val312) and the backbone of strand one with residue Thr197 (Thr78). The water molecule (red ball) is only found in glycolate oxidase.

The already mentioned increase of the level of background oxidase activity was also demonstrated by the use of stopped-flow spectrophotometry for mutant enzyme L436A (Figure 4.3). The absorbance change at 454 nm was simply monitored after rapidly mixing equal molarities of L-lactate and enzyme. The reduction of FMN is very fast compared to the reaction between reduced enzyme and dioxygen present in the solution. The traces were fitted to a double exponential function. The limiting rates for flavin re-oxidation, at atmospheric oxygen pressure, were determined to be 0.09 s^{-1} and 0.012 s^{-1} for the mutant enzyme L436A and wild-type, respectively. These values are slightly higher than the values obtained at steady-state, and could indicate that the product of reoxidation by dioxygen is a mixture of superoxide and hydrogen peroxide.

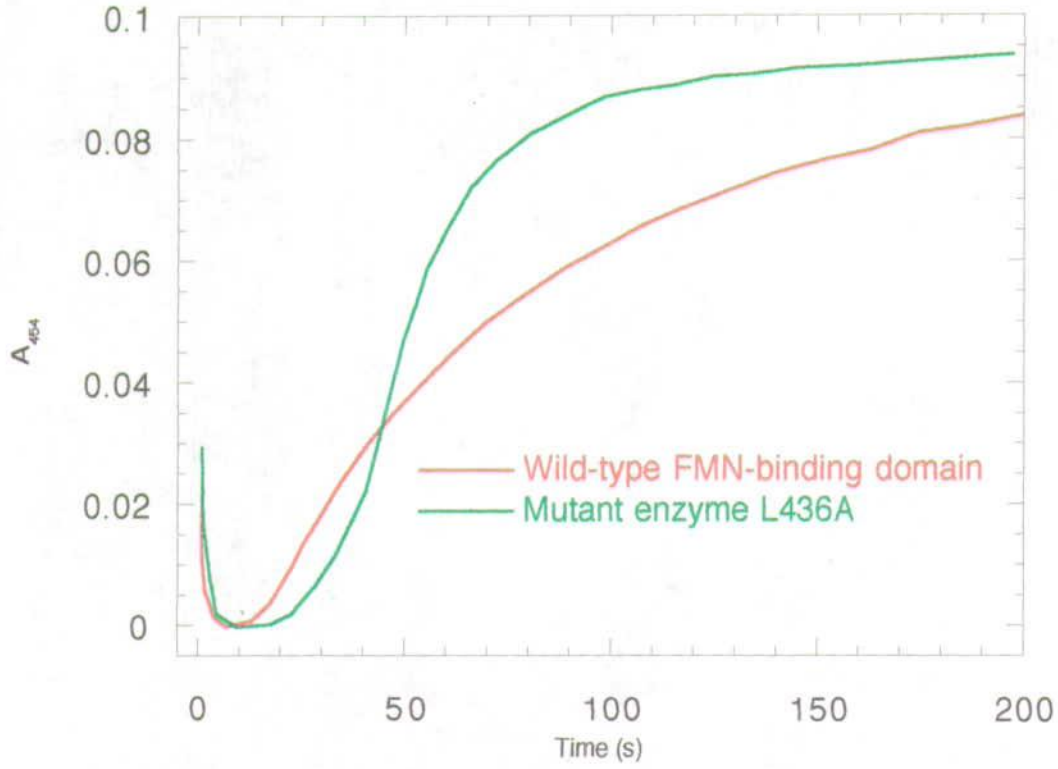

Figure 4.3. Stopped-flow traces generated by mixing equal volumes of enzyme and substrate (both at a concentration of 20 μM) in pressence of dioxygen. The reduction and reoxidation of FMN was monitored by the change in absorbance at 454 nm.

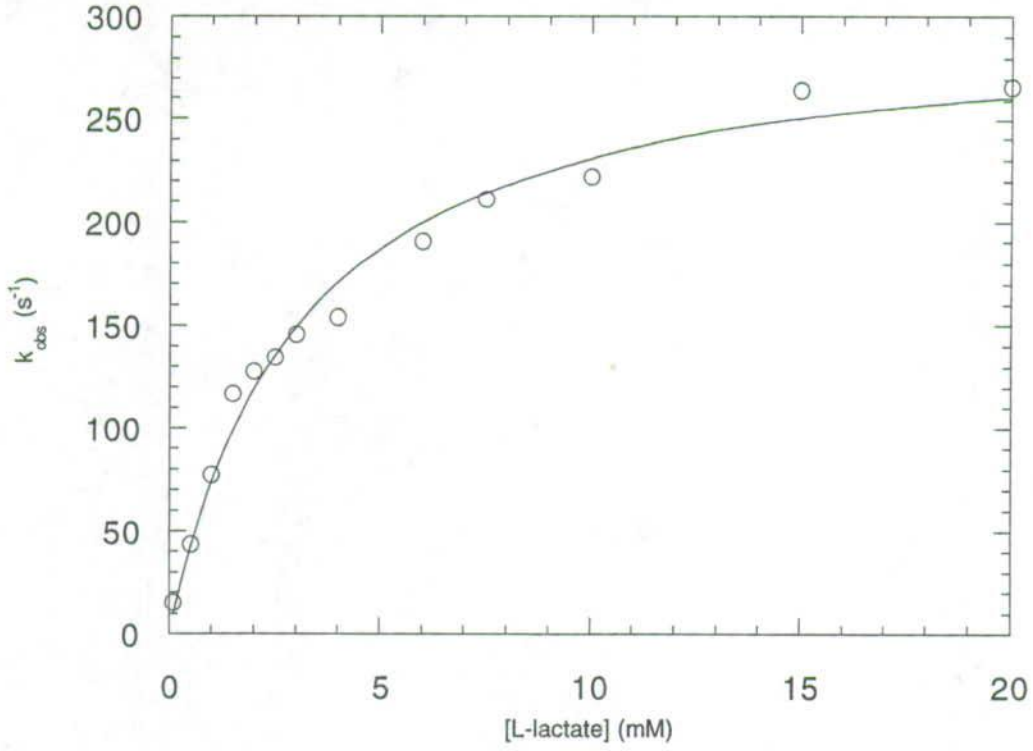

Figure 4.4. Pre-steady-state rate constants for reduction of flavin in mutant enzyme L436A plotted against L-lactate concentration. The rate constants were determined from the fast phase of double exponential fits. The curve is a fit to the Michaelis-Menten equation.

The limiting rate and Michaelis constant for reduction of FMN by L-lactate were also determined by stopped-flow spectrophotometry (Figure 4.4). The same reaction as described above was monitored, but on a much shorter time scale and at various substrate concentrations. The pre-steady state kinetic parameters, k_{cat} and K_m, were determined as 302±10 s^{-1} and 3.1±0.3 mM, respectively. The reductive half-reaction is obviously not the rate limiting step in the turn-over of L-lactate, as the limiting rate is nearly three-fold higher than that of the overall reaction as determined during steady-state.

4.2.2. The A198P mutation

A proline residue was introduced at position 198 instead of alanine (Figure 4.5). The corresponding position is in all members of the familiy occupied by small amino acid residues (glycine or alanine). This could naturally indicate that the amino acid residue must be flexible or that the available space is rather restricted. Nevertheless, a proline residue was introduced to investigate the effect of breaking the hydrogen bond between the main chain amide and position N5 of the isoalloxazine ring. This bond might be at least partly responsible for the different orientations of the flavin molecule observed in flavocytochrome b_2 and glycolate oxidase. The overall result of the mutation might then be the creation of sufficient space on the *re*-side of the ring system to accommodate dioxygen or increased mobility of FMN. Proline is an unique amino acid (really an imino acid), in that it is bonded covalently to the nitrogen atom of the peptide backbone. Therefore the peptide backbone at Pro residues has no amide hydrogen for use as a donor in hydrogen bonding. However, the cyclic five-membered ring also imposes rigid constraints on rotation about N-C^{α} bond of the backbone. Pro residues, consequently, can have significant effects on the conformation of the polypeptide backbone.

Unfortunately, the mutant enzyme turned out to be inactive. The overproduced enzyme could easily be purified, and identified both by absorption spectra and Western blotting. However, the bound flavin could not be reduced by L-lactate and was consequently always in its oxidised state. The problems arising from introduction of a proline residue at this position are easily visualised by molecular graphics. When the alanine is replaced with proline, without changing the conformation of the backbone, the distance between N5 and the amino acid side chain becomes critically short. The orientation of flavin or the conformation of the strand containing residue 198 simply has to change. This could very well result in disruption of the substrate binding site or

change the position of other active site residues. The distance between bound substrate and FMN is obviously of the utmost importance and very sensitive to any changes.

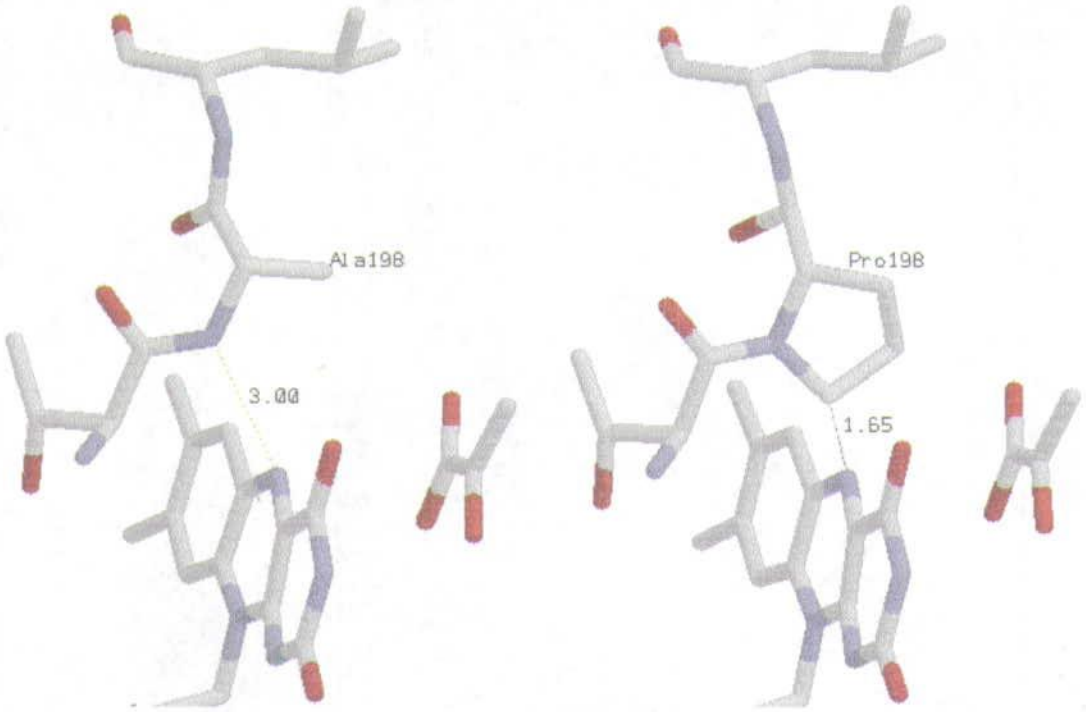

Figure 4.5. Models showing the wild type enzyme (left) and the mutant enzyme A198P (right). The alanine residue was substituted with proline, while keeping the main chain conformation as in the wild type enzyme. The dotted line indicates the closest contact between FMN and the residue 198 with the distance given in Ångström.

4.2.3. The A196P and A283T mutations

A couple of residues in and around the active site are completely conserved among the oxidases. One of these is the proline located at position 77 in strand one of glycolate oxidase, which corresponds to Ala196 in flavocytochrome b_2. Its two neighbouring amino acid residues both display some clear differences in the crystal structures of flavocytochrome b_2 and glycolate oxidase. A hydrogen bond from the side chain of Ser195 to the ribityl side chain is only present in flavocytochrome b_2. The other neighbouring residue, Thr197, has a completely different conformation. Thus, the effect of introducing a proline at this specific position (196) could be quite interesting, even though the alanine present in flavocytochrome b_2 and the proline of glycolate oxidase appear to have the same conformation.

The mutant enzyme, A196P, expressed very poorly in the pRC23 system. The ferricyanide reductase activity was detectable, but this was merely due to the high activity of the mutant enzyme. The bound flavin was at no point during the purification visible in the absorption spectrum. The gene encoding the mutation was therefore

transferred into the vector pJF118EH, and luckily the enzyme proved to be expressed at high level in this alternative system. The mutation had no negative effects whatsoever on the kinetic parameters (Table 4.1, p. 72). On the contrary, if anything, the substitution of alanine for proline was slightly beneficial with respect to dehydrogenase activity. Unfortunately, the mutation did not confer oxidase activity to the enzyme. Hence, in this particular case there is plenty of room for the proline side chain, which is located with the plane of its five-membered ring nearly parallel to that of the isoalloxazine ring system (Figure 4.6). The bulk of the sidechain has no effect on the orientation of FMN, and the substitution introduces no conformational changes to the backbone either. It thus appears to be of little significance whether the residue is a proline or an alanine in flavocytochrome b_2. However, the conclusion cannot just be extended to cover the other family members in which the residue indeed is fully conserved as a proline.

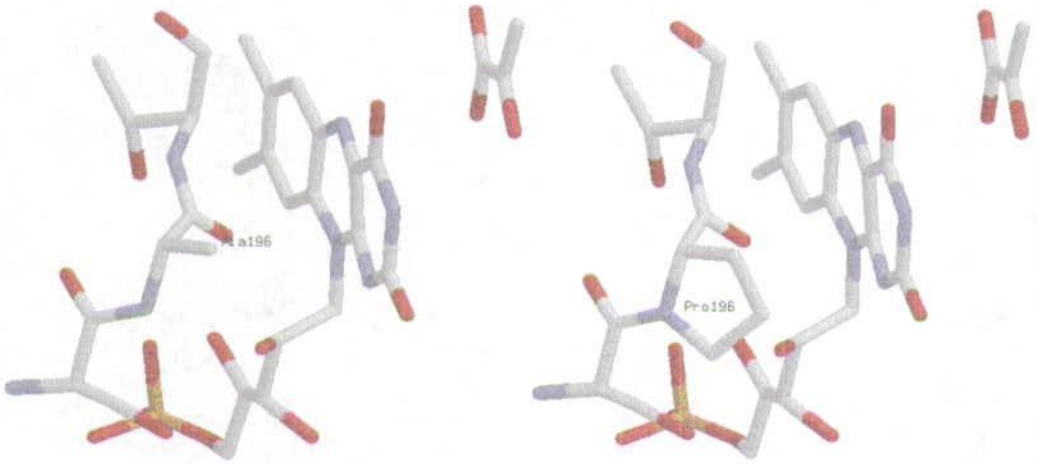

Figure 4.6. Models of the wild type enzyme (left) and mutant enzyme A196P (right). The alanine residue was substituted with a proline, while keeping the main chain conformation as in the wild type enzyme.

The position of amino acid residue 283 is, in flavocytochrome b_2, occupied by an alanine residue. However, the equivalent position in glycolate oxidase, and all other family members reacting with dioxygen, is conserved as a threonine residue. The residue in question is by no means remote from the active site (Figure 4.7). In sequence, it is situated right next to one of the active site residues, Asp282, which facilitate the proton abstraction by His373. An introduced threonine at this position could potentially interact with both residue Asp282 and His373, and change the kinetic characteristics of the enzyme significantly.

The mutant enzyme, A283T, was still functional as a ferricyanide reductase but had no increased L-lactate oxidase activity. The k_{cat} was more than five-fold lower than that of

the wild-type enzyme. The K_m went up nearly 10-fold, which is reflected in the 15-fold decrease in apparent rate constant for formation of complex between substrate and free enzyme (Table 4.1, p. 72). Given the large distance between the bound substrate and residue 283 in the crystal structure, such a large effect is rather surprising. However, it cannot be excluded that introduction of this more bulky residue is less compatible with L-lactate binding. The reported Michaelis constant of 22 mM for L-lactate monooxygenase (Maeda-Yorita *et al.*, 1995), which is the only one of the L-lactate utilising enzymes to contain a threonine at this position, is certainly quite high as well. However, the position seems to be able to accomodate a variety of different amino acid residues, as the L-lactate dehydrogenases from *E. coli* and *H. influenzae* both have a methionine at the corresponding position.

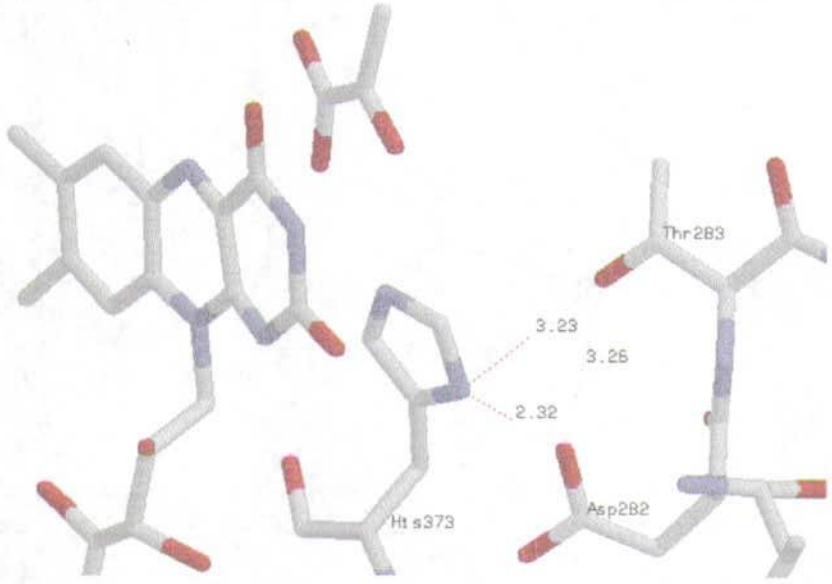

Figure 4.7. Model of mutant enzyme A283T. The closest distance to the active site residues His373 and Asp282 is given in Ångström and indicated by a dotted lined.

4.2.4. The L230W and D282N mutations

Two mutations of amino acid residues directly involved in the catalytic events were constructed and analysed in the search for increased oxidase activity. One of the amino acid residues is located at position 230 in flavocytochrome b_2. However, this particular residue is not conserved among the members of the family, and it is believed to be responsible for determining the substrate specificity (Daff, 1996). The size of the α-carbon side chain of the substrate seems to correlate with the size of the amino acid side chain at this position. The position is occupied by a leucine residue in flavocytochrome b_2, whereas a tryptophan is located at the corresponding position in glycolate oxidase. The tryptophan has been substituted for a serine, which seriously

impaired the catalytic function of glycolate oxidase (Stenberg *et al.*, 1995). Not only was the Michaelis constant increased some hundred fold, but the limiting rate was similarly decreased 500-fold. This result indicates that the tryptophan is of major importance in catalysis, and that it is involved in determining the substrate specificity of glycolate oxidase.

The possible role of a tryptophan at the position 230 was studied. The mutant enzyme L230W did not acquire the oxidase activity of glycolate oxidase. The enzyme was still a L-lactate dehydrogenase as monitored by the reduction of ferricyanide. However, the steady-state kinetic parameters were considerably different from those of the wild-type enzyme (Table 4.1, p. 72). The binding of L-lactate was seriously impaired, as demonstrated by the more than 50-fold decrease in the apparent rate constant between L-lactate and free enzyme. The rate of product formation, once the complex between enzyme and substrate is generated, was only down by three-fold. The mutation clearly alters the substrate specificity of the enzyme. The reason becomes obvious when replacing leucine with tryptophan in the model of flavocytochrome b_2 (Figure 4.8). There is simply no room for the methyl group of L-lactate, if keeping the same conformation of tryptophan as observed for leucine. The mutation does not make glycolate a better substrate (data not shown), and the specificity is obviously also influenced by other interactions.

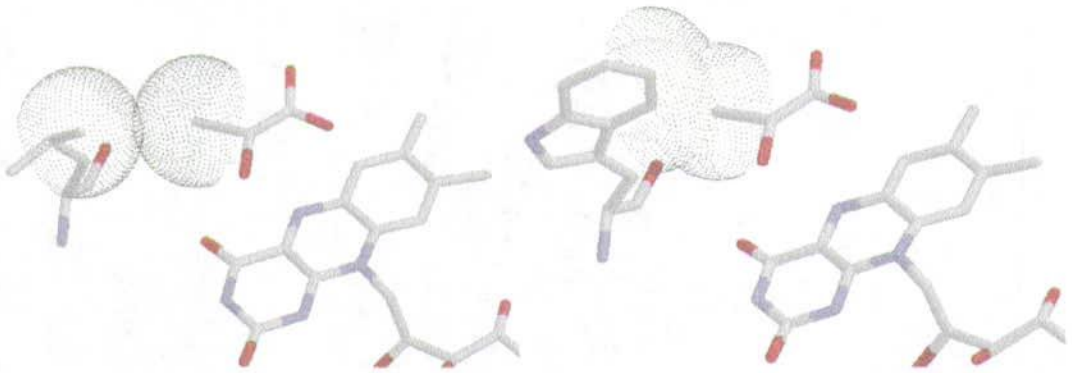

Figure 4.8. Model illustrating the steric interactions between pyruvate and tryptophan in mutant enzyme L230W (right), as compared to the interactions between Leu230 and substrate in the wild-type enzyme (left). The black spheres represent the van der Waal's radius'.

The mutant enzyme D282N, where aspartic acid 282 had been replaced with asparagine, was the only other mutant enzyme involving an active site residue to be investigated. The flavocytochrome b_2 enzyme carrying this mutation for some peculiar reason seemed to react slightly better with oxygen, when all of the existing mutant enzymes available were screened for oxidase activity. Previously reported results concerning the purification and kinetic analysis of the intact flavocytochrome b_2 mutant

enzyme (Gondry *et al.*, 1995) could not be confirmed. The yield from the purification of this enzyme was at the same level as normally observed. The synchrony between folding and flavin insertion did thus not appear to be disrupted as otherwise suggested. The idea that a simple mutation should affect the folding seemed highly unlikely in the first place, and even more so when taking into account that a portion of the overexpressed protein folded and incorporated flavin perfectly normally. The cause of flavin-free enzyme is much more likely to be due to excessive loss of flavin during a tedious purification procedure involving superfluous ammonium sulphate precipitation and dialysis. The k_{cat} observed for the intact mutant enzyme was also significantly different from previously published results (Table 4.2). The Michaelis constants were identical within the error though, as also observed for the wild-type enzyme when using different buffers. The phenomenon is at least partly explained by the use of different buffers and temperatures. However, loss of flavin during the experimental procedure involved when determining the kinetic parameters cannot be excluded as another important factor.

	k_{cat} s^{-1}	K_m mM	k_{cat}/K_m $x10^6$ $M^{-1}s^{-1}$
Wild-type (Tris-HCl, 25°C)[¶]	400±10	0.49±0.05	0.82±0.12
Wild-type (Phosphate, 30°C)[†]	270±30	0.49±0.10	0.55±0.22
D282N (Tris-HCl, 25°C)	26±4	0.63±0.10	0.04±0.02
D282N (Phosphate, 30°C)[†]	3.9±0.1	0.73±0.05	0.0053±0.0005

Table 4.2. Steady-state kinetic parameters for wild-type and mutant enzyme D282N of intact flavocytochrome b_2. Taken from [†]Gondry et al. (1995); [¶]Miles et al. (1992).

The flavin-binding domain mutant enzyme was also characterised by steady-state kinetics. The DNA fragment containing the mutation was transferred to the expression vector pJF118EH. The protein was overexpressed in TG1 cells, transformed with the recombinant vector, after induction with IPTG. Even the very high level of expression observed when using this expression system did not cause problems with lack of co-ordination between protein folding and flavin insertion. This observation provided further circumstantial evidence that any flavin-free enzyme is much more likely to result from loss of the cofactor rather than failure to incorporate it during folding. The steady-state kinetic parameters for the flavin-binding domain were also affected by the mutation (Table 4.1, p. 72). The k_{cat} decreased nearly 200-fold, whereas the Michaelis constant only went up slightly. Hence, the mutation decreased both the apparent rate constant for the combination of substrate with free enzyme (k_{cat}/K_m) and the capacity of this complex to form product (k_{cat}). The introduced asparagine residue simply fails to facilitate the proton abstraction from L-lactate by His373. This task is normally performed by the aspartic acid, and it was predictable that mutation of Asp282 would

have a major impact on the catalysis. The substrate was not able to reduce the bound FMN efficiently, and the reductive half-reaction was so slow that it could be followed by eye (Figure 4.9). Unfortunately, this mutation did not make an oxidase either, but merely an extremely poor L-lactate dehydrogenase.

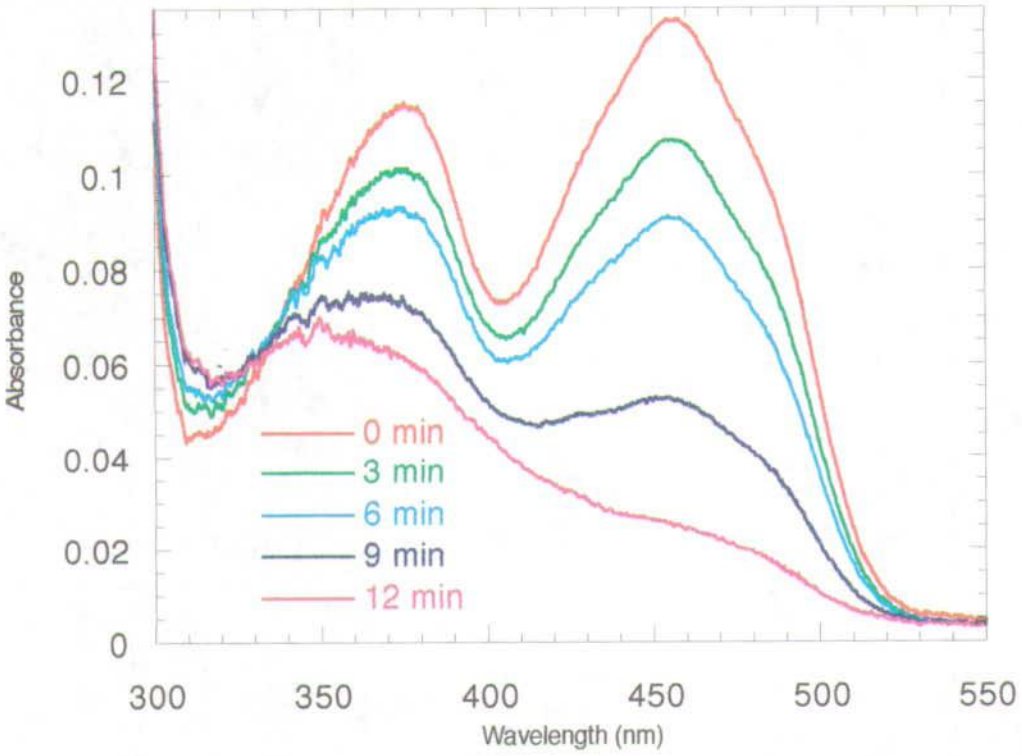

Figure 4.9. Absorption spectrum of 20.79 nmol mutant enzyme D282N of the flavin-binding domain in 10 mM Tris-HCl buffer pH 7.5 (I = 0.1M) recorded at 25°C in a 1 cm cuvette. An absorption spectrum was recorded every 3rd minute after addition of 10 µmol L-lactate (each spectrum was collected in about 10 seconds).

4.3. Conclusion

Site-specific mutagenesis obviously failed to generate the desired oxidase activity in the flavin-binding domain. The mutant enzymes created to generate more space around the bound flavin and thus better access of oxygen simply did not fulfil their promise. The reactivity towards dioxygen did generally appear to increase a little. However, this very minor increase in activity would probably also have arisen by introduction of many other mutations around the active site. The exclusion of oxygen is presumably evolutionarily optimised in flavocytochrome b_2, and perturbations will increase the level of background activity somewhat. Thus, none of the mutations really improved oxidase activity significantly.

It is not surprising that many of the introduced mutations cause a decrease in the dehydrogenase activity. All of the selected targets for mutation are located close to the active site, and are expected to change the conformation in this area. However, one exception was the mutation of Ala196 to a proline residue. The kinetic parameters remained unaffected even though this considerably more bulky side chain is situated right next to the flavin. The results confirmed that the residue at the position of Leu230 is important for determining the substrate specificity, but mutation of Ala198, Ala283, and Thr197 also seemed to influence the binding of substrate. The latter was possibly due to an indirect effect on the binding site, such as changes in the orientation of the isoalloxazine ring. Furthermore, the great importance of residue D282, in catalysis by facilitating the proton abstraction by His373, was confirmed.

The lack of success in producing oxidase activity by site-directed mutagenesis of the flavocytochrome b_2 flavin-binding domain suggests that a single mutation may not be sufficient to swing the function of the enzyme from being a dehydrogenase to being an oxidase. A number of double mutations, based on the above described mutations, were constructed and screened for oxidase activity. However, none had improved oxidase activity and their dehydrogenase activity was extremely poor. Any further characterisation was abolished due to the prohibitively large quantities of enzyme needed. Requirement of two or more simultaneous mutations to improve the oxidase activity significantly would make protein engineering an immensely difficult task.

Alternatives are obviously needed in the continued search for what determines oxidase activity. The possibilities includes construction of hybrid enzymes and introduction of multiple mutations at random before selecting or screening for clones with the wanted activity. The first alternative approach will be considered in the next chapter, where the role of a specific loop region is studied. The approach could be extended to cover other loop regions or other parts of the protein structure. The degree of the similarity between the three-dimensional structures of flavocytochrome b_2 and glycolate oxidase is so high that hybrid enzymes need not be misfolded and inactive by default. The identification of a chimera with oxidase activity could then be used as a starting point for either narrowing the region swapped or for construction of site-specific mutations. The techniques of DNA shuffling offers a convenient way of mixing the two genes as will be described later in chapter 6. The approach of random mutagenesis is somewhat related to the mixing of genes. However, it will mutate the gene for the flavin-binding domain at random, as opposed to mixing of the genes, which only introduce clusters of amino acid residues present in glycolate oxidase. The random mutagenesis approach combined with an appropriate selection procedure will also be dealt with in chapter 6.

5. The Role of the Disordered Loop Region in Controlling Oxidase Activity

5.1. Introduction

Comparison of the structures of flavocytochrome b_2 and glycolate oxidase provides very few clues as to the reasons for their marked difference in reactivity towards oxygen. Important information may indeed be hidden, as parts of both structures are "invisible". The crystal structures of flavocytochrome b_2 and glycolate oxidase both exclude parts of a surface loop between strand four and helix four of the β/α-barrel, which is disordered in the electron density map. The amino acid residues 300-311 are not visible and 298-299 are poorly ordered in subunit 2 of flavocytochrome b_2 (Xia & Mathews, 1990). In glycolate oxidase, residues 189-197 of the corresponding loop are disordered (Lindqvist, 1989). However, the observable course of the peptide chain in loop four is totally different between positions 296 and 325 of flavocytochrome b_2 and glycolate oxidase. Most of the segment in glycolate oxidase is located outside the carboxyl end of the β-strands of the barrel and forms a lid on the barrel, which partly shields the active site. The loop is moved away from the active site in flavocytochrome b_2, and is replaced by the cytochrome domain (Lindqvist *et al.*, 1991). The loop region is also sensitive to proteolytic attack, and is thus considered both exposed and flexible. Yet, the cleavage of a single bond caused an increase in the K_m and a decrease in the k_{cat} value (Ghrir & Lederer, 1981). This observation indicates some interactions between the loop and the active site. Mutation of residue Ala306 of the loop region to a serine has also been found to influence the kinetic parameters (Reid *et al.*, 1988). The substitution reduced the value of k_{cat} slightly, whereas K_m nearly doubled. These effects are presumably arising from conformational changes in the loop region, and substantiate the suggested interaction of this region with the active site.

The work described in this chapter was undertaken to elucidate the role of the disordered loop region in catalysis or the structure of the enzymes. Its function has naturally been impossible to deduce from structural information. Some indication of the importance of the loop region comes from other studies of analogous loops in related enzymes. The corresponding loop in L-mandelate dehydrogenase from *P. putida* seems to be responsible for the membrane association of this enzyme (Mitra *et al.*, 1993). Dihydroorotate dehydrogenase A from *L. lactis* also has a flexible loop at the same position of its β/α-barrel, which controls access to or from a cavity above the FMN (Rowland *et al.*, 1997). The reduced form of this enzyme is reoxidised by various electron acceptors including oxygen. Its closest known relative, as judged by structural similarity, is flavocytochrome b_2. Superposition of 234 C^{α}-atoms from the

two enzymes gave an root mean square deviation of 3.0 Å, with a corresponding sequence identity between equivalenced residues of 13%. Likewise, a mobile loop in lactate dehydrogenase from *B. stearothermophillus* has been linked to the substrate specificity of this enzyme, and several mutants with new specificities have been constructed by engineering changes into this loop (El Hawrani *et al.*, 1994). The possible function of the disordered loop in flavocytochrome b_2 in controlling oxygen reactivity and other kinetic parameters has been studied by construction and characterisation of several mutant enzymes. The results obtained from the study are presented in this chapter.

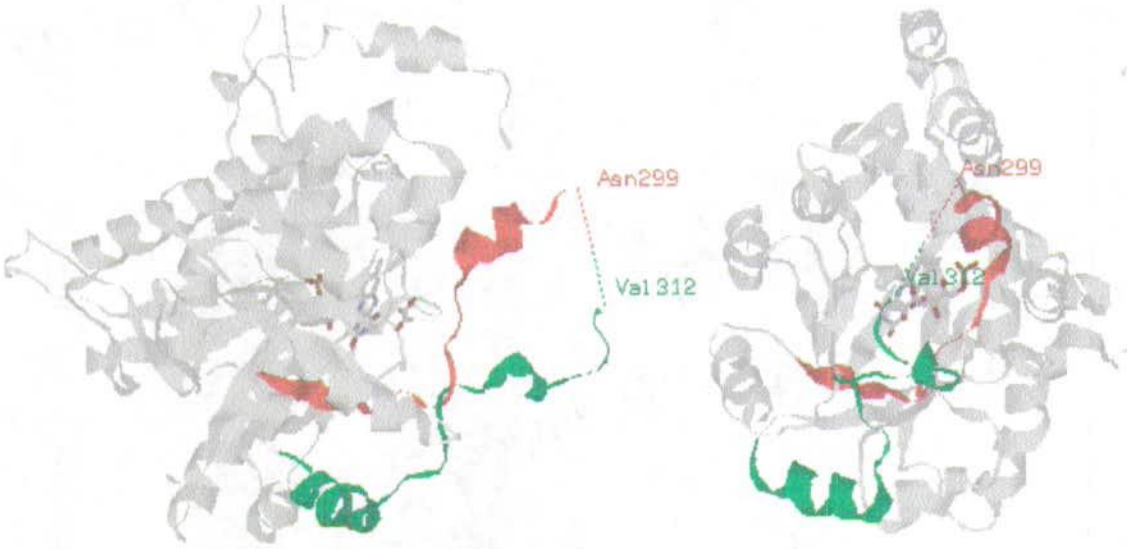

Figure 5.1. Subunit 2 of the crystal structure of flavocytochrome b_2. The model to the right is a view from the top of the TIM-barrel where the bound FMN is located. The figure to the left shows the same model, but rotated 90° around the y-axis. Strand four and helix four are highlighted in red and green, respectively. A part of the connecting loop is disordered, but indicated by a dotted line.

5.2. Results and discussion

5.2.1. The deletion and insertion mutations

The natural variation that exists among the FMN-dependent 2-hydroxy acid oxidising enzymes in the length and composition of the loop in question has been subject to discussion previously in section 1.10.1 (p. 25). It was established that there is no detectable sequence conservation in this region. The role of the loop has been studied by changing its length and replacing it with the loop from glycolate oxidase. The deletion and insertion mutations were performed in multiples of three amino acid residues (Figure 5.2). The rationale for doing so was that the loop of glycolate oxidase is six residues longer. Hence, replacement of the loop in flavocytochrome b_2 with that

of glycolate oxidase would increase the length by six residues. Besides, decreasing or increasing the length by three residues is much more likely to significantly change the kinetic parameters than smaller steps. The residues deleted are situated just prior to the site susceptible to attack by yeast proteases, but they are nevertheless a part of the disordered loop. The three residues were deleted by site-specific mutagenesis using the Kunkel strategy. The deletion (dAGP) only included aliphatic residues, changes in the charge were thus avoided, and the observations will merely reflect the effects of a physically shorter loop.

Figure 5.2. Sequence alignment of the loop regions of mutant and wild-type enzymes. The disordered residues are shown in red, whereas the green colour indicates deleted or inserted residues. The peptide bonds cleaved by yeast proteases are positioned between underlined residues.

Two insertion mutations were constructed by insertion of three (i3A) and six alanine residues (i6A) within the disordered loop region. Alanine is the smallest aliphatic amino acid, and confers some restriction to the flexibility of conformation as opposed to glycine. This amino acid also has the important property of not interacting favourably with water, but rather with other nonpolar atoms. These mutations will thus provide a framework for assessment of the consequences when increasing the length of the loop but not changing other properties. The alanine residues were inserted immediately after the three aliphatic residues that were removed in the deletion mutant enzyme. This task was also accomplished by the standard site-specific mutagenesis technique of Kunkel. The oligos used were constructed in a way that exploited the degeneracy of genetic code for alanine. This precaution eliminated formation of secondary structures in the sequence, which might otherwise have interfered with both mutagenesis and sequencing.

	k_{cat} s^{-1}	K_m (L-lactate) mM	k_{cat}/K_m (L-lactate) $10^6\ M^{-1}s^{-1}$	$\Delta\Delta G^{\neq}$ (J/mol)	$K_m(Fe(CN)_6^{3-})$ mM
WT	279±5	0.34±0.02	0.82±0.07	-	0.46±0.04 (4)
dAGP	88±2	1.55±0.10	0.055±0.005	6,700±400	0.36±0.04 (3)
i3A	265±5	0.40±0.03	0.66±0.07	500±500	0.35±0.04 (3.5)
i6A	166±2	1.00±0.04	0.166±0.009	4,000±300	0.27±0.05 (3.5)

Table 5.1. Steady-state kinetic parameters of mutant enzymes involving residues of the disordered loop region. Assays were performed in 10 mM Tris-HCl pH 7.5 (I = 0.1 M) at 25°C using ferricyanide as electron acceptor. The concentration of acceptor used is given in brackets after the K_m value obtained for ferricyanide at saturating L-lactate levels. The values of $\Delta\Delta G^{\neq}$ were calculated using the k_{cat}/K_m values (section 2.2.4, p. 47).

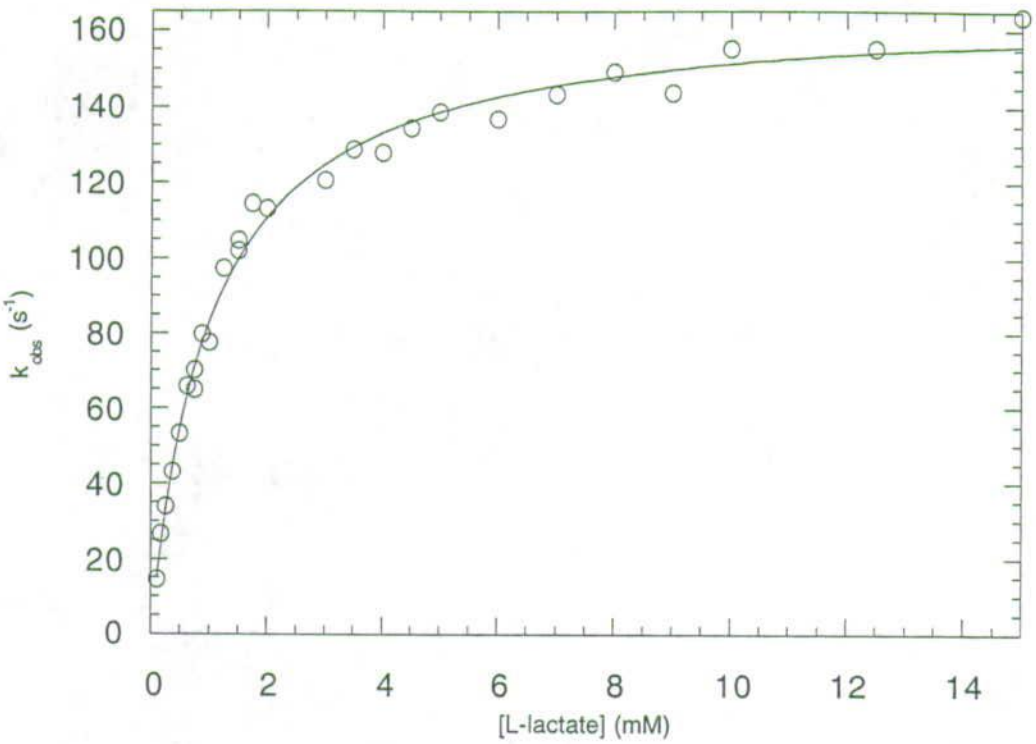

Figure 5.3. Plot of the steady state data for mutant enzyme i6A of the flavin-binding domain fitted to the Michaelis-Menten equation. The plot represents a typical set of data from steady-state assays using ferricyanide as the electron acceptor.

The constructed mutants were all subjected to analysis of their steady-state kinetic behaviour in terms of both dehydrogenase and oxidase activity. The maximum rate of hydrogen peroxide production when turning over L-lactate was determined as 0.002 s^{-1} for all four mutants. This is about 5000-fold less than the corresponding rate observed for glycolate oxidase. Although the rates are improved as compared to the wild-type enzyme, it can not be justified to label these mutant enzymes as being oxidases. It seems as if flavocytochrome b_2 has optimised the elimination of oxidase activity and that any small perturbation gives rise to a somewhat higher level of background activity. It is obvious when using ferricyanide as an artificial electron acceptor, that the mutant enzymes still function quite well in their capacity as L-lactate dehydrogenases (Table 5.1). These observations nevertheless reveal a number of interesting properties of the loop. The consequence of shortening the loop are much more dramatic than increasing the length of the loop (Figure 5.4). The apparent rate constant for combination of L-lactate with free enzyme only decreased five-fold even when inserting six alanine residues. Whereas, deletion of merely half as many residues decreased the value fifteen times. The shortened loop would presumably be less mobile than the wild-type loop. A consequence could possibly be that the active site becomes better shielded from the solvent. This would naturally make it more difficult for the substrate to access the site. However, the limiting rate was also affected and hence

deletion of three amino acid residues presumably also introduce some conformational changes in the active site. These changes could possibly be caused by strain forced upon the connecting or surrounding residues. Alternatively, specific residues in the loop itself are involved in the catalysis or interact with catalytically active residues. These interactions would then be disrupted due to conformational changes induced by the shortening. However, this seems unlikely due to the non-homogeneity in the loop region, as compared to the high degree of conservation in active site residues between family members.

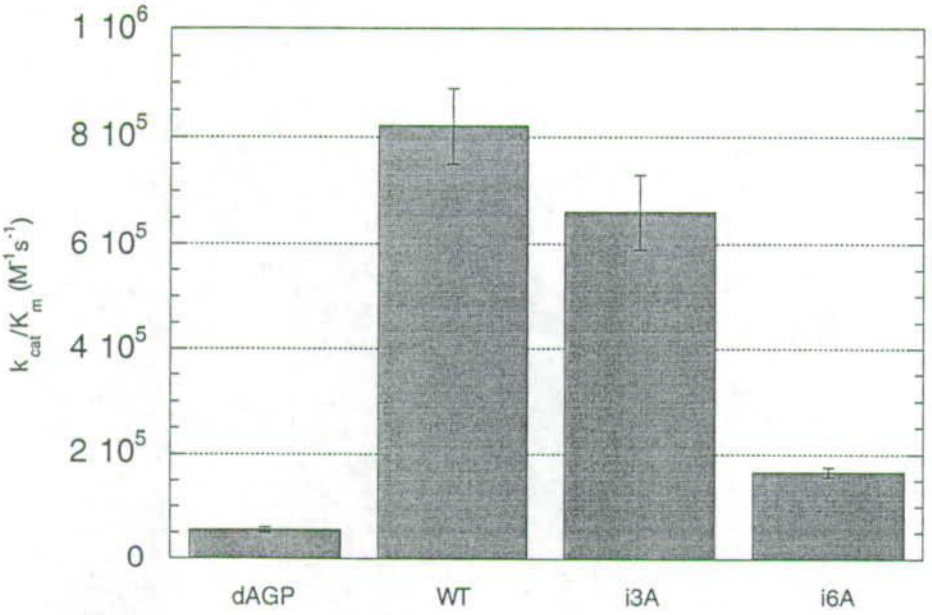

Figure 5.4. The apparent rate constant for combination of L-lactate and free mutant enzymes compared to the rate constant for the wild-type enzyme.

The possible involvement of the loop region in intra- and preceding inter-molecular electron transfer to flavocytochrome b_2-haem and cytochrome *c*, respectively, was briefly investigated. Only the mutant with six alanine residues inserted was studied, as this was considered representative all for the charge neutral deletion and insertion mutations. The intact flavocytochrome b_2, which carried the insertion, was purified and characterised as described in the relevant section of the methods. The steady-state kinetic parameters, using either ferricyanide or cytochrome *c* as electron acceptor, show the same trends as observed for the flavin-binding domain (Table 5.2). The values of the Michaelis constants increase, whereas the limiting rates decrease. This is naturally reflected in the calculated values of both the apparent rate constant for combination of L-lactate with free enzyme and change in the free energy of the transition state ($\Delta\Delta G^{\neq}$). However, the six residue insertion did not alter the parameters to the same extent in the intact enzyme as compared to the flavin-binding domain when using ferricyanide as electron acceptor. Instead, the transfer of electrons onto the

natural electron acceptor was more affected for the intact enzyme. The catalytic step, responsible for the observed changes, was attempted identified by measuring their individual rates by stopped-flow spectrophotometry.

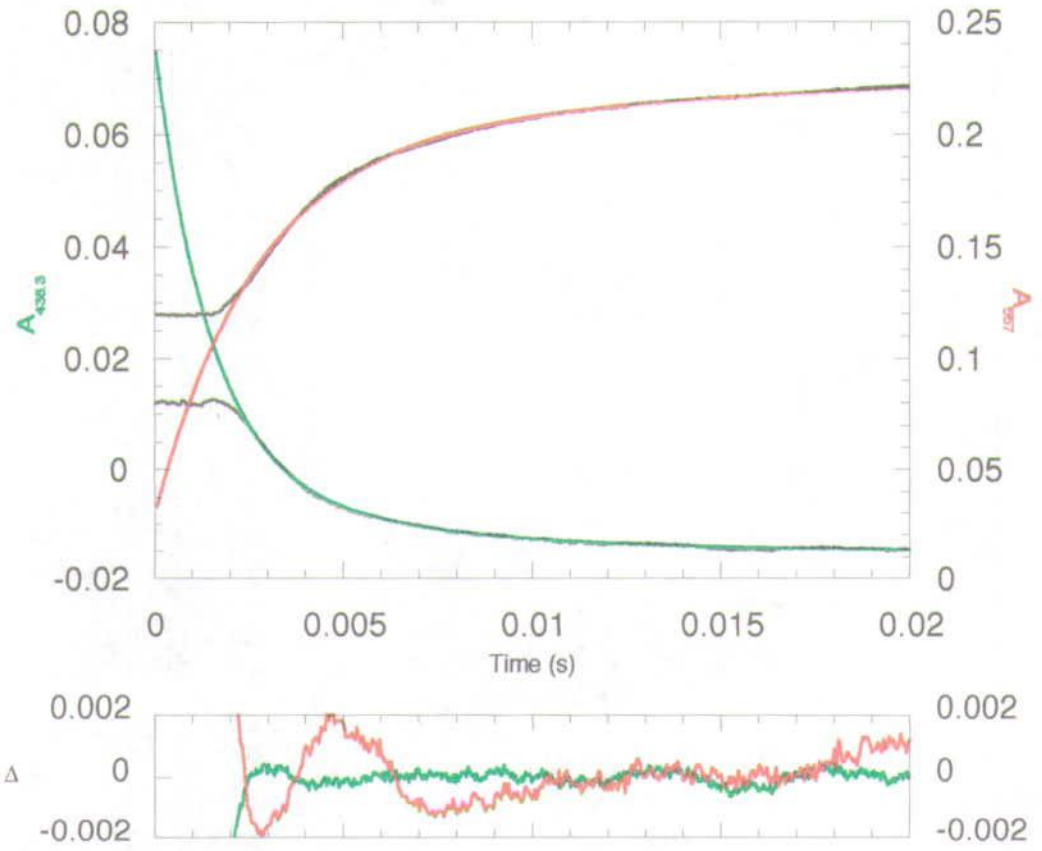

Figure 5.5. Stopped-flow traces showing reduction of FMN (black/green fit) and haem (black/red fit) after mixing 20 mM L-lactate with 20 μM enzyme. The traces were fitted by non-linear least-squares regression to a double exponential function. The difference plots shown were calculated by subtracting the fit functions from the acquired data.

	k_{cat} s^{-1}	K_m (L-lact) mM	k_{cat}/K_m (L-lact) $x10^6$ $M^{-1}s^{-1}$	$\Delta\Delta G^{\neq}$ J/mol	$K_m(Fe(CN)_6^{3-}]$ or [cyt. *c*]) mM or μM
WT† ($Fe(CN)_6^{3-}$)	400±10	0.49±0.05	0.82±0.11	-	« 0.1 (2)
i6A ($Fe(CN)_6^{3-}$)	272±4	0.63±0.04	0.43±0.04	1,600±600	0.022±0.005 (3)
WT† (cyt. *c*)	207±10	0.24±0.04	0.86±0.23	-	10±1 (35)
i6A (cyt. *c*)	97±3	0.71±0.08	0.14±0.02	4,500±1,000	18±3 (100)

Table 5.2. Steady-state kinetic parameters determined for intact flavocytochrome b_2 with six alanine residues inserted in the loop region. Assays were performed in 10 mM Tris-HCl pH 7.5 (I = 0.1 M) at 25°C. The concentration of acceptor used is given in brackets after the K_m value obtained for the acceptor at saturating L-lactate concentrations. The 3 mM ferricyanide used corresponds to 99.3% of saturation, while 100 μM cytochrome c corresponds to 84.8% saturation. The values of $\Delta\Delta G^{\neq}$ were calculated using the k_{cat}/K_m values (section 2.2.4, p. 47). The parameters for the wild-type enzyme are also listed and were taken from †Miles et al. (1992).

The pre-steady-state limiting rates for both flavin and haem reduction were determined by mixing 20 mM L-lactate with 20 μM enzyme and recording the change in absorbance at 557 nm and 438.3 nm in a stopped-flow apparatus (Figure 5.5). The rate of FMN-reduction by L-lactate was determined to be 692 s^{-1} by fitting the trace to a double exponential function, and hence nearly falls within range of 604±60 s^{-1} reported for the wild type enzyme (Miles *et al.*, 1992). The rate of haem reduction did not change significantly either. The value was 370 s^{-1} as compared to 445±50 s^{-1} for the wild type enzyme (Miles *et al.*, 1992). Thus, neither flavin nor haem reduction was slowed down by a longer loop. The affected step is likely to be the intramolecular electron transfer between FMN semiquinone and b_2-haem. This step has previously been identified to rate-limit the overall catalytic cycle for the wild type enzyme (Daff *et al.*, 1996a), and it thus makes sense that the rate is very susceptible to changes affecting this particular step. Hence, the length of the loop appears to either change the stability of the flavin semiquinone or interfere with the efficiency of flavin-haem interaction.

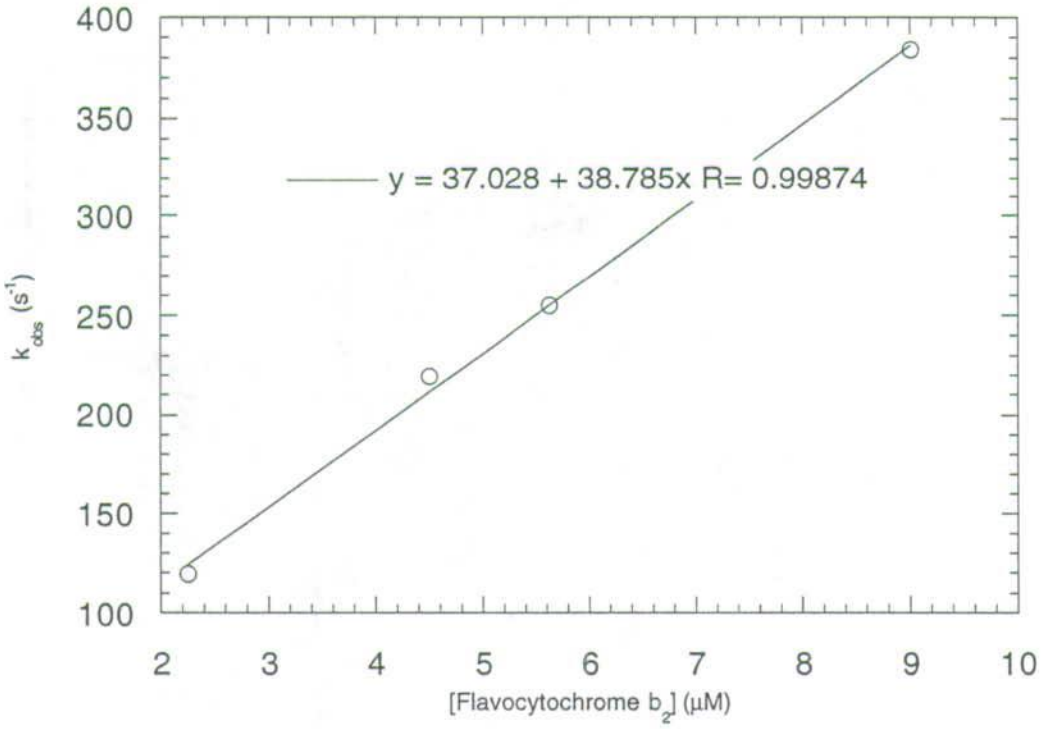

Figure 5.6. Derivation of the second-order rate constant for cytochrome c reduction. Pseudo-first order rate constants for cytochrome c reduction (k_{obs}) are plotted against flavocytochrome b_2 concentration and the data points are fitted to a straight line. Cytochrome c reduction was monitored by the change in absorbance at 416.5 nm on mixing 2 μM oxidised cytochrome c with 20 mM L-lactate and flavocytochrome b_2 in a stopped-flow apparatus. The rate constants were determined by fitting each trace to a single exponential function.

The insertion of six extra residues in the loop did not have any effect on the second-order rate constant for cytochrome *c* reduction. The rate constant was determined to 38.8 $\mu M^{-1}s^{-1}$ (Figure 5.6), which is identical to the rate of 34.8±0.9 $\mu M^{-1}s^{-1}$ observed for the wild-type enzyme (Daff *et al.*, 1996b). The loop is thus unlikely to be an important component of the cytochrome *c* binding site. Indeed, modelling studies have identified a region on the cytochrome domain as the docking site (Short, 1996).

5.2.2. The chimera mutations

Three different hybrid enzymes, consisting of loop regions from glycolate oxidase replaced with the corresponding loop of flavocytochrome b_2 (Figure 5.7), were constructed by cloning of fragments amplified by PCR. The number of possible constructs are limited by the necessity of restriction sites bordering the fragment to be replaced. Actually, no suitable restriction sites are present in the native DNA sequence of flavocytochrome b_2. Artificial restriction sites thus had to be engineered by site-specific mutagenesis. However, the introduced mutations should preferably be silent with respect to either flavocytochrome b_2 or glycolate oxidase. The new sites also ought to be unique sites to simplify the cloning and increase the rate of success greatly. Furthermore, the practical handling of PCR products puts a lower limit on the size of the DNA fragment to be replaced using this procedure.

```
FCb2       280 TVDAPSLGQREKDMKLKFSNTKAGP------KAMKKTNVEESQGASRALSKFIDPSL 330
Swap I         TVDTPRLGRREADIKNRFVLPPFLTLKNFEGIDLGKMDKANDSGLSRALSKFIDPSL
Swap II        TVDAPSLGQREKDMKLRFVLPPFLTLKNFEGIDLGKMDKANDSGLSSYVAGQIDPSL
Swap III       TVDAPSLGQREKDMKLRFVLPPFLTLKNFEGIDLGKMDKANDSGLSRALSKFIDPSL
GO         155 TVDTPRLGRREADIKNRFVLPPFLTLKNFEGIDLGRMDKANDSGLSSYVAGQIDRSL 211
```

Figure 5.7. Sequence alignment of hybrid enzymes involving replacements in the disordered loop region. Residues shown in red are disordered in the electron density maps. Residues from glycolate oxidase, which have replaced the corresponding loop residues in flavocytochrome b_2, are shown in green.

The longest loop replacement (swap I) was based on two restriction sites, *Sal*I and *Sac*I(*Sst*I), that had been engineered into the gene of flavocytochrome b_2 by Dr. Forbes D.C. Manson. The cloning of the amplified fragment from glycolate oxidase was relatively straight forward as illustrated in Figure 5.8. The medium length replacement (swap II) was not only shortened by six amino acid residues but also shifted downstream. The replacement was constructed to avoid changes in the conformation of residue Asp282, which is known to take part in the catalysis (see section 4.2.4, p. 79). The construction of this medium replacement required engineering of two new restriction sites, *Cla*I and *Hin*dIII, into the gene of flavocytochrome b_2. The *Cla*I site was found to be subject to methylation, and hence

all manipulation had to be performed in the dam⁻ *E. coli* strain JM110. Neither of the new sites were unique restriction sites, which further complicated the subsequent cloning of the amplified fragment from glycolate oxidase. The cloning procedure is summarised in Figure 5.9. Briefly, the two new restriction sites were introduced into separate copies of pGR401. These were then completely digested with *Eco*RI and the enzyme cutting at the new site. The two fragments were isolated by gel electrophoresis. Finally, these two fragments were ligated together with the amplified DNA fragment from glycolate oxidase in a three fragment ligation. The construct was transferred to an expression vector as a fragment digested with *Xba*I and partially with *Hin*dIII. The shortest replacement (swap III) was based on the restriction sites already used in the making of the previous two mutants. Use of the *Hin*dIII and *Sac*I sites generated a loop replacement involving seven residues fewer than the medium sized replacement. Hence, the residues involved in the replacement would include little more than the ones in the disordered loop region of flavocytochrome b_2. The basis of this construct was a vector with an additional *Hin*dIII site introduced into the version of pGR401 already having the *Sac*I and the *Sal*I site engineered. The PCR fragment was cloned into the vector after it had been partially digested with *Hin*dIII and then completely cut with *Sac*I (Figure 5.10). This construct was also transferred to an expression vector as a fragment digested with *Xba*I and partially with *Hin*dIII.

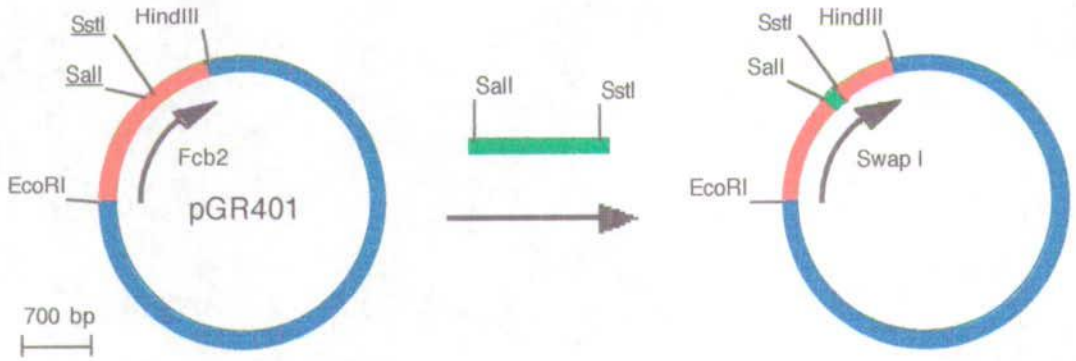


```
          ... Thr Val Asp Ala ... ... ... Ala Ser Arg Ala Leu ...
FCb2      ... ACT GTG GAT GCT ... ... ... GCT TCG AGA GCT TTA ...
SalI      ... ACT GTC GAC GCT ... ... ... GCT TCG CGA GCT CTA ...   SacI
PCR             TC GAC ACA ... ... ... CTT TCC AGA GCT
Hybrid    ... ACT GTC GAC ACA ... ... ... CTT TCC AGA GCT CTA ...
          ... Thr Val Asp Thr ... ... ... Leu Ser Arg Ala Leu ...
```

Figure 5.8. Scheme showing the construction of hybrid enzyme "Swap I". The product of the PCR reaction (not drawn to scale) replaced a SalI-SstI fragment of the gene encoding flavocytochrome b_2. The relevant parts of the nucleotide sequences are also shown. The two restriction sites (SalI & SstI), introduced by site-specific mutagenesis, are underlined. The sequence of the PCR product after digestion with SalI & SstI is displayed in green. Finally, the sequence of the resulting hybrid enzyme is shown along with the encoded amino acid sequence.

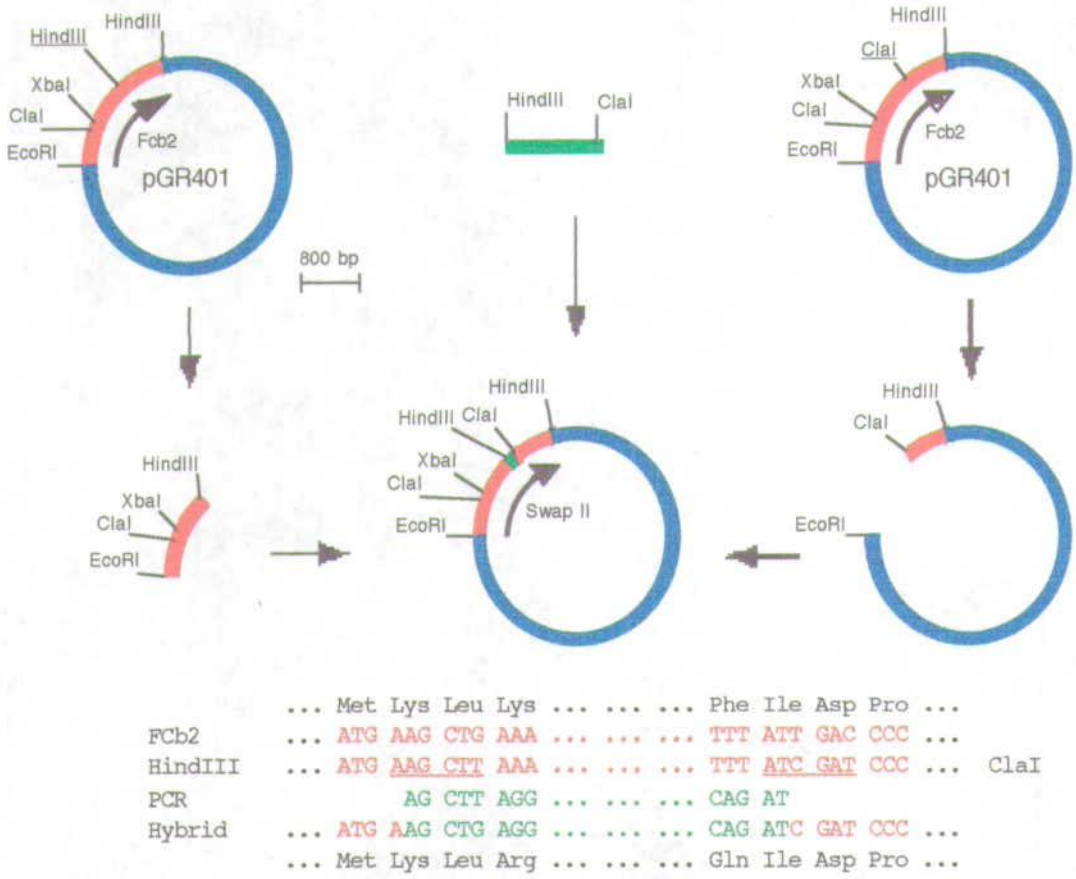

Figure 5.9. Scheme showing the construction of hybrid enzyme "Swap II". The product of the PCR reaction (not drawn to scale) replaced a HindIII-ClaI fragment of the gene encoding flavocytochrome b_2. The relevant parts of the involved nucleotide sequences are also shown. The two restriction sites, introduced by site-specific mutagenesis, are underlined. The sequence of the PCR product after digestion with HindIII and ClaI is displayed in green. The sequence of the resulting hybrid enzyme is also shown along with the encoded amino acid sequence.

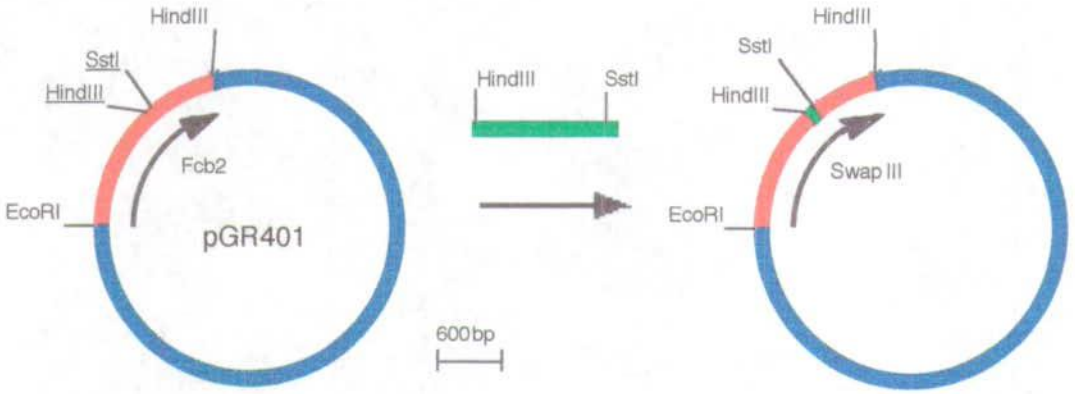

Figure 5.10. Scheme showing the construction of hybrid enzyme "Swap III". The product of the PCR reaction (not drawn to scale) replaced a HindIII-SstI fragment of the gene encoding flavocytochrome b_2. See Figure 5.8 and Figure 5.9 for details on the involved nucleotide sequence. The SalI site (upstream HindIII & SstI; not shown) does not introduce changes in the amino acid sequence of flavocytochrome b_2.

The constructed mutant enzymes with loop replacements were all analysed by steady-state kinetics to determine their dehydrogenase and oxidase activities. Again, all mutations failed to increase the oxidase activity above the basal level observed for every loop mutant enzyme. However, the L-lactate dehydrogenase activity was considerably lowered by swapping parts of the loop for the corresponding regions from glycolate oxidase (Table 5.3).

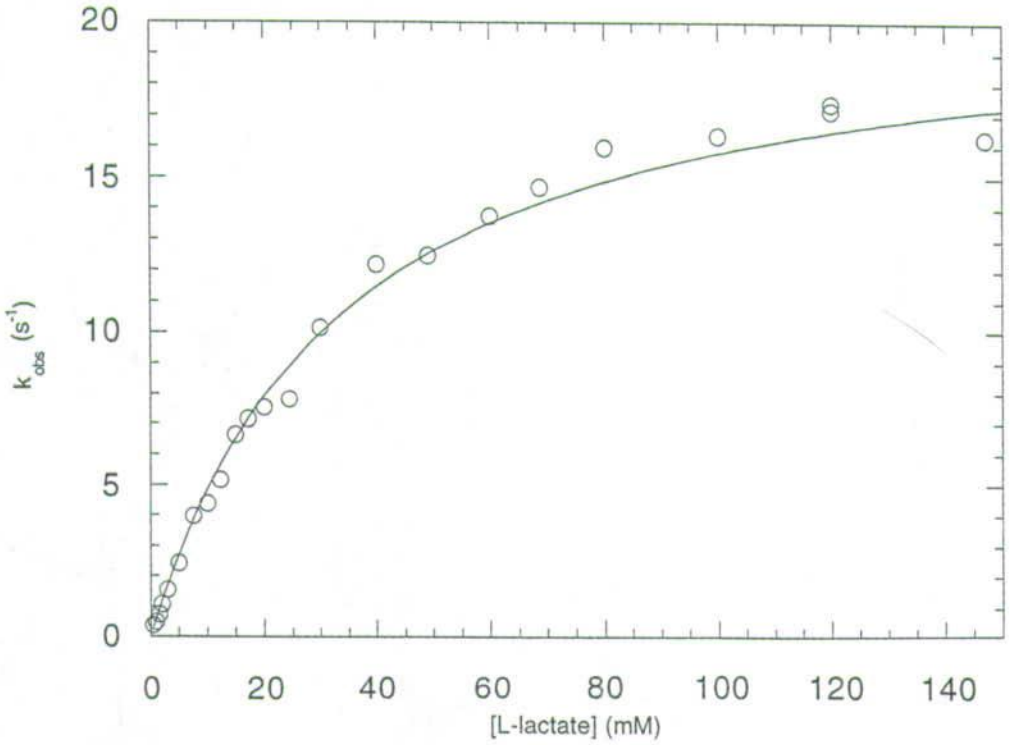

Figure 5.11. Plot of the steady state data for mutant enzyme "Swap I" of the flavin-binding domain fitted to the Michaelis-Menten equation. The plot represents a typical set of data from steady-state assays using ferricyanide as the electron acceptor.

	k_{cat} s^{-1}	K_m (L-lact) mM	k_{cat}/K_m (L-lact) $x10^6$ $M^{-1}s^{-1}$	$\Delta\Delta G^{\neq}$ J/mol	K_m ($Fe(CN)_6^{3-}$) mM
WT	279±5	0.34±0.02	0.82±0.07	-	0.46±0.04 (4)
Swap I	21.1±0.6	33±3	0.00064±0.00008	17,700±500	1.71±0.08 (15)
Swap II	14.2±0.3	5.0±0.5	0.0028±0.0004	14,100±600	0.44±0.07 (6)
Swap III	51.2±0.5	1.04±0.04	0.049±0.003	7,000±400	3.3±0.3 (7.5)

Table 5.3. Steady-state kinetic parameters of mutant enzymes involving residues of the disordered loop region. Assays were performed in 10 mM Tris-HCl pH 7.5 (I = 0.1 M) at 25°C using ferricyanide as electron acceptor. The concentration of acceptor used is given in brackets after the K_m value obtained for ferricyanide at saturating L-lactate levels. The values of $\Delta\Delta G^{\neq}$ were calculated using the k_{cat}/K_m values (section 2.2.4, p. 47).

The greatest effect was observed for the mutant enzyme involving the largest replacement. The K_m of L-lactate was badly affected and the Michaelis constant increased to around 33 mM. The limiting rate was not affected to the same extent. This

indicates that the enzyme-substrate complex still is able to form product with a reasonable rate, but that the formation of the complex in the first place is somewhat hindered. The apparent rate constant for combination of substrate with free enzyme was decreased more than 1,000-fold (Figure 5.12). The recombinant enzyme is such a very poor L-lactate dehydrogenase, that it barely deserves to be labelled as a L-lactate oxidising enzyme. However, the replacement of residues right next to the important Asp282 did not have detrimental consequence for the limiting rate. This becomes apparent when comparing the rate with that of the medium-sized loop replacement mutant, which was shortened with six residues and shifted downstream from Asp282. The limiting rate for this mutant enzyme is actually lowered even further. However, the Michaelis constant dropped drastically in comparison to that of the long loop replacement mutant. This causes an increase in the apparent rate constant for combination of substrate and free enzyme. The loop replacement of the third hybrid enzyme included yet fewer amino acid residues. Furthermore, these amino acid residues merely constitute the disordered fragment itself with a minor extension of about three residues on either side. The Michaelis constant of this mutant enzyme is identical to the one for the mutant enzyme with six neutral alanine residues inserted. The limiting rate is more than three times lower though, and the change in the composition of the region along with the number of residues replaced is obviously of great importance to the active site and its residues.

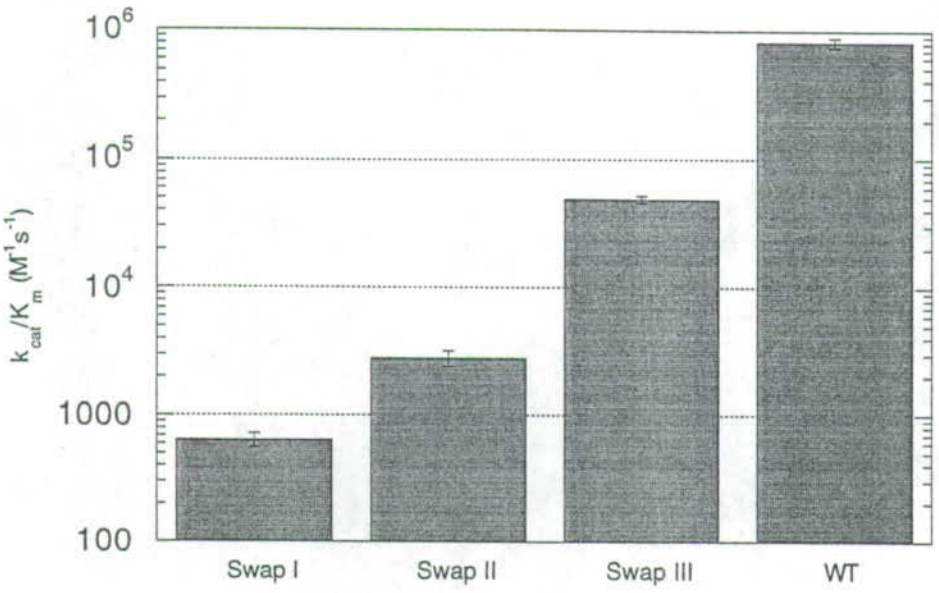

Figure 5.12. The apparent rate constant for combination of L-lactate and free loop replacement mutant enzymes compared to the rate constant for the wild-type enzyme.

This finding was confirmed by the visible absorption spectrum of the bound flavin. The absorption spectrum is determined by interactions between the protein moiety and FMN, and alterations in ionic and hydrogen bonds result in changed spectral properties. An overlay of the spectra for FMN bound in the flavin-binding domain and glycolate oxidase show shifts in both the positions of maxima and relative high of the peaks. The spectrum for the mutant enzyme with the largest loop replacement shares properties with the spectra for both wild-type enzymes, and is best described as an intermediate between the two (Figure 5.13). It is thus obvious that the amino acid residues in the loop region also interact, directly or indirectly, with the FMN molecule itself. The same observations were done for all the other replacement mutants, and the extent of these spectral changes corresponded to the number of amino acid residues involved in the replacement. The largest replacement thus also gave the largest degree of spectral changes. The altered composition was also observed to influence the reaction between reduced enzyme and ferricyanide. The explanation is probably that the replaced fragments had a more positive charge. Hence, the interaction with the highly negatively charged ferricyanide becomes less favourable due to electrostatic forces.

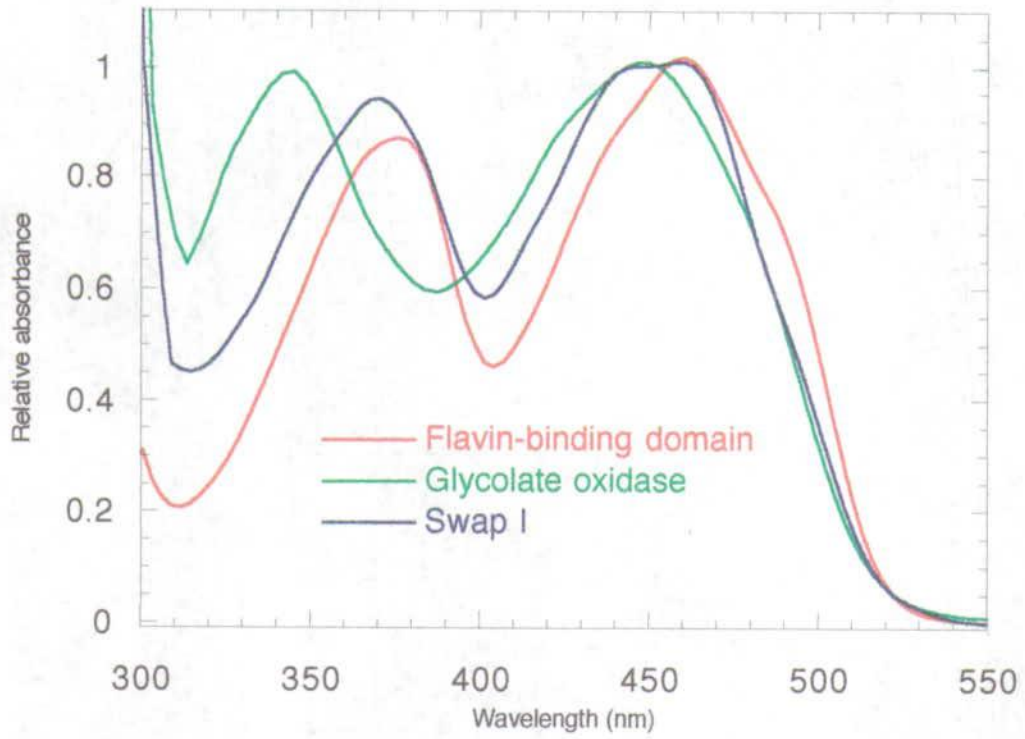

Figure 5.13. Absorption spectra of mutant enzyme "Swap I" and the wild-type enzymes normalised at λ = 454 nm. The original spectra were recorded in 10 mM Tris-HCl pH 7.5 (I = 0.1 M) at 25°C using a 1 cm cuvette.

5.3. Conclusion

This study has demonstrated that the loop region is able to accommodate quite dramatic changes in both length and composition without alteration of the overall structure. The protein is still folded correctly and retains dehydrogenase activity even when replacing the loop region with that of glycolate oxidase. The steady-state kinetic parameters do change significantly though, and this is primarily caused by the introduction of amino acids with chemically different properties. The length of the loop is not as critical, and insertion of three extra alanine residues hardly affects the steady-state kinetic parameters. The mutant enzyme with six inserted alanine residues has the same length of the loop as the replacement mutants, but functions much better as a L-lactate dehydrogenase in comparison with these. The steady-state parameters for the mutants with loop replacements depends both on the number of residues included and on the exact location of the replacement. The mutant, whose replacement covers merely the disordered fragment (Swap III), still works remarkably well as a dehydrogenase when the large number of effective mutations in close proximity to the active site are taken into consideration. The mutants, where the replaced region is extended either to the N- or C-terminal end, are much more affected. The Michaelis constant is dramatically increased for the mutant with an extension in the direction of the protein's N-terminal end (Swap I). This is naturally reflected in the apparent rate constant for the combination of substrate with free enzyme (k_{cat}/K_m). It is questionable whether labelling this mutant as a L-lactate dehydrogenase can be justified. However, the complex between enzyme and substrate definitely still has the capacity to form product once the complex itself is formed. Extending the replacement in the other direction (Swap II) does not affect the k_{cat}/K_m to the same extent, and the enzyme still recognises and binds L-lactate reasonably well. Instead, the capacity of the substrate-enzyme complex to form product (k_{cat}) is lowered even further.

The consequences of shortening the loop region by deleting three amino acid residues are surprisingly large. The effects are possibly the result of conformational changes imposed on the active site by steric effects. Furthermore, the mobility of the loop could be of great importance for the catalysis and would obviously be decreased by the shortening. The observation that increasing the length does not alter the steady-state kinetic parameters, along with the fact that the loop is disordered, support this idea of mobility. The hypothesis that the loop region includes catalytically active residues and their position or conformation change is unlikely. The main objection is that the loop region is hypervariable within the family. The loop does interact with the active site as demonstrated by the changed spectral properties observed for the mutant enzymes.

However, the region does not appear to control the reaction catalysed, that is, whether the reduced FMN is reoxidised by dioxygen or not. The interaction between the reduced enzyme and the artificial electron acceptor ferricyanide is affected by the alterations in charge of the loop though (see values of K_m for ferricyanide in Table 5.3, p. 95), but this can not be ascribed any physiological importance. Instead, the loop region seems to fulfil a role in the interaction between substrate and free enzyme, as the k_{cat}/K_m values changed considerably. However, the mutant enzymes with loop replacements did not turn glycolate over any better than the wild-type enzyme. Indeed, the interaction is known to be influenced by non-loop residues as well (see section 4.2.4 on the L230W mutation, p. 79). It is all too obvious that the loop region has evolved along with the rest of the enzyme. The integrity of the loops is obviously of great importance for the specific reaction catalysed by the individual enzymes in the family, and simply swapping the loops around does not confer changes in the reactivity although the activity is affected.

It has become painfully obvious that the exact interpretation of the kinetic data in relation to function of the loop region is somewhat difficult. The problem is the lack of structural data for major parts of this region. The deficiency could theoretically be alleviated by molecular modelling. However, modelling of a loop region is normally considered highly inaccurate and unreliable. The rule of thumb is that loops consisting of three to six are reasonably predictable, but the disordered segment of flavocytochrome b_2 includes at least twice as many residues. Furthermore, a disordered part in a crystal structure is normally taken as an indication of the region either being mobile or existing in several different conformations. Another difficulty in modelling a loop region is that energy minimisation often generates rather meaningless results. Instead, good results generally rely on comparison with similar loops of known structure. None of the related proteins, whose crystal structures have been elucidated, have a well ordered loop. Hence, the idea of modelling the loop region was abandoned, and the nature of the interactions between the loop and the active site remain undisclosed.

6. Forced Evolution of a Dehydrogenase to an Oxidase

6.1. Introduction

The limitations of site-specific mutagenesis have been demonstrated only too well in the previous chapters. Engineering oxidase activity into a dehydrogenase failed because the structural features controlling the reactivity are not defined. There is a striking lack of knowledge about the chemistry of the reaction between oxygen and reduced FMN in oxidases. Furthermore, the structural information available does not provide many clues as to why the reactivity of glycolate oxidase differs from that of the flavin-binding domain in flavocytochrome b_2. The two enzymes are simply too similar, and the main difference appears to reside with the cofactor itself (Lindqvist *et al.*, 1991). However, its orientation and other properties are impossible to change in a predictable way by mutagenesis. Besides large variability exists even among known structures of glycolate oxidase. The co-factor has thus been observed to have an orientation much more similar to that of flavocytochrome b_2 in presence of active-site inhibitors (Stenberg & Lindqvist, 1997). Hence, it was decided to complement the protein engineering approach by forced evolution. The principle is to introduce mutations at random within the gene and then select or screen for clones expressing protein with the desired activity. The method has a number of advantages over site-specific mutagenesis. Ideally, the mutations are introduced at random without bias. This makes it possible to identify amino acid changes that rather unpredictably influence activity. These may include subtle changes remote from the active site, and mutations that only in combination alters the reactivity but not individually.

Naturally, the approach also has a few drawbacks. The major one is the astronomical number of combinations in a protein the size of the flavin-binding domain, even when changing just a couple of amino acids. This problem is worsened further by the degeneracy of the genetic code. About two-thirds of the introduced mutations will thus merely result in amino acid changes already encountered previously. A related issue is how random the mutations really are. Any preference for a certain type of mutation would also increase the number of clones needed to be screened, before encounter with a clone expressing an enzyme with improved oxidase activity. The major obstacle is thus the numbers involved, and makes a highly efficient selection system an absolute necessity. Manually screening such a large number of clones is a sheer impossibility.

6.2. Results and discussion

6.2.1. The selection system

The need for a selection system lead to the construction of an *E. coli* strain that is able to grow only when expressing an enzyme with the desired oxidase activity. The L-lactate metabolism in *E. coli* has already been described in detail, and it was concluded that the enzyme responsible for this ability is L-lactate dehydrogenase. This dehydrogenase converts L-lactate to pyruvate, which is utilised by the pyruvate dehydrogenase complex to generate acetyl CoA for the citric acid cycle (Spiro & Guest, 1991). A strain lacking the L-lactate dehydrogenase would thus be able to sustain growth on L-lactate if and only if expressing an enzyme converting the L-lactate to pyruvate. The most likely scenario also has the cloned enzyme using dioxygen as terminal electron acceptor and thus being an oxidase. *E. coli* has no equivalent of cytochrome *c*, and the flavin-binding domain is unable to interact with this electron acceptor anyhow. The L-lactate dehydrogenase of *E. coli* instead tranfers electrons to ubiquinol, but these processes occur in the bilayer where the enzyme is embedded. The cloned dehydrogenase is soluble and the most obvious oxidant is thus molecular oxygen. Furthermore, the two enzymes are evolutionary so distant relatives that the flavin-binding domain of flavocytochrome b_2 is rather unlikely to be able to replace the natural dehydrogenase in the respiratory chain.

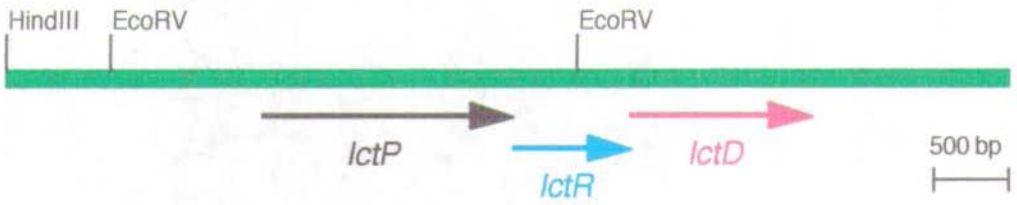

Figure 6.1. E. coli lct operon deposited in GeneBank (accession number L13970).

The ability of *E. coli* to grow on L-lactate is associated with the *lct* locus at min 80.8 on the chromosome map (Dong *et al.*, 1993). The lct locus contain three overlapping genes in the clockwise order of *lctD*, *lctR*, and *lctP* on the chromosome map (Figure 6.1). These genes, however, are transcribed in the counterclockwise direction. The flavin mononucleotide-dependent dehydrogenase is encoded by the *lctD* gene, while *lctR* and *lctP* encode a putative regulator of transcription and a L-lactate permease, respectively. Professor E. Lin's group at Harvard Medical School had already both

cloned the *lct* region and constructed a mutant strain with lost ability to grow on L-lactate. The cloned *lct* operon and the strain was kindly placed at my disposal. The *lacD* null mutant strain was created by λp*lac*Mu9(kan) fusion in the downstream *lctD*. Unfortunately, the strain also lost its L-lactate permease activity encoded by the upstream *lctP*. Another disadvantage was the use of insertion mutagenesis by λp*lac*Mu9(kan), which makes other lambda infections impossible. Another mutant strain was simply required, and the gene had to be deleted by an alternative procedure. The approach of employing a suicide vector was taken, as the cloned *lctD* gene was readily available and no λ phage infection was involved. The deletion was performed in MC4100, a K-12 strain, which has not undergone excessive previous genetic manipulation. The chosen suicide vector, pMAK705, makes use of the temperature sensitive replicon pSC101 (Hamilton *et al.*, 1989). The plasmid thus become integrated into the chromosome at elevated temperatures by homologous recombination between the chromosomal gene and a homologous sequence cloned into the plasmid. Subsequent growth of the co-integrants at low temperature leads to a second recombination event. The chromosome will then either have undergone a gene replacement or retain the original copy of the gene, depending on the position of the second recombination event. The construction of the suicide vector is described in the scheme below (Figure 6.2). A kanamycin resistance cassette was inserted into the *lctD* gene at the very end, and simultaneously a minor fragment was deleted just upstream from the insertion. The possibility of spontaneous recombination to regenerate the original gene was thus eliminated. The suicide vector is easily lost after the second recombination has taken place simply by elevating the temperature again while not selecting for the resistance carried by the plasmid itself. The mutants which have actually undergone gene replacement are selected by their resistance to kanamycin.

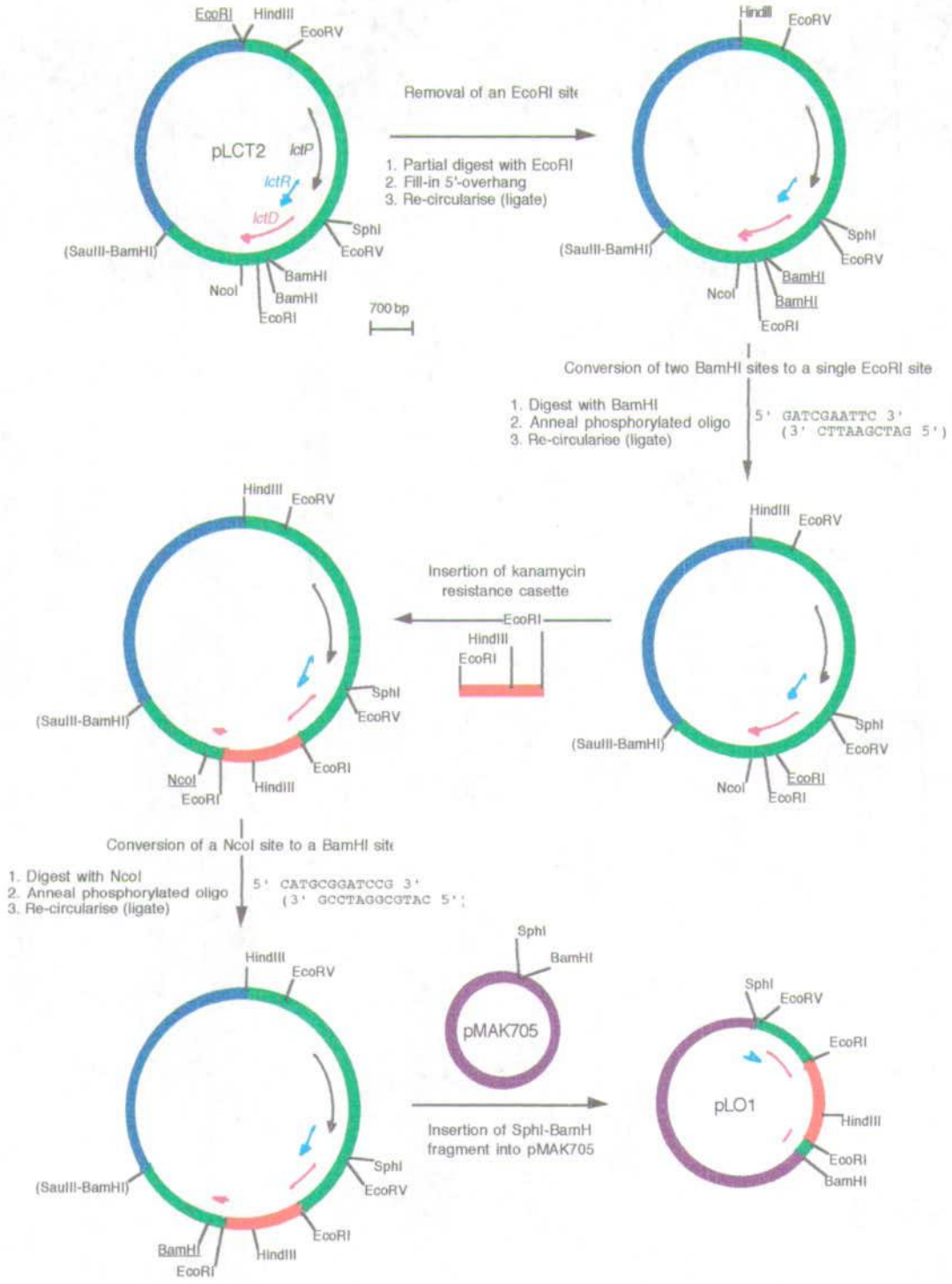

Figure 6.2. Construction of the suicide vector, pLO1. The lct operon (coloured green) encoding the L-lactate dehydrogenase from E. coli was cloned in pLCT2. A number of restriction enzyme sites were removed or converted to other sites (the names of these sites are underlined). A kanamycin resistance cassette was then inserted into the lctD gene replacing an EcoRI-EcoRI fragment. The gene with the inserted resistance cassette was finally transferred to the plasmid pMAK705 as a SphI-BamHI fragment thus generating plasmid pLO1.

The construct was verified by Southern blotting using the *Bam*HI-*Eco*RV fragment from pLCT2 as probe, and was annealed to genomic DNA digested with *Eco*RV and *Hin*dIII (Figure 6.3). The inserted kanamycin resistance cassette introduced a *Hin*dIII site, which is not present in the original gene. The probe should thus identify a fragment with a size of either 1586 or 1918 bp depending on the orientation of the inserted cassette. Chromosomal DNA retaining the original gene would instead result in a minimal size of 4157 bp. Twelve clones were found to have kanamycin resistance after having lost the suicide plasmid. All these proved to contain the kanamycin resistance cassette inserted within the gene for L-lactate dehydrogenase, and all with the same orientation of the cassette resulting in a fragment of the size 1586 bp being identified. The genotype had thus been confirmed, and indeed the phenotype proved to be a lack of ability to grow on L-lactate as expected. The gene replacement was transferred to TG1 by P1 transduction, as the transformation efficiency was better for this strain. The major question was now whether these strains would be able to sustain growth on L-lactate when expressing glycolate oxidase. However, first a suitable expression system had to be established.

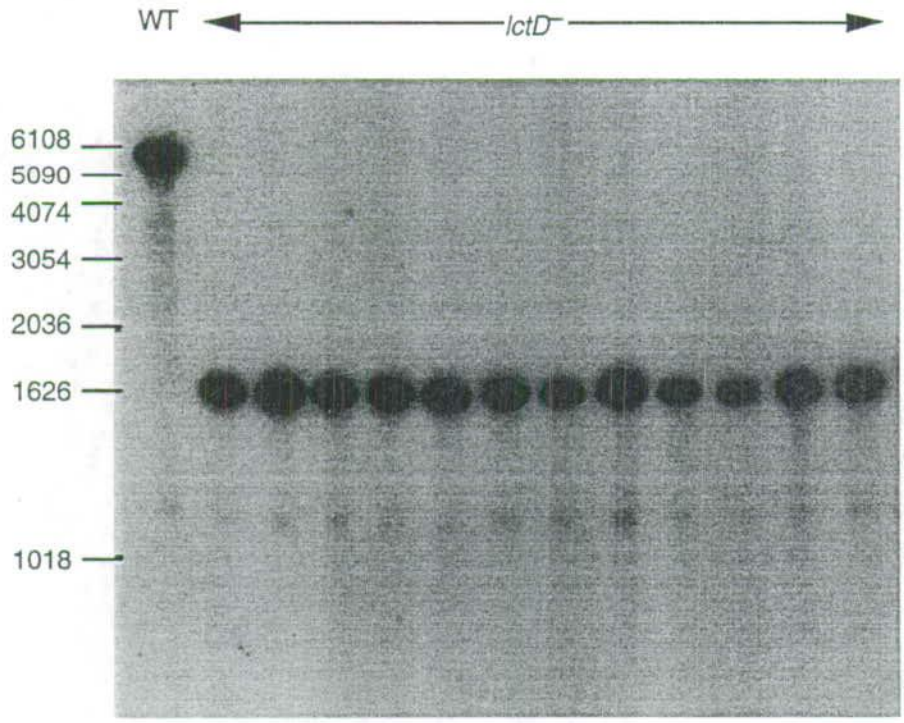

Figure 6.3. Southern blot of wild-type MC4100 and lctD⁻ clones. The null strain was constructed by homologous recombination between the constructed suicide plasmid and chromosomal DNA. The genomic DNA was digested with EcoRV/HindIII and probed with a radio-labelled BamHI-EcoRV fragment of pLCT2.

6.2.2. The expression system

Several different expression systems were explored. A system able to express both the flavin-binding domain and glycolate oxidase was required. Furthermore, the level of expression had to be sufficiently high to sustain growth of the selection strain when producing glycolate oxidase. This was an essential positive control to test the selection system. It had previously been reported that glycolate oxidase did not express particularly well in several expression systems in *E. coli*. Attempts to express glycolate oxidase directly under control of the heat-inducible λP_L promoter had failed and had given rise to an inactive protein of lower molecular weight (Macheroux *et al.*, 1992). Hence, it was obvious that the system used for expression of the flavin-binding domain was unsuitable. An alternative expression system was needed. Glycolate oxidase is expressed quite well using one of the pET vectors, in which expression is under control of the T7 promoter. The T7 RNA polymerase may be supplied either by a chromosomal copy of gene *1* under control of the *lac*UV5 promoter (Studier & Moffatt, 1986) or by a plasmid-borne copy under control of the λP_L promoter (Tabor & Richardson, 1985). The preference was to use IPTG to induce expression and not heat. The level of expression would be much easier to control when using IPTG instead of temperature. Beside, the problems encountered when trying to express glycolate oxidase under direct control of the λP_L promoter might very well be caused by the elevated temperature needed. The heat-shock system is also induced during temperature induction, and some of these genes encode potent proteases. Besides, working with just one plasmid would be simpler and eliminate unforeseen events e.g. caused by incompatible plasmids. The two plasmid system could not be adopted directly anyhow as the L-lactate dehydrogenase gene was knocked out by inserting a kanamycin resistance cassette also carried by the required second plasmid.

Hence, attempts were made to insert a chromosomal copy of gene *1* into the manipulated strain by making it lysogenic for DE3. Bacteriophage DE3 is a λ derivative that has the immunity region of phage 21 and carries a DNA fragment containing the *lac*I gene, the *lac*UV5 promoter, the beginning of the *lac*Z gene and the gene encoding T7 RNA polymerase. This fragment has been inserted into the *int* gene, and DE3 thus needs a helper for either integration into or excision from the chromosome. The strain was made lysogenic by a co-infection with λNM75, to provide Int *in trans*. Lysogens with the immunity of phage 21 were selected, purified, and the immunity confirmed. Monolysogen imm^{21} hosts were presumed to have been lysogenised by λDE3. Bacteria with the correct immunity were obtained, but

unfortunately no expression of glycolate oxidase was observed upon induction with IPTG.

A new vector, that enabled expression of both the flavin-binding domain and glycolate oxidase, was needed. The genes were cloned into two different vectors, pBAD18 (Guzman *et al.*, 1995) and pJF118EH (Fürste *et al.*, 1986). The gene for the flavin-binding domain was simply excised from the original construct of vector pRC23. Glycolate oxidase cloned into pET-3d had kindly been provided by Dr. P. Macheroux (University of East Anglia). Unfortunately, the construction of this vector had lead to the destruction of the restriction enzyme cleavage site at the C-terminal end. New restriction enzyme cleavage sites were introduced by amplification of the cloned gene by PCR using primers containing the sequence recognised by *Eco*RI and *Hin*dIII. The two vectors were chosen because everything needed for expression are enclosed in vectors themselves, and thus in principle any strain may be used for expression. The vector pBAD18 contain the P_{BAD} promoter of the *araBAD* (arabinose) operon and the gene, araC, encoding the positive and negative regulator of this promoter. The vector offers tight regulation of expression, modulation by varying the concentration of the inducer arabinose, and repression by glucose to very low levels. However, the vector did not express significantly levels of either the flavin-binding domain or glycolate oxidase. Improvement could possibly be achieved by optimising the ribosome binding site. The other vector, pJF118EH, is based on the controllable *tac* promoter. The gene for the *lac* repressor (*lac*I^q) had been inserted to render the plasmid strain-independent. The *tac* promoter is an artificial hybrid promoter, which consists of parts of the *trp* and *lac* promoter. The *trp* promoter belongs to the strongest class of promoters known in *E. coli* (Pühler, 1993). Thus, the hybrid promoter is much stronger than the *lac*UV5 promoter, but is still regulated by overproduction of lac repressor. Luckily, the two enzymes were both produced in high quantities when cloned into this expression system. Actually, the expression system overproduced the flavin-binding domain even better than pRC23, which is controlled by the λP_L promoter. The level of expression is determined by various factors. The initiation of translation requires a ribosome binding site. The efficiency of translation is also affected by the primary and secondary structure of mRNA. One primary structure feature known to be of importance is the presence of a Shine-Dalgarno sequence (Winnacker, 1987). Its typical primary structure is $AGGN_{6-9}ATG$, G should not occur at position -3, positions +5 and +10 should be occupied by either A or T, and less than two G residues should occur between positions -1 and -7. It is quite obvious that pJF118EH complies much better to these rules than pBAD18 (Figure 6.4), which probably explains the observed difference in the level of expression.

```
16S rRNA            3' OH AUU CCU CCA CU---5'
                          ||| ||| ||| ||
complementary       5'    TAA GGA GGT GA---3'
strand
                                    -5   -1+1
pJF118EH            5'--- CAG GAA ACA GAA TTC ATG ---3'
pBAD18              5'--- TGG GCT AGC GAA TTC ATG ---3'
pRC23               5'--- ATT AAG GAG GAA TTC ATG ---3'
pPM1                5'--- AGA AGG AGA TAT ACC ATG ---3'
```

Figure 6.4. Comparison of primary structure of translation initiation sites. The top line shows the sequence of the 3' end of E. coli 16S rRNA. The DNA sequence below is that of the corresponding complementary strand which is the prototype of a Shine-Dalgarno sequence. The plasmid sequences are aligned with respect to the position of their ATG codons. Start codons and regions of homology with 16S rRNA are underlined.

The genetically manipulated strain was indeed able to sustain growth on L-lactate, when expressing glycolate oxidase cloned into pJF118EH. Cells overproducing the flavin-binding domain was not able to grow with L-lactate as sole source for energy and carbon. However, the cells expressing glycolate oxidase grew very poorly when only supplied with L-lactate and M9 salts (Figure 6.5). The reason was lack of thiamine and Mg^{2+}, which are needed in the pyruvate oxidation (Levy *et al.*, 1973). The formation of acetyl CoA involves a series of intermediate steps that require the stepwise participation of Mg^{2+} and thiamine-pyrophosphate. The minimal medium used for the selection was hence supplemented with thiamine and Mg^{2+}. The last hurdle had thus been overcome and the actual selection procedure itself could get under way.

Figure 6.5. Photograph of plates streaked with cells of the null strain expressing the flavin-binding domain (left side of each plate) and glycolate oxidase (right). The plate to the left was supplied with M9 salts and 100 mM pyruvate, while the other plate was supplied with M9 salts and 100 mM L-lactate. Expression was induced by addition of 1 mM IPTG to the agar.

The selection system was complemented with a colourmetric screen for oxidase activity (Maeda-Yorita *et al.*, 1995). The screen was based on the coupled assay between horse radish peroxidase utilising hydrogen peroxide and the oxidase producing it. The agar plates used for screening were simply seeded with horse radish peroxidase, the dye *o*-dianisidine, and naturally L-lactate (Figure 6.6). The screen was merely used as an alternative to selection, but the two could in principle be combined to allow distinction between various levels of activity.

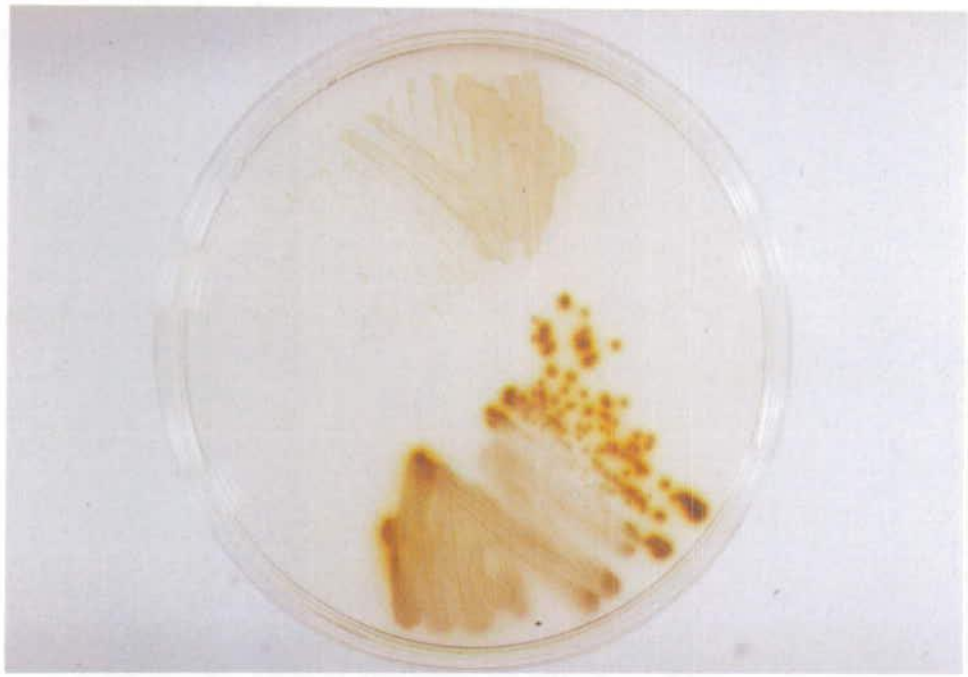

Figure 6.6. Photograph of cells expressing the flavin-binding domain (top) and glycolate oxidase (bottom). The plate was seeded with horse radish peroxidase, o-dianisidine and L-lactate. Expression was induced by addition of 1 mM IPTG to the agar.

6.2.3. Random mutagenesis

A wide range of techniques is available for introduction of random mutations into DNA. Some are based on the use of mutagenic chemicals (Myers *et al.*, 1985), whereas other have a biological foundation. The biological approach was preferred to the chemical, because it is much simpler, easier to control, and less labour-intensive. The term "biological mutagenesis" is used to describe incorporation of mistakes in the DNA by enzymes during replication. The mutagenesis is either executed *in vivo* or *in vitro*. Plasmid DNA is typically mutated *in vivo* using a bacterial mutator strain, that is, a strain lacking parts of the normal proof-reading machinery. Random mutagenesis performed *in vitro* include amplification of DNA by the polymerase chain reaction (Leung *et al.*, 1989). The use of PCR to generate mutation has many advantages. The

level of mistakes is easily controlled, cloning of the mutated product is simple, and mutations may be targeted to specific areas.

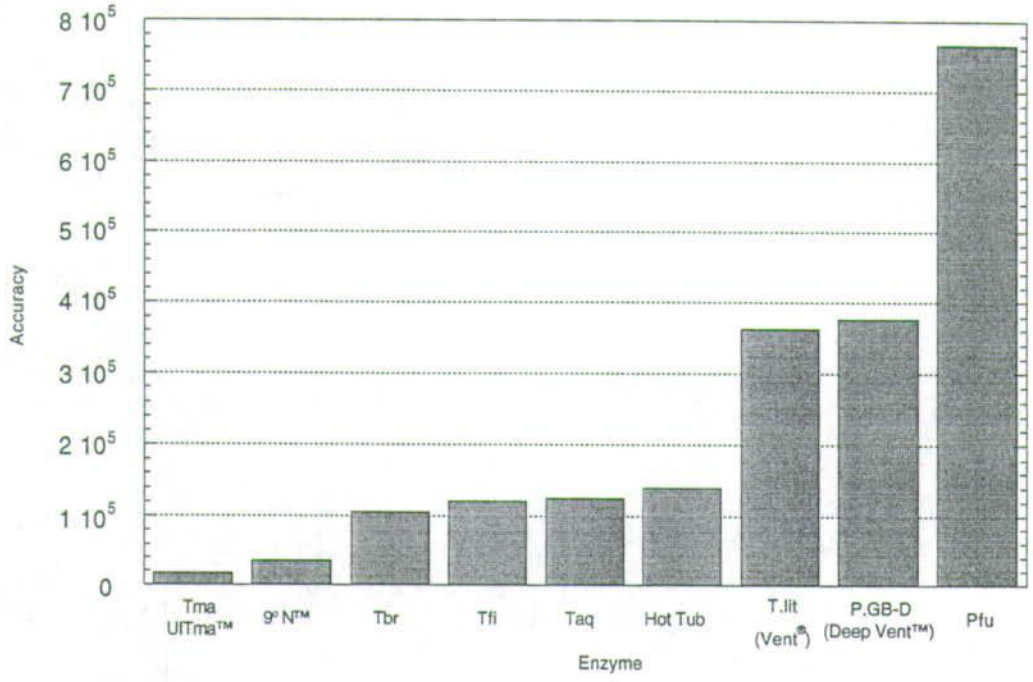

Figure 6.7. Accuracy is represented as the average number of correct nucleotides a given polymerase incorporates before making an error. Source: Stratagene® catalogue 1997.

The enzymes used for PCR have no 3' → 5' proof-reading exonuclease activity, and this give rise to a certain background error rate depending on the enzyme (Figure 6.7). Thus, *Taq* DNA polymerase is naturally error-prone, and indeed commercial suppliers generally offer engineered polymerase with decreased error rate. While higher fidelity in PCR is normally desired, the opposite is relatively easy to achieve. Several parameters, such as pH, dNTP concentration, type and concentration of divalent metal ion, influence the fidelity of the reaction (Eckert & Kunkel, 1990). The presence of the base analogue dITP also induces misincorporation (Spee *et al.*, 1993). However, the hyper-mutagenic conditions generated by varying the concentration of Mn^{2+} was preferred. It was attractive due to simple control of mutation frequency, and the level of mutations generated seemed within an appropriate range. The Mn^{2+} does not work by replacing Mg^{2+} by occupying sites on the polymerase. The mode of action for enzyme-mediated manganese mutagenesis is rather believed to be binding of Mn^{2+} to the DNA template or to the incoming dNTP substrates (Beckman *et al.*, 1985). The binding would affect the polymerase discrimination of the incoming nucleotide triphosphates.

The study demonstrated that the concentration of Mn^{2+} added was inversely proportional to the yield of PCR product. Concentrations up to 0.3 mM were tolerated,

whereas higher levels resulted in complete loss of product. The result from several independent PCRs were compared. A concentration of 0.1 mM Mn^{2+} gave both a good yield of product and an appropriate level of mutation (0.8%). This level of mutation equals around ten point mutations in a gene the size of the flavin-binding domain. However, a number of these mutations will not result in an actual change of the amino acid encoded due to the degeneracy of the genetic code. Furthermore, most of the mutations occur in remote parts of the enzyme far away from the active site, and are unlikely to affect dehydrogenase or oxidase activity. Mutations occurring during an early cycle of the polymerase chain reaction were not prevailing, as demonstrated by the random distribution of mutations in clones from the same reaction. No true mutagenic hotspots were detected either, as the clones from different reactions also resulted in a random distribution of the mutations. However, the number of transition mutations is higher than those of the transversion type. Although this is expected, the mutations are thus not introduced completely at random. It is a fairly good approximation though, as all different types of mutations are likely to occur albeit with different frequencies (Table 6.1). Another point to make here is unequal degeneracy of the genetic code. Some amino acid are encoded by only a single codon, while others have as many as six different codons. This will naturally increase the chances of some mutations to be encountered much more frequently than others, yet another reason why 'random' mutagenesis does not introduce new amino acids completely at random. All the described observations are in very good correlation with available published data (Leung *et al.*, 1989).

From\To	A	C	G	T
A	-	1	9	1
C	0	-	1	5
G	3	0	-	2
T	3	7	0	-

Table 6.1. List of the different type of mutations encountered when sequencing randomly mutated PCR products. Parts of the DNA from six clones (a total of 4000 bases) were sequenced from both ends of the gene. Addition of 0.1 mM Mn^{2+} to the standard PCR reaction proved to generate 6-10 mutations per 1000 bases. About 60% of these mutations were transitions (AT ↔ GC).

6.2.4. DNA shuffling

The purpose of molecular evolution is to mimic the natural "design" process in biological systems and speed it up by selection *in vitro*. However, the application of error-prone PCR is a rather poor substitute for the real thing. The problem is that homologous recombination, combined with a low number of point mutations, is very important for the evolution of a linear sequence. Error-prone PCR is by no means

combinatorial, but introduce a low level of point mutations randomly over a long sequence. The vast number of possible combinations combined with the limited size of a library means that many rounds of selection are needed for protein optimisation. Repeated cycles will inevitably also lead to an increase in the number of neutral mutations though. The search in sequence space is thus somewhat limited for error-prone PCR. The newly developed process of DNA shuffling offer a remedy to this deficiency. DNA shuffling is a technique for *in vitro* recombination of homologous genes (Stemmer, 1994b). The initial population of molecules are artificially cleaved into random fragments by DNase I. These fragments are then reassembled into full-length genes by a PCR-like reaction without added primers. Incomplete strands become progressively longer as they find complementary strands to template extension of their 3' ends. The complete strands are finally amplified by conventional PCR and cloned into the expression vector. The process is repeated after selection of the most fit clones for use in the next cycle. Each strand thus acquires many of its new mutations by swapping genetic material with other strands in the population. The acquired mutations have a better chance of improving the protein function, as they have already survived selection in favour of the target function. This argument naturally assumes that the effect of mutations is additive. The required number of cycles is thus considerably lowered compared to that of error-prone PCR. Error-prone PCR may be employed to enhance the level of mutagenesis in the initial cycles of DNA shuffling. The homologous recombination process of DNA shuffling, coupled with selection and screening, will then combine the positive mutations and simultaneously remove the negative mutations from the sequence pool. Any neutral mutations may be removed in the later cycles by addition of excess of parental DNA to the pool. Backcross with wild-type DNA enables elimination non-essential mutation, when also combined with selection and screening.

The method has been applied to the flavin-binding domain of flavocytochrome b_2, and DNA fragments within the range 100-300 bp have successfully been reassembled to the full-length gene. The cloned genes do indeed still encode proteins with dehydrogenase activity, and sequencing has further confirmed the identity. The process of DNA shuffling of hypermutated DNA coupled with selection is being performed at present. DNA shuffling also offers another exciting application: The mixing of genes encoding related proteins (Stemmer, 1994a). Shuffling requires the presence of homologous regions, but these may be separated by regions of diversity. Scaffold-like proteins, as flavocytochrome b_2 and glycolate oxidase, thus seem potentially suitable for shuffling. The similarity between the two genes is illustrated by their alignment in the appendix (section 9.2, p. 131). Crossover between genes of

such low homology is forced by very low annealing temperature. The use of the Klenow fragment, instead of *Taq* DNA polymerase, permits a low annealing temperatures. Indeed, recombination between segments with an average of only 4.1 bases of uninterrupted identity has been reported. The degree of relatedness may thus be rather modest. The construction of a library of chimeras of the flavin-binding domain and glycolate oxidase is currently under way. The diversity present in such a mixture is arguably a lot more meaningful than random mutations. It certainly eliminates a number of fruitless mutations, and merely includes actual differences between the two genes.

6.3. Conclusion

Although the application of forced evolution so far has been unsuccessful, it is a very promising approach. Molecular evolution has the potential to solve the complex problem of making an oxidase without the need to define the structure and function relationship. Furthermore, oxidase activity is not very likely to be switched on/off by a single amino acid change, which makes site-specific mutagenesis an even more impossible mission. All the tools needed for success are now available, and the rest is merely a numbers game. The number of possibilities can seem prohibitively high, but there is a remedy (provided that the effect of beneficial mutations is additive). DNA shuffling has already proved very powerful in molecular evolution, and reduce the required number of selection rounds significantly. The technique increase the number of positive mutation and removes the negative mutations at the same time. Finally, the neutral mutations may also be eliminated by this combination of *in vitro* homologous recombination and selection.

The number of mutant enzymes needed to be screened, before detecting a clone with significant improvement in the level of oxidase activity, may possible be lowered even further. The frequency of relevant mutations can be increased by merely introducing the amino acid present at that specific position in glycolate oxidase. Again, DNA shuffling offers a convenient way of mixing two related genes. The positive combinations of these would be used as starting point for further studies. The minimal changes needed may then be identified by backcross with wild-type DNA or by introducing site-specific mutation in the wild-type DNA. DNA shuffling is thus a very powerful tool, and is by far the most promising one. The presence of L-lactate itself during selective pressure could possibly also induce changes by adaptive mutations, but this technique has not been taken into consideration during this study. The forced

evolution described may potentially be applied in a number of related studies. The most obvious of these is to introduce new substrate specificities into glycolate oxidase. Everything needed in the screening procedure is already available. A suitable expression system has been set up. Agar plates seeded with substrate (for example L-mandelate), horse radish peroxidase and *o*-dianisidine would make up a suitable screen. The system could also be employed in an attempt to enhance the not too impressive oxidase activity of glycolate oxidase.

7. Final Conclusion

The present study has clearly demonstrated the limitations of site-specific mutagenesis. One of the major obstacles, in engineering flavocytochrome b_2 into an oxidase, is the lack of knowledge on the structure-function relationship. The understanding of the reductive half-reaction is reasonably well-established, although there still remains controversy about the exact mechanism involved. The elucidation of the mechanism behind the oxidative half-reaction poses a much bigger challenge. Free reduced flavin itself reacts reasonably well with molecular oxygen, but the oxidases somehow manage to enhance this reactivity even further. The dehydrogenases have evolved a quite different biochemistry, and practically eliminated the reaction with oxygen. Flavocytochrome b_2 appears to be a dehydrogenase by virtue of specifically excluding oxygen as a potential electron acceptor. If so, engineering some level of oxidase activity into this enzyme would simply be a question of generating access to the active site. This would presumably increase the level of reactivity to that of free FMN, which would represent an immense improvement. However, all attempts to achieve this objective by site-specific mutagenesis have been unsuccessful. The mutant enzymes all influenced the dehydrogenase activity, but failed to provide the promised oxidase activity. Hence, it has to be concluded either that access to the active site is not the real problem, or that a single mutation is not sufficient to swing the function. Naturally, it is possible that none of the mutant enzymes actually generated any significant difference in the access. Another important issue, which may seem to have been somewhat ignored in the present study, is the question of the overall architecture of the active-site itself. Oxidases enhance the reactivity of the reduced FMN towards molecular oxygen. The redox potentials fail to explain this phenomenon, as free FMN actually has a lower potential than the FMN of glycolate oxidase. Furthermore, the redox potentials for glycolate oxidase and flavocytochrome b_2 are not significantly different. The relevance of these potentials is thus somewhat limited for this enzymatic mechanism. The reaction catalysed by oxidases is not a bimolecular collision reaction. A sufficiently strong binding of the initial reduction product, superoxide, could drive the reaction and eliminate any barriers. Increased hydrophobicity has been proposed an important factor (Malmström, 1982), and could possibly explain why glycolate oxidase reacts so poorly with ferricyanide. However, effective hydride transfer also requires a hydrophobic environment (Stoll *et al.*, 1996), and hence the active site of flavocytochrome b_2 is presumably shielded from solvent as well - at least during the reductive half-reaction.

A structural feature, which potentially could be of importance in shielding the active site from solvent, is a flexible loop located just outside the substrate binding site. The function of this loop region was studied by construction and characterisation of a

number of mutant enzymes, including hybrid enzymes. All of the mutant enzymes retained dehydrogenase activity, and did unfortunately not introduce oxidase activity. However, they demonstrated that the loop interacts with the active site. The consequence of introducing aliphatic amino acid residues was not especially pronounced, whereas the effect of a shorter loop was more dramatic. The greatest effects on the kinetic parameters were observed for the chimeras though. Three mutant enzymes were constructed by replacing parts of the loop region with the corresponding regions from glycolate oxidase. Their K_m for the reaction with ferricyanide was significantly changed, and could indicate involvement of this region in determination of the hydrophobicity. The Michaelis constant for L-lactate was also increased, and the value for the chimera involving the largest replacement went up by a factor of about 100. The loop is hence also partly responsible for the interaction between enzyme and substrate. Other evidence of the functional role of this loop includes the absorption spectra. Again the hybrid enzyme with the largest replacement appeared to be have a spectrum which was an intermediate between those of the flavin-binding domain and glycolate oxidase. Thus, the environment around the bound FMN had obviously changed in the direction of that found in glycolate oxidase. However, these alterations were not sufficient to shift the catalytic events taking place. Actually, the apparent rate constant for combination of L-lactate with the free enzyme (k_{cat}/K_m) was considerably more affected than the rate constant for the enzyme-substrate complex, once formed, to form product (k_{cat}). However, it seems reasonably justified to conclude that the loop region is somehow involved in controlling catalysis, but the control exercised by this region is more subtle than regulating the reactivity with dioxygen. It is quite likely that the solution to this particular puzzle reside in other loop regions, maybe through combinational effects. The active sites residues are all located in these loops at the carboxyl end of the β-strands making up the interior of the TIM-barrel. The barrel structure itself constitutes a scaffold upon which these residues are held in position. It would thus be interesting to construct other hybrid enzymes involving replacement of other loop regions. It is naturally of the utmost importance that the folded structure of these chimeras remain unchanged, but this is indeed also most likely to be the case (El Hawrani *et al.*, 1994). Any hybrid enzymes with improved oxidase activity would provide a firm basis for subsequent site-specific or targeted random mutagenesis. This approach would allow identification of individual amino acid residues responsible for switching the activity.

Another promising approach is that of forced evolution. The above described difficulties make random mutagenesis coupled with selection a very interesting alternative. The technique obviously eliminates the requirement for a well defined

structure-function relationship. Mutations are introduced at random without bias, which enables identification of beneficial, but unpredictable, mutations. However, the number of possible combinations, when considering a gene the size of flavin-binding domain, are rather overwhelming. The selection procedure is the Achilles' heel. Screening of a vast number of mutant enzymes is simply not feasible. A selection system based on expression in *E. coli* has been established. The principle is that expression of the mutant enzyme is essential for survival of the clone. This has been achieved by construction of an *E. coli* strain unable to metabolise L-lactate, but still capable of growing on pyruvate. The enzyme responsible for *E. coli* ability to grow on L-lactate is L-lactate dehydrogenase, and this gene was knocked-out by gene replacement. The strain is thus only able to grow on L-lactate when an enzyme converting this to pyruvate is present. The flavin-binding domain and glycolate oxidase are both able to catalyse this reaction. However, the flavin-binding domain has no redox partner in *E. coli,* whereas glycolate oxidase is able to reduce dioxygen. The approach also requires a good expression system. Several different expression vectors were tested, but only pJF118EH was capable of expressing both enzymes. Its expression is under control of the strong *tac* promoter, and is inducible by IPTG due to the presence of the *lacI*^{q} gene on the plasmid itself. The vector thus offers control of the level of expression and is furthermore strain-independent. The selection system was proved to work, when expressing flavin-binding domain and glycolate oxidase. Random mutations were then introduced in the gene for the flavin-binding domain by error-prone PCR. These PCR products were subsequently cloned into the expression vector and subjected to the selection. The effort has been in vain until now, which probably is due to the prohibitive large number of combinations. The odds could be improved considerably by various tricks. The introduction of random mutations in the whole gene is unnecessary. A large portion of the proteins is unlikely to actually make any difference in the reactivity whatsoever. The mutagenesis could be concentrated to the loop regions, which are very probable to be in control of the reaction catalysed. The application of PCR for introducing mutations allows targeting specific areas simply by the choice of primers. The cloning of the PCR products is naturally hindered by the lack of appropriate restriction enzyme site, but these are easily introduced by site-specific mutagenesis. Currently, five new sites are being engineered into the gene of the flavin-binding domain, and will thus enable six smaller areas to be specifically targeted by random mutagenesis. Another method, DNA shuffling, has been set up to lower the number of mutant enzymes needed to be screened before generating a good oxidase. The technique mimics natural evolution by exploiting the process of homologous recombination. The principle is again selection of positive clones, but

these subsequently swap genetic material with other clones in the population. The combination of acquired mutations are quite likely to improve the activity further, since they are all the result of a selection. The technique could be employed to blend a population of clones generated by error-prone PCR, which naturally would increase the rate of mutagenesis. Likewise, the number of mutation could be lowered by blending in wild-type DNA, which theoretically also would lower the number of neutral mutations. Finally, the technique also offers a convenient way of mixing closely related genes (Stemmer, 1994a). This is a particular exciting application, which hold great promises in solving the problem discussed in this thesis. The flavin-binding domain of flavocytochrome b_2 and glycolate oxidase exhibit quite high similarity at the DNA level, and both encoded enzymes contain the same structural motif, the TIM-barrel. This makes them ideal candidates for DNA shuffling, while still keeping their structural integrity. DNA shuffling of the genes encoding these two enzymes will presumably exclude fruitless mutations, as the only amino acid residues introduced will be those existing in glycolate oxidase. The approach very much resembles the suggested manual loop replacement, but is much less laborious and involves the complete gene.

8. References

Anraku, Y. & Gennis, R. B. (1987). The aerobic respiratory chain of *Escherichia coli*. *TIBS* **12**, 262-266.

Appleby, C. A. & Morton, R. K. (1954). Crystalline cytochrome b, and lactic dehydrogenase of yeast. *Nature* **173**, 749-752.

Bainbridge, G., Madgwick, P., Parmar, S., Mitchell, R., Paul, M., Pitts, J., Keys, A. J. & Parry, M. A. J. (1995). Engineering Rubisco to change its catalytic properties. *Journal of Experimental Botany* **46**, 1269-1276.

Balme, A., Brunt, C. E., Pallister, R. L., Chapman, S. K. & Reid, G. A. (1995). Isolation and characterisation of the flavin-binding domain of flavocytochrome b_2 expressed independently in *Escherichia coli*. *Biochem. J.* **309**, 601-605.

Beckman, R. A., Mildvan, A. S. & Loeb, L. A. (1985). On the Fidelity of DNA Replication: Manganese Mutagenesis in Vitro. *Biochemistry* **24**, 5810-5817.

Belmouden, A., Diêp Lê, K. H., Lederer, F. & Garchon, H. J. (1993). Molecular cloning and nucleotide sequence of cDNA encoding rat kidney long chain L-2-hydroxyacid oxidase - expression of the catalytically active recombinant protein as a chimera. *Eur. J. Biochem.* **214**, 17-25.

Bernard, H.-U., Remaut, E., Hershfield, M. V., Das, H. K. & Helinski, D. R. (1979). Construction of plasmid cloning vehicles that promote gene expression from the bacteriophage p_L promoter. *Gene* **5**, 59-76.

Black, M. T., White, S. A., Reid, G. A. & Chapman, S. K. (1989). High-level expression of fully active yeast flavocytochrome b_2 in *Escherichia coli*. *Biochem. J.* **258**, 255-259.

Brändén, C.-I., Schneider, G., Lindqvist, Y., Anderson, I., Knight, S. & Lorimer, G. (1987). Structural and Evolutionary Aspects of the Key Enzymes in Photorespiration; RuBisCo and Glycolate Oxidase. *Cold Spring Harbor Symposia on Quantitative Biology* **LII**, 491-498.

Brunt, C. E., Cox, M. C., Thurgood, A. G. P., Moore, G. R., Reid, G. A. & Chapman, S. K. (1992). Isolation and characterisation of the cytochrome domain of flavocytochrome b_2 expressed independently in *E. coli*. *Biochem. J.* **283**, 87-90.

Brüstlein, M. & Bruice, T. C. (1972). Demonstration of a Direct Hydrogen Transfer between NADH and a Deazaflavin. *JACS* **94**(18), 6548-6549.

Cederlund, E., Lindqvist, Y., Söderlund, G., Brändén, C.-I. & Jörnvall, H. (1988). Primary structure of glycolate oxidase from spinach. *Eur. J. Biochem.* **173**, 523-530.

Clark, W. M. (1960). *Oxidation Reduction Potentials of Organic Systems*, Williams & Wilkins, Baltimore.

Crameri, A., Whitehorn, E. A., Tate, E. & Stemmer, W. P. C. (1996). Improved Green Flourescent Protein by Molecular Evolution Using DNA Shuffling. *Nature Biotechnology* **14**, 315-319.

Creighton, T. E. (1993). *Proteins*. Second edit, W.H. Freeman and Company, New York.

Crowl, R., Seamans, C., Lomedico, P. & McAndrew, S. (1985). Versatile expression vectors for high-level synthesis of cloned gene products in *Escherichia coli*. *Gene* **38**, 31-38.

Daff, S., Ingledew, J., Reid, G. A. & Chapman, S. K. (1996a). New Insights into the Catalytic Cycle of Flavocytochrome b_2. *Biochemistry* **35**(20), 6345-6350.

Daff, S., Sharp, R. E., Short, D. M., Bell, C., White, P., Manson, F. D. C., Reid, G. A. & Chapman, S. K. (1996b). Interaction of Cytochrome *c* with Flavocytochrome b_2. *Biochemistry* **35**(20), 6351-6357.

Daff, S. N. (1996). Analysis of the Catalytic cycle & Manipulation of Substrate Specificity in Flavocytochrome b_2. Ph.D., University of Edinburgh.

Daum, G., Böhni, P. C. & Schatz, G. (1982). Import of proteins into mitochondria. Cytochrome b_2 and cytochrome *c* peroxidase are located in the intermembrane space of yeast mitochondria. *J. Biol. Chem.* **257**(21), 13028-13033.

Dey, P. M. & Harborne, J. B., Eds. (1997). Plant Biochemistry. First edit. London: Academic Press.

Diêp Lê, K. H. & Lederer, F. (1991). Amino Acid Sequence of Long Chain α-Hydroxy Acid Oxidase from Rat Kidney, a Member of the Family of FMN-dependent α-Hydroxy Acid-oxidizing Enzymes. *J. Biol. Chem.* **266**(31), 20877-20881.

Dong, J. M., Taylor, D. J., Iuchi, S. & Lin, E. C. C. (1993). Three Overlapping *lct* Genes Involved in L-Lactate Utilization by *Escherichia coli*. *J. Bact.* **175**(20), 6671-6678.

Doyle, K., Ed. (1996). Protocols and Applications Guide. Third edit. Madison: Promega.

Ebsworth, E. A. V., Connor, J. A. & Turner, J. J. (1975). *The Chemistry of OXYGEN*. First edit. Comprehensive Inorganic Chemistry (Bailar Jr., J. C., Emeléus, H. J., Nyholm, R. & Trotman-Dickenson, A. F., Eds.), 22, Pergamon Press, Oxford.

Eckert, K. A. & Kunkel, T. A. (1990). High fidelity DNA synthesis by the *Thermus aquaticus* DNA polymerase. *Nucleic Acids Research* **18**(13), 3739-3744.

El Hawrani, A. S., Moreton, K. M., Sessions, R. B., Clarke, A. R. & Holbrook, J. J. (1994). Engineering surface loops of proteins - a preferred strategy for obtaining new enzyme function. *TIBTECH* **12**, 207-211.

Engels, B. (1996). Amplify 2.52β edit. University of Wisconsin, Madison.

Fersht, A. R., Leatherbarrow, R. J. & Wells, T. N. C. (1987). Structure-Activity Relationships in Engineered Proteins: Analysis of Use of Binding Energy by Linear Free Energy Relationships. *Biochemistry* **26**, 6030-6038.

Fisher, A. J., Raushel, F. M., Baldwin, T. O. & Rayment, I. (1995). Three-dimensional Structure of Bacterial Luciferase from *Vibrio harveyi* at 2.4 Å Resolution. *Biochemistry* **34**, 6581-6586.

Frigerio, N. A. & Harbury, H. A. (1958). Preparation and some properties of crystalline glycolic acid oxidase of spinach. *J. Biol. Chem.* **231**, 135-155.

Fürste, J. P., Pansegrau, W., Frank, R., Blöcker, H., Scholz, P., Bagdasarian, M. & Lanka, E. (1986). Molecular cloning of the plasmid RP4 primase region in a multi-host-range *tacP* expression vector. *Gene* **48**, 119-131.

Gasser, S. M., Ohashi, A., Daum, G., Böhni, P. C., Gibson, J., Reid, G. A., Yonetani, T. & Schatz, G. (1982). Imported mitochondrial proteins cytochrome b_2 and cytochrome c_1 are processed in two steps. *Proc. Natl. Acad. Sci. U.S.A.* **79**, 267.

Gatti, D. L., Palfey, B. A., Lah, M. S., Entsch, B., Massey, V., Ballou, D. P. & Ludwig, M. L. (1994). The Mobile Flavin of 4-OH Benzoate Hydroxylase. *Science* **26**, 110-114.

Ghisla, S. & Massey, V. (1986). New flavins for old: artificial flavins as active site probes of flavoproteins. *Biochem. J.* **239**, 1-12.

Ghisla, S. & Massey, V. (1989). Mechanisms of flavoprotein-catalyzed reactions. *Eur. J. Biochem.* **181**, 1-17.

Ghisla, S. & Massey, V. (1992). L-lactate oxidase. In *Chemistry and Biochemistry of Flavoenzymes* (Müller, F., ed.), Vol. II, pp. 244-289. CRC Press, Inc., Boca Raton, FL.

Ghrir, R. & Lederer, F. (1981). Study of a Zone Highly Sensitive to Proteases in Flavocytochrome b_2 from *Saccharomyces cerevisiae*. *Eur. J. Biochem.* **120**, 279-287.

Gibson, Q. H. & Hastings, J. W. (1962). The Oxidation of Reduced Flavin Mononucleotide by Molecular Oxygen. *Biochem. J.* **83**, 368-377.

Giegel, D. A., Williams, C. H. J. & Massay, V. (1990). L-Lactate 2-Monooxygenase from *Mycobacterium smegmatis*. *J. Biol. Chem.* **265**(12), 6626-6632.

Gondry, M., Diêp Lê, K. H., Manson, F. D. C., Chapman, S. K., Mathews, F. S., Reid, G. A. & Lederer, F. (1995). On the lack of coordination between protein folding and flavin insertion in *Escherichia coli* for flavocytochrome b_2 mutant forms Y254L and D282N. *Protein Science* **4**(5), 925-935.

Gordon, E. H. J. (1997). The physiological role of a novel flavocytochrome *c* from *Shewanella putrefaciens*. Ph.D., University of Edinburgh.
Green, M. J. & Hill, H. A. O. (1984). Chemistry of Dioxygen. *Methods in Enzymology* **105**, 3-23.
Guiard, B. (1985). Structure, expression and regulation of a nuclear gene encoding a mitochondrial protein: the yeast L(+)-lactate cytochrome *c* oxidoreductase (cytochrome b_2). *EMBO J.* **4**(12), 3265-3272.
Gutteridge, S., Newman, J., Herrmann, C. & Rhoades, D. (1995). The crystal structures of Rubisco and opportunities for manipulating photosynthesis. *Journal of Experimental Botany* **46**, 1261-1267.
Guzman, L.-M., Belin, D., Carson, M. J. & Beckwith, J. (1995). Tight Regulation, Modulation, and High-Level Expression by Vectors Containing the Arabinose P_{BAD} Promoter. *J. Bact.* **177**(14), 4121-4130.
Hamilton, C. M., Aldea, M., Washburn, B. K., Babitzke, P. & Kushner, S. R. (1989). New Method for Generating Deletions and Gene Replacements in *Escherichia coli*. *J. Bact.* **171**, 4617-4622.
Haumont, P.-Y., Thomas, M.-A., Labeyrie, F. & Lederer, F. (1987). Amino-acid sequence of the cytochrome-b_5-like heme-binding domain from *Hansenula anomala* flavocytochrome b_5. *Eur. J. Biochem.* **169**, 539-546.
Hazzard, J. T., Cusanovich, M. T., Tainer, J. A., Getzoff, E. D. & Tollin, G. (1986). Kinetic Studies of Reduction of a 1:1 Cytochrome *c*-Flavodoxin Complex by Free Flavin Semiquinone and Rubredoxin. *Biochemistry* **25**, 3318-3328.
Ingraham, L. L. & Meyer, D. L. (1985). *Biochemistry of Dioxygen*, Plenum Press, New York.
Iwatsubo, M., Mével-Ninio, M. & Labeyrie, F. (1977). Rapid kinetic studies of partial reactions in heme free derivative of L-lactate cytochrome *c* oxidoreductase (flavocytochrome b_2); the flavodehydrogenase function. *Biochemistry* **16**(16), 3558-3566.
Jorns, M. S., Ballinger, C., Kinney, G., Pokora, A. & Vargo, D. (1983). Reaction of Enzyme-bound 5-Deazaflavin with Peroxides. *J. Biol. Chem.* **258**(14), 8561-8567.
Kasha, M. & Brabham, D. E. (1979). Singlet Oxygen Electronic Structure and Photosensitization. In *Singlet Oxygen* (Kasha, M., ed.). Academic Press, Inc.
Keevil, T. & Mason, H. S. (1978). Molecular Oxygen in Biological Oxidations - An Overview. *Methods Enzymol.* **LII**, 3-40.
Kemal, C., Chan, T. W. & Bruice, T. C. (1977). Reaction of $^3O_2$ with Dihydroflavins. 1. *N*3,5-Dimethyl-1,5-dihydrolumiflavin and 1,5-Dihydroisoallozines. *JACS* **99**(22), 7272-7286.
King, G. & Murray, N. E. (1995). Restriction alleviation and modification enhancement by the Rac prophage of *Escherichia coli* K-12. *Molecular Microbiology* **16**(4), 769-777.
Kunkel, T. A. (1985). Rapid and efficient site-directed mutagenesis without phenotypic selection. *Proc. Natl. Acad. Sci. USA* **82**, 488-492.
Kunkel, T. A., Roberts, J. D. & Zakour, R. A. (1987). Rapid and Efficient Site-Specific Mutagenesis without Phenotypic Selection. *Methods in Enzymology* **154**, 367-382.
Lederer, F., Cortial, S., Becam, A.M., Haumont, P.Y. & Perez, L. (1985). Primary structure of flavocytochrome b_2 from baker's yeast. *Eur. J. Biochem.* **139**, 59-65.
Lederer, F. (1991). Flavocytochrome b_2. In *Chemistry and Biochemistry of Flavoenzymes* (Müller, F., ed.), Vol. II, pp. 153-242. CRC Press, Inc., Boca Raton.
Leegood, R. C., Lea, P. J., Adcock, M. D. & Häusler, R. E. (1995). The regulation and control of photorespiration. *Journal of Experimental Botany* **46**, 1397-1414.
Leenders, A., Kooijman, M., van Hoek, A., Veeger, C. & Visser, A. J. W. G. (1993). Flavin dynamics in reduced flavodoxins. *Eur. J. Biochem.* **211**, 37-45.

Leung, D. W., Chen, E. & Goeddel, D. V. (1989). A method for random mutagenesis of a defined DNA segment using a modified polymerase chain reaction. *Technique* **1**(1), 11-15.

Levy, J., Campbell, J. J. R. & Blackburn, T. H. (1973). *Introductory microbiology*. First edit, John Wiley & Sons, Inc., New York.

Lide, D. R., Ed. (1993). CRC Handbook of Chemistry and Physics. 73rd edit. Boca Raton: CRC Press.

Lindqvist, Y. (1989). Refined structure of spinach glycolate oxidase at 2Å resolution. *J. Mol. Biol.* **209**, 151-166.

Lindqvist, Y. & Brändén, C.-I. (1985). Structure of glycolate oxidase from spinach. *Proc. Natl. Acad. Sci. USA* **82**, 6855-6859.

Lindqvist, Y. & Brändén, C.-I. (1989). The Active Site of Spinach Glycolate Oxidase. *J. Biol. Chem.* **264**(6), 3624-3628.

Lindqvist, Y., Brändén, C.-I., Mathews, F. S. & Lederer, F. (1991). Spinach Glycolate Oxidase and Yeast Flavocytochrome b_2 Are Structurally Homologous and Evolutionarily Related Enzymes with Distinctly Different Function and Flavin Mononucleotide Binding. *J. Biol. Chem.* **266**, 3198-3207.

Macheroux, P., Kieweg, V., Massey, V., Sönderlind, E., Stenberg, K. & Lindqvist, Y. (1993). Role of tyrosine 129 in the active site of spinach glycolate oxidase. *Eur. J. Biochem.* **213**, 1047-1054.

Macheroux, P., Massey, V., Thiele, D. J. & Volokita, M. (1991). Expression of Spinach Glycolate Oxidase in *Saccharomyces cerevisiae*: Purification and Characterisation. *Biochemistry* **30**, 4612-4619.

Macheroux, P., Mulrooney, S. B., Williams Jr., C. H. & Massey, V. (1992). Direct expression of active spinach glycolate oxidase in *Escherichia coli*. *Biochimica et Biophysica Acta* **1132**, 11-16.

Maeda-Yorita, K., Aki, K., Sagai, H., Misaki, H. & Massey, V. (1995). L-lactate oxidase and L-lacate monooxygenase: Mechanistic variation on a common structural theme. *Biochimie* **77**, 631-642.

Malmström, B. G. (1982). Enzymology of oxygen. *Ann. Rev. Biochem.* **51**, 21-59.

Massey, V. (1994). Activation of Molecular Oxygen by Flavins and Flavoproteins. *J. Biol. Chem.* **269**, 22459-22462.

Mattevi, A., Vanoni, M. A., Todone, F., Rizzi, M., Teplyakov, A., Coda, A., Bolognesi, M. & Curti, B. (1996). Crystal structure of D-amino acid oxidase: A case of active site mirror-image convergent evolution with flavocytochrome b_2. *Proc. Natl. Acad. Sci. USA* **93**, 7496-7501.

Mejean, V., Iobbi-Nivol, C., Leppelletier, M., Giordano, G., Chippaux, M. & Pascal, M.-C. (1994). TMAO anaerobic respiration in *Escherichia coli*: involvement of the *tor* operon. *Molecular Microbiology* **11**(6), 1169-1179.

Mewies, M., Basran, J., Packman, L. C., Hille, R. & Scrutton, N. S. (1997). Involvement of a flavin iminoquinone methide in the formation of 6-hydroxyflavin mononucleotide in tromethylamine dehydrogenase: A rationale for the existence of 8 alpha-methyl and C6-linked covalent flavoproteins. *Biochemistry* **36**(23), 7162-7168.

Miles, C. S., Rouvière-Fourmy, N., Lederer, F., Mathews, F. S., Reid, G. A., Black, M. T. & Chapman, S. K. (1992). Tyr-143 facilitates interdomain electron transfer in flavocyochrome b_2. *Biochem. J.* **285**, 187-192.

Miller, J. H. (1992). *A short Course in Bacterial Genetics*. First edit, Cold Spring Harbor Laboratory, New York.

Mitra, B., Gerlt, J. A., Babbitt, P. C., Koo, C. W., Kenyon, G. L., Joseph, D. & Petsko, G. A. (1993). A Novel Structural Basis for Membrane Association of a Protein: Construction of a Chimeric Soluble Mutant of (*S*)-Mandelate Dehydrogenase from *Pseudomonas putida*. *Biochemistry* **32**, 12959-12967.

Morton, R. K., Armstrong, J. M. & Appleby, C. A. (1961). The chemical and enzymic properties of cytochrome b_2 of bakers' yeast. In *Haematin Enzymes* (Falk,

J. E., Lemberg, R. & Morton, R. K., eds.), pp. 501-523. Pergamon Press, Oxford.
Mott, J. E., Grant, R. A., Ho, Y.-S. & Platt, T. (1985). Maximizing gene expression from plasmid vectors containing the λ P_L promoter: Strategies for overproducing transcription termination factor ρ. *Proc. Natl. Acad. Sci. USA* **82**, 88-92.
Müh, U., Williams Jr., C. H. & Massey, V. (1994). Lactate Monooxygenase: II. Site-directed Mutagenesis of the Postulated Active Site Base Histidine 290. *Journal of Biological Chemistry* **269**(11), 7989-7993.
Mullis, K. B. (1990). The Unusual Origin of the Polymerase Chain Reaction. *Scientific American*(April), 36-43.
Murray, N. E., Brammar, W. J. & Murray, K. (1977). Lambdoid Phages that Simplify the Recovery of in vitro Recombination. *Mol. Gen. Genet.* **150**, 53-61.
Myers, R. M., Lerman, L. S. & Maniatis, T. (1985). A general Method for Saturation Mutagenesis of Cloned DNA Fragments. *Science* **229**, 242-247.
Pace, C. & Stankovich, M. (1986). Oxidation-Reduction Proporties of Glycolate Oxidase. *Biochemistry* **25**, 2516-2522.
Pajot, A. P. & Claisse, M. L. (1974). Utilisation by yeast of D-lactate and L-lactate as sources of energy in the presence of antimycin. *Eur. J. Biochem.* **49**, 275-285.
Pajot, P. & Groudinsky, O. (1970). Molecular Weight and Quaternary Structure of Yeast L-Lactate Dehydrogenase (Cytochrome b_2). *Eur. J. Biochem.* **12**, 158-164.
Pallister, R. L., Reid, G. A., Brunt, C. E., Miles, C. S. & Chapman, S. K., Eds. (1990). Isolation and Characterisation of the Flavin Domain of Flavocytochrome b_2 expressed independently in *E. coli*. Flavins and Flavoproteins 1990. Edited by Curti, B., Ronchi, S. & Zanetti, G. Berlin: Walter de Gruyter.
Pompon, D. & Lederer, F. (1979). Deazaflavins as Cofactors for Flavocytochrome b_2 from Baker's Yeast. *Eur. J. Biochem.* **96**, 571-579.
Pühler, A., Ed. (1993). Genetic Engineering of Microorganisms. First edit. Weinheim: VCH.
Reid, G. A., White, S., Black, M. T., Lederer, F., Mathews, F. S. & Chapman, S. K. (1988). Probing the active site of flavocyochrome b_2 by site-directed mutagenesis. *Eur. J. Biochem.* **178**, 329-333.
Rowland, P., Nielsen, F. S., Jensen, K. F. & Larsen, S. (1997). The crystal structure of the flavin containing enzyme dihydroorotate A from *Lactococcus lactis*. *Structure* **5**, 239-252.
Rychlik, W. (1992). Oligo® 4.02 edit. National Biosciences, Inc., Plymouth.
Sambrook, J., Fritsch, E. F. & Maniatis, T. (1989b). *Molecular Cloning, a laboratory manual*. 2nd edit (Nolan, C., Ed.), 2. 3 vols, Cold Spring Harbor Laboratory Press, Cold Spring Harbor.
Sambrook, J., Fritsch, E. F. & Maniatis, T. (1989c). *Molecular Cloning, a laboratory manual*. 2nd edit (Nolan, C., Ed.), 1. 3 vols, Cold Spring Harbor Laboratory Press, Cold Spring Harbor.
Sambrook, J., Fritsch, E. F. & Maniatis, T. (1989a). *Molecular Cloning, a laboratory manual*. 2nd edit (Nolan, C., Ed.), 3. 3 vols, Cold Spring Harbor Laboratory Press, Cold Spring Harbor.
Scopes, R. K. (1987). *Protein Purification*. Second edit. Springer Advanced Texts in Chemistry (Cantor, C. R., Ed.), Springer-Verlag, New York.
Scrutton, N. S. (1994). α/β Barrel Evolution and the Modular Assembly of Enzymes: Emerging Trends in the Flavin Oxidase/Dehydrogenase Family. *BioEssays* **16**(2), 115-122.
Sharp, R. E., White, P., Chapman, S. K. & Reid, G. A. (1994). Role of Interdomain Hinge of Flavocytochrome b_2 in Intra- and Inter-Protein Electron Transfer. *Biochemistry* **33**, 5115-5120.
Short, D. M. (1996). The location of the cytochrome *c* binding site on flavocytochrome b_2. Ph.D., University of Edinburgh.

Silhavy, T. J. (1984). *Experiments with Gene Fusions*, Cold Spring Harbor Laboratory, New York.
Singer, T. P. & Edmondson, D. E. (1978). Flavoproteins (Overview). *Meth. Enz.* **LIII**, 397-419.
Smékal, O., Yasin, M., Fewson, C. A., Reid, G. A. & Chapman, S. K. (1993). L-Mandelate dehydrogenase from *Rhodotorula graminis*: comparisons with the L-lactate dehydrogenase (flavocytochrome b_2) from *Saccharomyces cerevisiae*. *Biochem. J.* **290**, 103-107.
Southern, E. (1975). Detection of specific sequences among DNA fragments separated by gel electrophoresis. *J. Mol. Biol.* **98**, 503-517.
Spee, J. H., de Vos, W. M. & Kuipers, O. P. (1993). Efficient random mutagenesis method with adjustable mutation frequency by use of PCR and dITP. *Nucleic Acids Research* **21**(3), 777-778.
Spencer, R., Fisher, J. & Walsh, C. (1977). One- and Two-Electron Redox Chemistry of 1-Carba-1-deazariboflavin. *Biochemistry* **16**(16), 3586-3594.
Spiro, S. & Guest, J. R. (1991). Adaptive responces to oxygen limitation in *Escherichia coli*. *TIBS* **16**, 310-314.
Stemmer, W. P. C. (1994a). DNA shuffling by random fragmentation and reassembly: *In vitro* recombination for molecular evolution. *Proc. Natl. Acad. Sci. USA* **91**, 10747-10751.
Stemmer, W. P. C. (1994b). Rapid evolution of a protein *in vitro* by DNA shuffling. *Nature* **370**, 389-391.
Stenberg, K., Clausen, T., Lindqvist, Y. & Macheroux, P. (1995). Involvement of Tyr24 and Trp108 in substrate binding and substrate specificity of glycolate oxidase. *Eur. J. Biochem.* **228**, 408-416.
Stenberg, K. & Lindqvist, Y. (1997). Three-dimensional structures of glycolate oxidase with bound active-site inhibitors. *Protein Science* **6**(5), 1009-1015.
Stoll, V. S., Kimber, M. S. & Pai, E. F. (1996). Insights into substrate binding by D-2-ketoacid dehydrogenases from the structure of *Lactobacillus pentosus* D-lactate dehydrogenase. *Structure* **4**(4), 437-447.
Streitwieser, A. J. & Heathcock, C. H. (1985). *Introduction to Organic Chemistry*. Third edit, Macmillan Publishing Company, New York.
Studier, F. W. & Moffatt, B. A. (1986). Use of Bacteriophage T7 RNA Polymerase to Direct Selective High-level Expression of Cloned Genes. *J. Mol. Biol.* **189**, 113-130.
Studier, F. W., Rosenberg, A. H., Dunn, J. J. & Dubendorff, J. W. (1990). Use of T7 RNA Polymerase to Direct Expression of Cloned Genes. *Methods in Enzymology* **185**, 60-89.
Tabor, S. & Richardson, C. C. (1985). A bacteriophage T7 RNA polymerase/promoter system for controlled exclusive expression of specific genes. *Proc. Natl. Acad. Sci. USA* **82**, 1074-1078.
Torssell, K. B. G. (1989). *Natural Product Chemistry*. First edit, John Wiley & Sons Limited, Chichester.
Tsou, A. Y., Ransom, S. C., Gerlt, J. A., Buechter, D. D., Babbitt, P. C. & Kenyon, G. L. (1990). Mandelate Pathway of *Pseudomonas putida*: Sequence Relationships Involving Mandelate Racemase, (*S*)-Mandelate Dehydrogenase, and Benzoylformate Decarboxylase and Expression of Benzoylformate Decarboxylase in *Escherichia coli*. *Biochemistry* **29**, 9856-9862.
Tye, B., Chien, J., Lehman, I., Duncan, B. & Warner, H. (1978). Uracil incorporation: A source of pulse-labeled DNA fragments in the replication of *Escherichia coli* chromosome. *Proc. Natl. Acad. Sci. USA* **75**, 233-237.
Urban, P. & Lederer, F. (1984). Baker's yeast flavocytochrome b_2. A mechanistic study of the dehydrohalogenation reaction. *Eur. J. Biochem.* **144**, 345-351.
Volokita, M. & Somerville, C. R. (1987). The primary structure of spinach glycolate oxidase deduced from the DNA sequence of a cDNA clone. *J. Biol. Chem.* **262**, 15825-15828.

Walsh, C. (1980). Flavin Coenzymes: At the Crossroads of Biological Redox Chemistry. *Acc. Chem. Res.* **13**, 148-155.
Willetts, A. (1997). Structural studies and synthetic applications of Baeyer-Villiger monooxygenases. *TIBTECH* **15**, 55-62.
Winnacker, E.-L. (1987). *From Genes to Clones*. First edit. Trans. Ibelgaufts, H., VCH, Weinheim.
Xia, Z.-x. & Mathews, F. S. (1990). Molecular Structure of Flavocytochrome b_2 at 2.4 Å Resolution. *J. Mol. Biol.* **212**, 837-863.
Yanisch-Perron, C., Vieira, J. & Messing, J. (1985). Improved M13 phage cloning vectors and host strains: nucleotide sequences of the M13mp18 and pUC19 vectors. *Gene* **33**(1), 103-119.

9. Appendix

9.1. Abbreviations

Textual abbreviation	
A	absorbance
amp	ampicillin
ATP	adenosine-5'-triphosphate
BSA	bovine serum albumin
cam	chloramphenicol
Cyt. c	cytochrome *c*
DEAE	diethylaminoethyl
DNA	deoxyribonucleic acid
dNTP	deoxyribonucleotide 5'-triphosphate
DTT	dithiothreiol
ε	molar absorption coefficient
EDTA	ethylenediaminetetraacetic acid
EtBr	ethidium bromide
EtOH	ethanol
FCb2	flavocytochrome b_2
FDH	flavin-binding domain of flavocytochrome b_2
FMN	flavin mononucleotide
GO	glycolate oxidase
I	ionic strength
IPTG	isopropyl β-D-thiogalactopyranoside
k_A	specificity constant (k_{cat}/K_m)
kan	kanamycin
k_{cat}	limiting rate
K_m	Michaelis constant
NaOAc	sodium acetate
OD	optical density
PCR	polymerase chain reaction
PMSF	phenylmethylsulphonyl fluoride
RNA	ribonucleic acid
rpm	rotation per minute
Rubisco	ribulose-1,5-bisphosphate carboxylase/oxygenase
SDS	sodium dodecyl sulphate
Tris	Tris(hydroxymethyl)aminomethane
UV	ultraviolet
WT	wild-type

Units	
A	ampere
°C	degree Celcius
Da	Daltons
g	gram
J	joule
K	degree Kelvin
L	litre
m	metre
M	molar
s	second
V	volt
Å	Ångström

Amino acid	Code	
Alanine	A	ala
Cysteine	C	cys
Aspartic acid	D	asp
Glutamic acid	E	glu
Phenylalanine	F	phe
Glycine	G	gly
Histidine	H	his
Isoleucine	I	ile
Lysine	K	lys
Leucine	L	leu
Methionine	M	met
Asparagine	N	asn
Proline	P	pro
Glutamine	Q	gln
Arginine	R	arg
Serine	S	ser
Threonine	T	thr
Valine	V	val
Tryptophan	W	trp
Tyrosine	Y	tyr

Base of deoxyribonucleic acid	Code
Adenine	A
Cytosine	C
Guanine	G
Thymine	T

9.2. Sequence alignment

Sequence alignment of the gene encoding glycolate oxidase and the part of the gene encoding the corresponding amino acid sequence in the flavin-binding domain of flavocytochrome b_2.

9.3. Bacterial strains

Strain	Genotype	Reference
AR120	λN99 (F', galK2, LAM-, *rpsL*200)	(Mott *et al.*, 1985)
BL21(DE3)	F$^-$,*ompT*, *hsdS*$_B$, (r_B^-,m_B^-), *dcm*, *gal*, λ(DE3)	(Studier & Moffatt, 1986)
BW313	*dut*, *ung*, *thi*-1, *relA*, *spoT*1/F'lysA	(Tye *et al.*, 1978; Kunkel, 1985)
DH5α®	ϕ80d*lacZ*ΔM15, *recA*1, *endA*1, *gyrA*96, *thi*-1, *hsdR*17 (r_K^-,m_K^+), *supE*44, *relA*1, *deoR*, Δ(*lacZYA- argF*)U169	(Doyle, 1996)
ECL901	*araD*139, Δ(*argF-lac*)U169, *rpsL*150, *relA*1, *deoC*1, *flb*-5301, *ptsF*15, *frd*-101, ϕ(*lctA-lac*)	(Dong *et al.*, 1993)
ED8654	*supE*44, *supF*58, *hsdR*514($r_K^-m_K^+$), *metB*1, *lacY*1, *galK*2, *galT*22, *trpR*55	(Murray *et al.*, 1977)
JM109	*endA*1, *recA*1, *gyrA*96, *thi*, *hsdR*17 (r_K^-,m_K^+), *relA*1, *supE*44, Δ(*lac-proAB*), [F', *traD*36, *proAB*, *lacI*^{q}ZΔM15]	(Yanisch-Perron *et al.*, 1985)
JM109(DE3)	JM109, λ(DE3)	(Doyle, 1996)
JM110	*rpsL*, *thr*, *leu*, *hsdR*17 (r_K^-,m_K^+), *lacY*, *galK*, *galT*, *ara*, *tonA*, *tsx*, *dam*, *dcm*, *supE*44, Δ(*lac-proAB*), [F', *traD*36, *proAB*, *lacI*^{q}ZΔM15]	(Yanisch-Perron *et al.*, 1985)
LO1	MC4100, *lctD*(kanR)	this study
MC4100	*araD*139, Δ(*argF-lac*)U169, LAM-, *flhD*5301, *fruA*25, *relA*1, *rpsL*150(strR), *rbsR*22, *deoC*1, *ptsF*25	(Silhavy, 1984)
NF1	F$^-$*lac*$^-$, λ*c*I857*N*7*N*53ΔH1	(Bernard *et al.*, 1979)
pop2136	F$^-$*lac*$^-$, λ*c*I857*N*7*N*53ΔH1	(Bernard *et al.*, 1979)
TG1	*supE*, Δ(*hsdM-mcrB*), *thi*, Δ(*lac-proAB*), [F', *traD*36, proAB$^+$, *lacI*^{q}lacZΔM15]	(Sambrook *et al.*, 1989c)

9.4. Plasmids

Plasmid	Relevant features	Reference
pBAD18	P_{BAD} promoter and its regulatory gene *araC* (amp^R)	(Guzman *et al.*, 1995)
pDSb2	Gene encoding flavocytochrome b_2 under control of $P_{N25X/0}$ promoter (amp^R)	(Black *et al.*, 1989)
pEG10	kanamycin resistance casette (kan^R)	(Gordon, 1997)
pET3d	T7 RNA polymerase promoter (amp^R)	(Studier *et al.*, 1990)
pGP1-2	Gene *1* under control of λP_L promoter and its regulatory gene *c*I857(kan^R)	(Tabor & Richardson, 1985)
pGR401	Gene encoding flavocytochrome b_2 cloned in shuttle vector with a f1 ori (amp^R)	(Reid *et al.*, 1988)
pJF118EH	*tac* promoter and the repressor gene *lacI*^{q} (amp^R)	(Fürste *et al.*, 1986)
pLCT2	*lctD*$^+$, *lctT*$^+$ (amp^R)	(Dong *et al.*, 1993)
pLO1	pMAK705, *lctD*$^-$::kan^R (cam^R)	this study
pLysS	Gene for lysozyme under control of *tet* promoter (cam^R)	(Studier *et al.*, 1990)
pMAK705	Temperature sensitive pSC101 origin of replication (cam^R)	(Hamilton *et al.*, 1989)
pPM1	Gene encoding glycolate oxidase cloned in pET3d (amp^R)	(Macheroux *et al.*, 1992)
pRC23	λp_L promoter (amp^R)	(Crowl *et al.*, 1985)
pT7-5	T7 RNA polymerase promoter (amp^R)	(Tabor & Richardson, 1985)
pT7-7	T7 RNA polymerase promoter (amp^R)	(Tabor & Richardson, 1985)

The resistance confered by the plasmid is indicated in brackets.

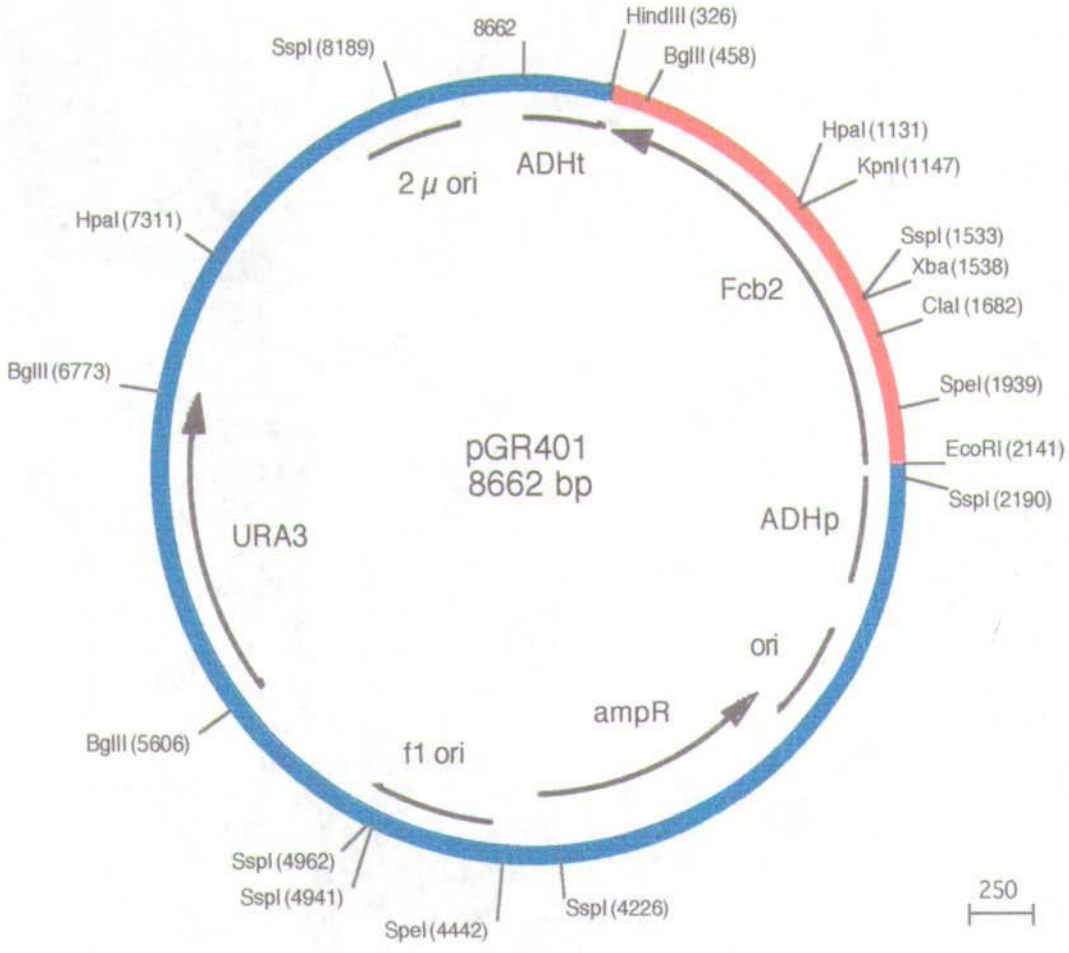

Map of the yeast expression vector pGR401. The flavocytochrome b_2 coding sequence (FCb2), shown in red, lies between the promoter (ADH_p) and terminator (ADH_t) of the *S. cerevisiae ADH1* gene. The plasmid contains origins of replication and selectable markers for maintainance in *E. coli* (ampR) and in yeast (URA3). The presence of the origin of replication from bacteriophage f1 (f1 ori) allowed isolation of single-stranded DNA for site-specific mutagenesis and DNA sequence determination. Restriction enzyme sites occuring only once within the gene for flavocytochrome b_2 are indicated along with their position on the plasmid (Reid *et al.*, 1988).

Used for production of single-stranded DNA in TG1 under ampicillin selection, and for production of uracil-containing single-stranded DNA in BW313 also under ampicillin selection.

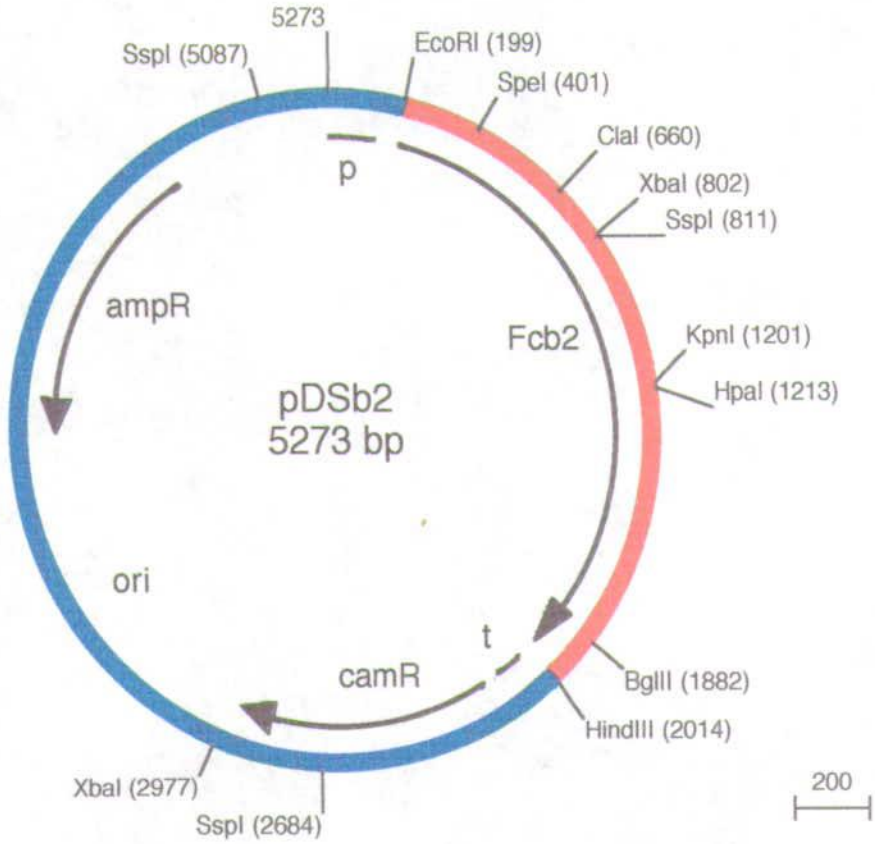

Map of *E. coli* expression vector pDSb2. The flavocytochrome b_2 coding sequence (FCb2), shown in red, lies between the promoter (p) and terminator (t) from coliphage T_5. The plasmid contains origin of replication and selectable markers for maintainance in *E. coli*. Restriction enzyme sites occuring only once within the gene for flavocytochrome b_2 are indicated along with their position in the plasmid (Black *et al.*, 1989).

Used for constitutive expression of flavocytochrome b_2 in TG1 under ampicllin selection.

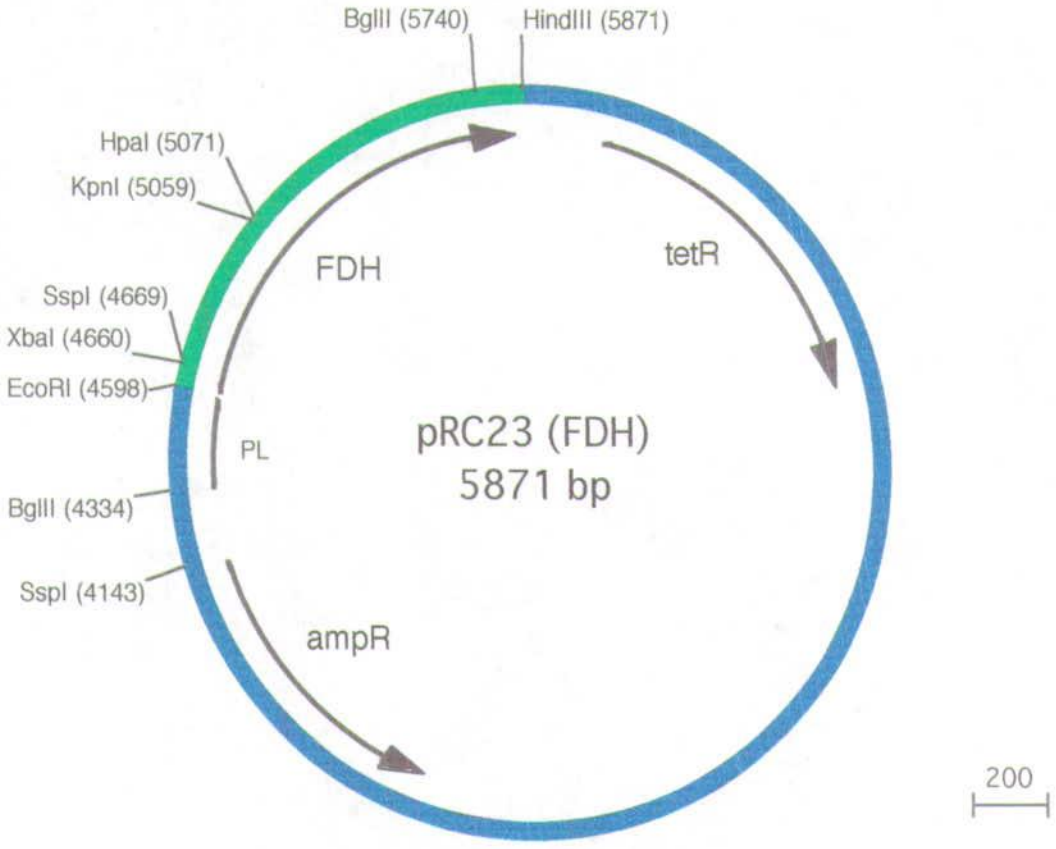

Map of *E. coli* expression vector pRC23(FDH). The coding sequence for the flavin-binding domain of flavocytochrome b_2 (FDH), shown in green, is cloned downstream the bacteriophage λ P_L promoter. The plasmid contains origin of replication and selectable markers for maintainance in *E. coli*. Restriction enzyme sites occuring only once within the gene for the flavin-binding domain are indicated along with their position in the plasmid (Crowl *et al.*, 1985).

Used for expression of the flavin-binding domain in pop2136 or NF1, both of which overproduce the λ *c*I repressor. Expression was induced by growth at 42°C under ampicillin selection.

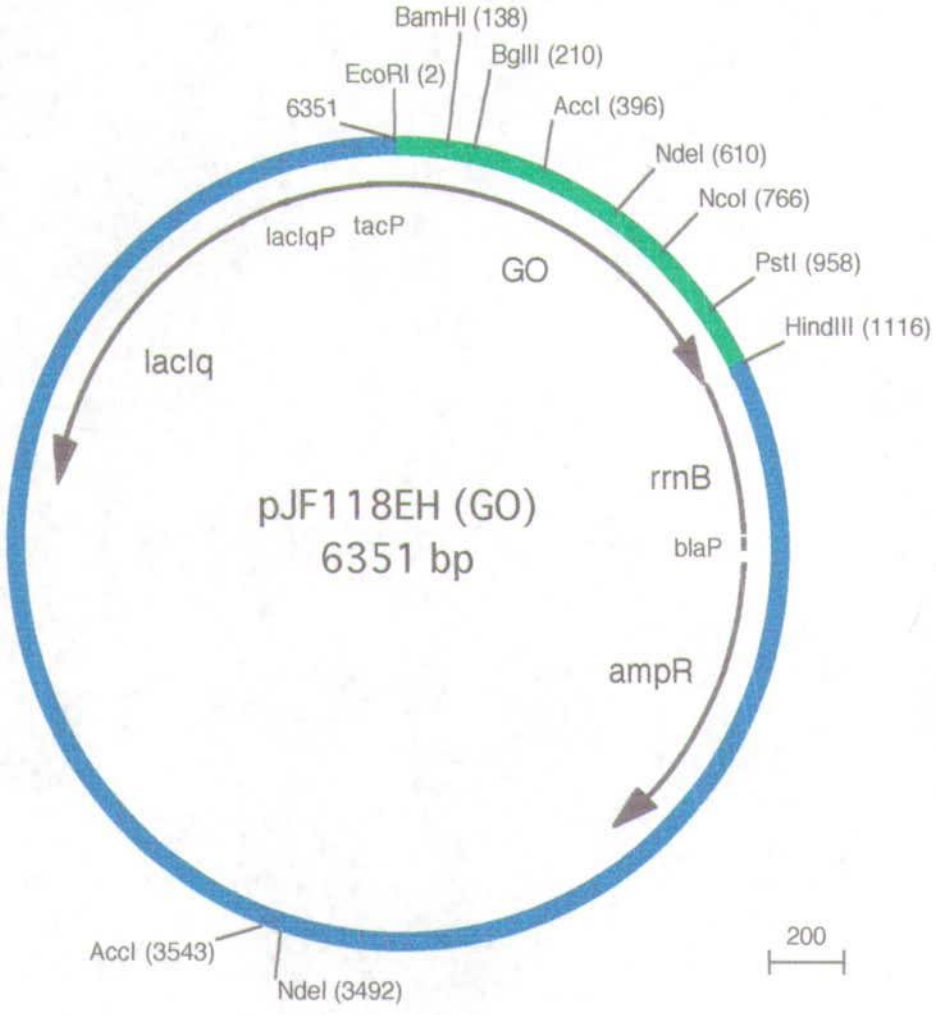

Map of *E. coli* expression vector pJF118EH(GO). The glycolate oxidase coding sequence, shown in green, is cloned downstream the *tac* hybrid promoter. The plasmid also contains origin of replication and selectable markers for maintainance in *E. coli*. The presence of the *lacI*^{q} gene renders the use of the plasmid independent from repressor-overproducing strains. rrnB represents part of the *E. coli rrnB* operon containing the gene for 5S RNA and its two transcriptional terminators, and prevents interference between transcription and replication. Restriction enzyme sites occuring only once within the gene for glycolate oxidase are indicated along with their position in the plasmid (Fürste *et al.*, 1986).

Used for expression of glycolate oxidase in TG1 under ampicillin selection. Expression was induced by addition of 1 mM IPTG.

9.5. Primers and oligonucleotides

Name	Sequence	Description
102A	CTGCACAATATTTCAAGC	Sequencing of flavocytochrome b_2
127A	TAGACAACaAGCCGAA	Sequencing of flavocytochrome b_2
H43M	CTACCAAATatgCCAGGTGGG	Sequencing of flavocytochrome b_2
b2-730	AATGCGTATCATAGG	Sequencing of flavocytochrome b_2
Y254F	CCAACTATtTGTTAACTC	Sequencing of flavocytochrome b_2
K349R	CTATTGTTATCAtgGGTGTTCAA	Sequencing of flavocytochrome b_2
Hind1500	CTTGAAAGCtTTATGTCT	Sequencing of flavocytochrome b_2
L436A	AGACCATTCgcGTATGCGAACTC	Mutation of Leu436 to Ala
A196P	CTACGTGTCTcCTACAGCTTTG	Mutation of Ala196 to Pro
A198P	GTCTGCTACAcCTTTGTGTAAAC	Mutation of Ala198 to Pro
A283T	CACTGTGGATaCTCCAAGTTT	Mutation of Ala283 to Thr
L230W	GATATCTACTTgGGCTTCATGT	Mutation of Leu230 to Trp
T197A	CGTGTCTGCTgCAGCTTTGTG	Mutation of Thr197 to Ala
dAGP	CCAATACAAAG--------AAAGCGATGA	Deletion of three amino acid residues (AGP)
i3A	GGCTGGTCCAgctgcggctAAAGCGATGA	Insertion of three alanine residues
i6A	GGCTGGTCCAgctgcagctgcggcagccAAAGCGATGA	Insertion of six alanine residues
FHI	GATATGAAGCTtAAATTTTCC	Introduction of *Hin*dIII site in FDH
FCL	CAAAGTTTATcGAtCCCTCTTTGAC	Introduction of *Cla*I site in FDH
GHI	cccAAGcttAGGTTTGTTTTACC	Amplification of GO, incl. *Hin*dIII site
GCL	ccATCgATCTGACCAGCGAC	Amplification of GO, incl. *Cla*I site
Sal1	acgcgtcGACACACCCCGATTG	Amplification of GO, incl. *Sal*I site
Sst1	gtcgagctctGGAAAGGCCAGAGTC	Amplification of GO, incl. *Sst*I site
EcoRI	GGAGGAATTCATGGAAACTAAGG	Amplification of FDH, incl. *Eco*RI site
HindIII	CATTAAAGCTTCAGAAAGTAGCC	Amplification of FDH, incl. *Hin*dIII site
GOMG1	cggaattcATGGAGATCACA	Amplification of GO, incl. *Eco*RI site
GOMG2	cccaagcTTATAATCTGGCAA	Amplification of GO, incl. *Hin*dIII site
BTOE	GATCGGAATTCC	Convert BamHI site to *Eco*RI site
LO2	CATGCGGATCCG	Convert NcoI site to *Bam*HI site

Capital letter indicates perfect match with target DNA.